arXiv:astro-ph/0310218v1 8 Oct 2003

Tidal dissipation in rotating giant planets

G. I. Ogilvie[1,2] and D. N. C. Lin[2,1]

ABSTRACT

Many extrasolar planets orbit sufficiently close to their host stars that significant tidal interactions can be expected, resulting in an evolution of the spin and orbital properties of the planets. The accompanying dissipation of energy can also be an important source of heat, leading to the inflation of short-period planets and even mass loss through Roche-lobe overflow. Tides may therefore play an important role in determining the observed distributions of mass, orbital period, and eccentricity of the extrasolar planets. In addition, tidal interactions between gaseous giant planets in the solar system and their moons are thought to be responsible for the orbital migration of the satellites, leading to their capture into resonant configurations.

Traditionally, the efficiency of tidal dissipation is simply parametrized by a quality factor Q, which depends, in principle, in an unknown way on the frequency and amplitude of the tidal forcing. In this paper, we treat the underlying fluid dynamical problem with the aim of determining the efficiency of tidal dissipation in gaseous giant planets such as Jupiter, Saturn, or the short-period extrasolar planets. Efficient convection enforces a nearly adiabatic stratification in these bodies, which may or may not contain rocky cores. With some modifications, our approach can also be applied to fully convective low-mass stars.

In cases of interest, the tidal forcing frequencies are typically comparable to the spin frequency of the planet but are small compared to its dynamical frequency. We therefore study the linearized response of a slowly and possibly differentially rotating planet to low-frequency tidal forcing. Convective regions of the planet support inertial waves, which possess a dense or continuous frequency spectrum in the absence of viscosity, while any radiative regions support generalized Hough waves. We formulate the relevant equations for studying the excitation of these disturbances and present a set of illustrative numerical calculations of the tidal dissipation rate.

[1]Institute of Astronomy, University of Cambridge, Madingley Road, Cambridge CB3 0HA, UK; gogilvie@ast.cam.ac.uk

[2]UCO/Lick Observatory,University of California, Santa Cruz, CA 95064; lin@ucolick.org

We argue that inertial waves provide a natural avenue for efficient tidal dissipation in most cases of interest. The resulting value of Q depends, in principle, in a highly erratic way on the forcing frequency, but we provide analytical and numerical evidence that the relevant frequency-averaged dissipation rate may be asymptotically independent of the viscosity in the limit of small Ekman number. For a smaller viscosity, the tidal disturbance has a finer spatial structure and individual resonances are more pronounced.

In short-period extrasolar planets, tidal dissipation via inertial waves becomes somewhat less efficient once they are spun down to a synchronous state. However, if the stellar irradiation of the planet leads to the formation of a radiative outer layer that supports generalized Hough modes, the tidal dissipation rate can be enhanced, albeit with significant uncertainty, through the excitation and damping of these waves. The dissipative mechanisms that we describe offer a promising explanation of the historical evolution and current state of the Galilean satellites as well as the observed circularization of the orbits of short-period extrasolar planets.

Subject headings: hydrodynamics — planets and satellites: general — waves

1. INTRODUCTION

1.1. Tidal interactions in planetary systems

The discovery of the very first extrasolar planet orbiting a main-sequence star, 51 Peg b, brought the surprising revelation that other planetary worlds can revolve around their host stars in extraordinarily tight orbits (Mayor & Queloz 1995). Around approximately one per cent of all the stars targeted by radial-velocity searches, similar planets are found with periods of a few days. These short-period planets were probably formed within a protostellar disk several AU away from their host stars through a sequence of physical processes outlined in the conventional 'core-accretion' theories of planetary formation (Lissauer 1993; Pollack et al. 1996). During its final accretion phase, strong interactions between a protoplanet and its natal disk lead to the formation of a gap near its orbit, which effectively terminates its growth. Angular momentum exchange with the disk causes a protoplanet formed in the inner region of the disk to migrate towards its host star (Goldreich & Tremaine 1980; Lin & Papaloizou 1986). Near the star, the protoplanet's migration may be halted either by its tidal interaction with a rapidly spinning host star or by entering a cavity in the disk associated with the stellar magnetosphere (Lin, Bodenheimer, & Richardson 1996). Planets

may also terminate their migration with intermediate-period orbits when their natal disks are rapidly depleted (Trilling, Lunine, & Benz 2002; Armitage et al. 2002; Ida & Lin 2003).

Short-period planets may be scattered to the vicinity of (or far away from) the stellar surface owing to dynamical instabilities associated with their long-term post-formation gravitational interaction (Rasio & Ford 1996; Weidenschilling & Marzari 1996). In this case, the protoplanet's orbit may initially be highly eccentric and subsequently undergo circularization owing to the tidal dissipation within its envelope (Rasio et al. 1996). Scattering by residual planetesimals is another promising avenue for planetary orbital migration (Murray et al. 1998). It has also been suggested that short-period planets may be formed *in situ* through a sequence of planetesimal migration, coagulation, and gas accretion (Papaloizou & Terquem 1999; Bodenheimer, Hubickyj, & Lissauer 2000; Sasselov & Lecar 2000). Finally, a totally different theory of protoplanetary formation relies upon gravitational instability in a massive gaseous protostellar disk (Kuiper 1951; Cameron 1978; Boss 1997), which produces a subcondensation with a composition close to that of the central star and having little, if any, solid core. Although the inferred presence of solid cores in Jupiter, Saturn, Uranus, and Neptune (Hubbard 1984) favors the orderly growth scenario in our solar system, there is as yet no direct evidence for or against the existence of cores in extrasolar planets.

In the past eight years, more than 100 planets have been discovered, around approximately ten per cent of the target stars in various planet search programs. A comprehensive distribution of planetary mass, period, and eccentricity has begun to emerge. These data are particularly useful for constraining and differentiating some scenarios for the formation and evolution of short-period planets. For example, there appears to be a minimum cut-off period at about three days. If the short periods of some planets were attained through orbital migration, their observed period distribution could be attributable to the stopping mechanism involved. It is also possible that the present period distribution is established through post-formation evolution, e.g., planets with extremely short periods may have perished subsequent to their formation. A particularly interesting characteristic of the planet-bearing stars is that they tend to be metal-rich with respect to the Sun and the F–G field-star average in the solar neighborhood (e.g., Gonzalez et al. 2001; Santos, Israelian, & Mayor 2001). This correlation may result from planets having being consumed following either migration through the protoplanetary disk (Lin 1997; Laughlin & Adams 1997; Sandquist et al. 1998) or gravitational interaction with other planets (Rasio & Ford 1996). It may also be interpreted as evidence that an enhanced metallicity in the planet-forming disk, probably resulting from a metal-rich parent cloud, is especially conducive to planet formation (Pollack et al. 1996; Fischer & Valenti 2003; Ida & Lin 2003).

Another important set of observational data is the planets' eccentricities. While the

eccentricities of planets with periods $P > 21$ days are uniformly distributed up to about 0.7, all planets with $P < 7$ days have nearly circular orbits. This observed dichotomy in the eccentricity–period distribution has been attributed to the circularization of the orbits of short-period planets induced by their internal tidal dissipation (Rasio et al. 1996; Marcy et al. 1997). Such a scenario would be necessary to account for the small eccentricities of the short-period planets if they were scattered into, or strongly perturbed in, the vicinity of their host stars by their planetary siblings. If, instead, the short-period planets acquired their small semi-major axes through tidal interaction with their natal disks (Lin et al. 1996), such a process may be able to damp the eccentricities of planets with masses $M_p \lesssim 10\,M_J$ (where M_J is the mass of Jupiter) (Goldreich & Tremaine 1980; Artymowicz 1992), although this hypothesis remains uncertain (Papaloizou, Nelson, & Masset 2001; Goldreich & Sari 2003). However, some of the potential stopping mechanisms, such as the planets' tidal interaction with rapidly spinning host stars (Lin et al. 1996), can also excite their orbital eccentricities (Dobbs-Dixon, Lin, & Mardling 2003). An efficient post-formation eccentricity damping mechanism may still be needed to account for the small eccentricities of the short-period planets.

Although no information is available on the rotation of extrasolar planets, tidal interaction with the host star is expected to bring the rotation of a short-period planet into synchronism with its orbit and to eliminate any obliquity of its rotation axis. Since the spin of a planet accounts for much less angular momentum than its orbit, synchronization proceeds more rapidly than circularization. This assumption neglects the possible effects of thermal tides, which may tend to drive the planet away from synchronism (Thomson 1882; Gold & Soter 1969).

Tidal interaction can also modify the radii and internal structures of short-period planets. In principle, the actual sizes of extrasolar planets may be used, at least as a partial test, to infer whether they formed through core accretion or through gravitational instability of massive gaseous protostellar disks. In the fully convective envelopes of gaseous giant planets, it is difficult for the refractory elements to condense into droplets and become differentiated from the volatile elements (cf. Guillot et al. 2003). Therefore planets formed through orderly core accretion are more likely to have solid cores and to be relatively compact, whereas those formed through gravitational instability are likely to retain a nearly uniform solar composition throughout their interiors and to be more extended.

The detection of a transiting planet around the star HD 209458 provides an opportunity for us to measure its radius directly and thereby to constrain its present internal structure. The observed radius, $1.35\,R_J$, of this $0.63\,M_J$ planet (Brown et al. 2001) is larger than that expected for a coreless planet with a similar mass and age. A planet with a core would be still

more compact, leading to an even larger discrepancy with the observational measurement. For this short-period planet, the presence of a small residual orbital eccentricity or non-synchronous rotation could lead to internal tidal dissipation with a heating rate comparable to or larger than that released by the Kelvin–Helmholtz contraction. Provided that the dissipation of the host star's tidal disturbance occurs well below the planet's photosphere, it increases the planet's internal temperature and equilibrium radius (Bodenheimer et al. 2000).

Planet–star interactions may also have altered the mass distribution of the short-period planets. Above a critical eccentricity, which is a function of the planet's semi-major axis, tidal dissipation of energy during the circularization process can cause a planet to inflate in size before its eccentricity is damped. For moderate eccentricities, the planet adjusts through a sequence of stable thermal equilibria in which the rate of internal tidal dissipation is balanced by the enhanced radiative flux associated with the planet's enlarged radius. For sufficiently large eccentricities, the planet swells beyond $2\,R_J$ and its internal degeneracy is partially lifted. Thereafter, the thermal equilibria become unstable and the planet undergoes runaway inflation until its radius exceeds the Roche radius (Gu, Lin, & Bodenheimer 2003). The critical eccentricity of about 0.2 (for a young Jupiter-mass planet with a period less than three days) may be easily attained, with the result that many short-period planets may have migrated to the vicinity of their host stars and perished there.

The above discussion clearly indicates the importance of planet–star tidal interactions to the origin and destiny of short-period planets. They may determine (1) the asymptotic semi-major axis of migrating protoplanets, (2) the absence of planets with periods less than three days, (3) the structure of those planets that survive in the vicinity of their host stars, and (4) the small eccentricities and relatively low masses of the short-period planets. However, the efficiency of these processes depends crucially on the ability of the planet to dissipate tidal disturbances, which is poorly understood.

1.2. Theory of the equilibrium tide

An early analysis of the nature of the tidal interaction between Earth and the Moon was introduced by Darwin (1880) based on the concept of the equilibrium tide (see Cartwright 2000 for a historical discussion). In this model, due originally to Newton, a homogeneous spherical body continually adjusts to maintain a state of quasi-hydrostatic equilibrium in the varying gravitational potential of its orbital companion. Darwin introduced a phase lag into the response, the lag being proportional to the tidal forcing frequency and attributable to the viscosity of the body. The phase lag gives rise to a net tidal torque and dissipation of energy.

Subsequent formulations (Munk & MacDonald 1960; Goldreich & Soter 1966) parametrize the efficiency of the tidal dissipation, whatever its origin, by a specific dissipation function or Q-value (quality factor). Although, in principle, Q is an unknown function of the frequency and amplitude of the tidal forcing, in the planetary science community it is usually treated as a constant property of each body in the solar system, corresponding to a constant phase lag of $\arcsin Q^{-1}$ (e.g., Murray & Dermott 1999). Indeed, studies of the Earth's rotation provide evidence that its Q-value is approximately constant over a wide range of frequency (Munk & MacDonald 1960), even though a variety of mechanisms may be responsible. The tidal Q-value may be predominantly determined by turbulent dissipation in the shallow seas (Taylor 1920; Jeffreys 1920; see Munk & MacDonald 1960 for a discussion). In the case of the Moon, the observational constraints on Q are much weaker, but the synchronized spin of the Moon suggests that the presence of an ocean is not necessary for tidal dissipation. In the context of binary stars, the assumption of a constant lag time is usually adopted (Hut 1981; Eggleton, Kiseleva, & Hut 1998) as in Darwin's viscous model.

Evidence of tidal dissipation can also be found in gaseous giant planets such as Jupiter and Saturn. For example, the Laplace resonance of Io, Europa, and Ganymede may be entered through the tidal interaction of the moons with Jupiter (Goldreich 1965; Peale, Cassen, & Reynolds 1979; Lin & Papaloizou 1979b). In order to maintain this resonant configuration despite the dissipation inside Io, tidal dissipation within Jupiter must continually induce angular momentum transfer from its spin to Io's orbit. The magnitude of the Q-value for Jupiter, inferred from Io's dissipation rate, is in the range $6 \times 10^4 - 2 \times 10^6$ (Yoder & Peale 1981). These values are similar to those inferred, for solar-type stars, from the circularization of close binaries as a function of their age and semi-major axis (Mathieu 1994; Terquem et al. 1998). Using these values of Q, the orbital evolution of a planetary or a stellar companion of a main-sequence star can be estimated by extrapolation, under the assumption of either a constant lag angle (Goldreich & Soter 1966), a constant lag time (Hut 1981; Eggleton et al. 1998), or an intermediate approach (Mardling & Lin 2002).

In the extended convective envelopes of gaseous giant planets and low-mass stars, turbulence can lead to dissipation of the motion that results from the continual adjustment of the equilibrium tide. However, the turbulent viscosity estimated from the mixing-length theory ought to be reduced by a frequency-dependent factor owing to the fact that the convective turnover timescale is usually much longer than the period of the tidal forcing. Estimating this reduction in the efficiency of the turbulent viscosity, Zahn (1977, 1989) analyzed the dissipation of equilibrium tides in low-mass stars and computed an efficiency of angular momentum transfer for a non-rotating star that matches the observationally inferred circularization timescale of solar-type binary stars (Mathieu 1994). However, with a different prescription for the efficiency reduction factor (Goldreich & Keeley 1977; Goodman & Oh

1997), the derived rate of angular momentum transfer falls short of that required by nearly two orders of magnitude (Terquem et al. 1998). Based on a similar approach, which gives $Q \approx 5 \times 10^{13}$ from the dissipation of the equilibrium tide in Jupiter, Goldreich & Nicholson (1977) suggested that the tidal interaction between the Galilean satellites and Jupiter cannot drive any significant orbital evolution. For the short-period extrasolar planets, such a high Q-value would imply circularization times considerably longer than the ages of their host stars.

1.3. Dynamical tides

The problem of tidal dissipation is even more acute for high-mass stars in close binaries because they have extended radiative envelopes that may be expected to be free from turbulence. Yet their orbits are indeed circularized despite their short lifespans (Primini, Rappaport, & Joss 1977). In these systems, the tidal perturbation of the companion can induce the resonant excitation of low-frequency g-mode oscillations in the radiative region, which carry both energy and angular momentum fluxes (Cowling 1941; Zahn 1970). This wavelike, dynamical tide exists in addition to the equilibrium tide and provides an alternative avenue for tidal dissipation. The g modes are primarily excited in the radiative envelope close to the convective core where the Brunt–Väisälä frequency is comparable to the tidal forcing frequency and the wavelengths of the gravity waves are sufficiently long to couple well with the tidal potential (Goldreich & Nicholson 1989). Using asymptotic methods in the limit that the forcing frequency is small compared to the dynamical frequency of the star, Zahn demonstrated the existence of resonant modes that amplify the dynamical response of the star at particular frequencies. This local analysis was generalized to modest frequencies in a numerical analysis by Savonije & Papaloizou (1983, 1984). Despite the absence of convectively driven turbulence in the radiative envelope, the g-mode oscillations can be dissipated through radiative damping on the wavelength scale. The radiative loss in the stellar interior is generally weak so that the waves can propagate in an approximately adiabatic manner to the stellar surface where they are dissipated and the angular momentum they carry is deposited. This concept gives rise to the interesting suggestion that the stars become synchronized from the outside in (Goldreich & Nicholson 1989). As the dissipation layer first establishes a synchronized rotation, it presents a barrier to the outwardly propagating waves in the form of a corotation resonance at which the group velocity of the waves vanishes. Just below the corotation resonance, waves are stalled with large amplitude and dissipated. This process continues, initially inducing differential rotation but eventually leading to the global synchronization of the stellar spin. This theoretical model is in agreement with the observed spin and orbital evolution of high-mass close binary stars (Giuricin, Mardirossian,

& Mezzetti 1984a, 1984b).

In the interior of a solar-type star, where a radiative core is surrounded by a convective envelope, g-mode oscillations are also excited in the radiative region and, inasmuch as they extend into the outer convective region, they are dissipated by turbulent viscosity. For some special forcing frequencies, these g-mode oscillations can also attain a global resonance that strongly enhances the oscillation amplitude in the radiative region and the rate of dissipation in the convective region (Terquem et al. 1998). Nevertheless, the overall synchronization process is limited by the less efficient tidal dissipation that occurs in between resonant frequencies. A calibration with the observed circularization periods suggests that the required viscosity is nearly two orders of magnitude larger than that inferred from the standard mixing-length model for turbulent convection and the Goldreich & Keeley (1977) reduction factor.

Although g-mode excitation is a powerful process that drives the dynamical tidal response in stars, it can be effective only in radiative regions. Since the envelopes of gaseous giant planets are mostly convective, the relevance of g-mode oscillations is less well established. In a series of papers, Ioannou & Lindzen (1993a, 1993b, 1994) considered the dynamical response of Jupiter to the tidal perturbation of Io with a prescribed model for Jupiter's interior. They showed that g modes can be resonantly excited if the interior is slightly subadiabatic to the extent that an appropriately tuned wave cavity is created. When these waves are transmitted into the atmosphere and dissipated, they can produce an effective Q-value comparable to that inferred from the supposed orbital evolution of Io. However, current models suggest that convection may extend throughout the entire envelope of Jupiter and is such an efficient heat-transport process that Jupiter's envelope is adiabatically stratified and neutrally buoyant to a very high degree (Guillot et al. 2003). In this limit, Ioannou & Lindzen's mechanism does not work and only a non-wavelike dynamical response to Io's tidal perturbation would remain with a much reduced amplitude and $Q > 10^{10}$.

In contrast to Jupiter, the surface layers of short-period extrasolar planets may be stabilized against convection because they are intensely heated by their host stars and may attain a radiative state. If so, g-mode oscillations may be excited in the radiative layer just above its interface with the planet's convective envelope and dissipated through radiative or nonlinear damping (Lubow, Tout, & Livio 1997) as suggested for high-mass stars. However, the one-sided stellar irradiation of the surface of a synchronized planet induces a large-scale, shallow circulation (Burkert et al. 2003), which does not necessarily suppress convection and enhance the Brunt-Väisälä frequency over an extended region in the atmosphere. Thus the efficiency of dynamical tidal dissipation via g-mode oscillations remains an outstanding issue.

In their calculation Ioannou & Lindzen (1993a, 1993b) also considered the effects of uniform rotation. For the excitation of the dynamical response, they adopted the so-called 'traditional approximation' in which only the radial component of the angular velocity is included in the computation of the Coriolis force (Eckart 1960; Chapman & Lindzen 1970; Unno et al. 1989). This approach was justified in their model on the basis that the dynamical response occurs primarily near the atmosphere of Jupiter where the horizontal scale of the motion is large and the radial velocity perturbation is relatively small. It enabled them to separate the radial and angular variables in the governing linearized equations for the perturbations. The meridional structure of Jupiter's response due to Io's perturbation is then determined by Laplace's tidal equation, the solutions of which are Hough modes (Hough 1897, 1898) instead of spherical harmonics, while the radial structure is determined by a set of ordinary differential equations. Using a local (WKB) approximation, they obtained a dispersion relation describing a mixture of gravity, inertial, and acoustic oscillations. Although inertial waves can be excited in the nearly adiabatic planetary interior, Ioannou & Lindzen (1993b) did not consider them relevant for tidal dissipation. In fact the main effect of rotation in their model is that tidal forcing by a single solid harmonic projects on to many Hough modes, each with the potential to resonate. They noted that the traditional approximation of neglecting the latitudinal component of the angular velocity is, in fact, not appropriate in the planet's interior.

The effects of uniform rotation have been investigated in greater depth by Savonije, Papaloizou, & Alberts (1995) in the context of high-mass binary stars, which consist of extended radiative envelopes around small convective cores. These authors were the first to attempt a two-dimensional numerical solution of the linearized equations governing tidal disturbances, including the full Coriolis force. By 'switching off' terms deriving from the non-radial component of the angular velocity, they were able to verify that the traditional approximation can give a reasonably accurate measure of the tidal torque on a highly stratified, slowly rotating star. Like Ioannou & Lindzen (1993b), they found that the possibilities for resonant excitation of g modes are enhanced in a rotating star because the Coriolis force couples spherical harmonics of different degrees. Recently Savonije & Witte (2002) applied the traditional approximation to carry out a high-resolution study of the dynamical tidal interaction between a uniformly rotating solar-type star and an orbital companion including the effects of stellar evolution.

At the same time, Savonije et al. (1995) noted that the Coriolis force introduces a rich spectrum of inertial modes in a certain frequency range, which are not adequately represented by the traditional approximation. When the full Coriolis force is included, the response of the star to tidal forcing in the frequency range of the inertial modes contains large-amplitude, very short-wavelength components that could not be resolved on the grid. Using

an improved finite-difference numerical scheme including viscosity (Savonije & Papaloizou 1997) and an asymptotic perturbation analysis (Papaloizou & Savonije 1997), they later showed that inertial modes can be resonantly excited in the adiabatic convective cores of high-mass stars and can interact with the rotationally modified g modes and torsional r modes in the radiative envelopes. When these waves are dissipated through radiative damping, the efficiency of the tidal interaction is greatly enhanced.

1.4. Inertial waves

The study of inertial waves is said to have originated with Poincaré (see Greenspan 1968). Much attention has been devoted to the oscillations of an incompressible fluid contained in a rotating spherical, spheroidal, or cylindrical container. When the Ekman number is small, the Coriolis force provides the only significant restoring force, away from viscous boundary layers, and the resulting inertial waves have remarkable mathematical and physical properties. The low-frequency oscillations of an adiabatically stratified star or planet in uniform rotation are governed by a very similar problem (Papaloizou & Pringle 1981, 1982). In each case the inertial waves have frequencies (as observed in the rotating frame) no greater in magnitude than twice the angular velocity of the fluid, and have a rich spectrum that is dense or continuous in the absence of viscosity.

In the simplest problems, such as that of a full sphere of incompressible fluid, an apparently complete set of inviscid inertial wave solutions can be obtained analytically (Greenspan 1968; Zhang et al. 2001). However, the calculation of inertial waves in a spherical annulus, or in a star or planet with an arbitrary density stratification, requires two-dimensional numerical computations. Moreover, since the inviscid Poincaré equation is spatially hyperbolic in the relevant range of frequencies, the problem is ill-posed unless an explicit viscosity is included. Rieutord & Valdettaro (1997) calculated inertial waves in a spherical annulus, noting the behavior of the frequencies, damping rates, and eigenfunctions in the limit of small Ekman number. Their results were further elucidated by Rieutord, Georgeot, & Valdettaro (2001), who explained the important influence of the solid core. In particular, the viscous eigenfunctions are concentrated on characteristic rays of the Poincaré equation, which typically converge towards limit cycles as they reflect repeatedly from the inner and outer boundaries. A balance between the focusing of the wave energy along the converging rays and a lateral viscous diffusion sets the characteristic width of the eigenfunctions and determines the damping rates of the modes.

Dintrans & Ouyed (2001) used similar methods to calculate inertial waves in a slowly rotating polytrope at more modest Ekman numbers, with potential application to Jovian

seismology. They considered a pure inertial wave problem, eliminating acoustic and gravity waves by adopting the anelastic approximation and using a neutrally buoyant model. Indeed, in contrast to either high-mass or solar-type stars in close binaries, the entire envelope of a gaseous giant planet is likely to be convective except for a shallow atmospheric layer. In contrast to the assumption adopted by Ioannou & Lindzen (1993b), efficient heat transport by convection prevents the propagation or excitation of g-mode oscillations. Inertial modes, however, can propagate throughout the planetary envelope.

Jupiter's spin frequency is a significant fraction of its dynamical frequency and is more than twice the orbital frequencies of the Galilean satellites. Short-period extrasolar planets probably formed as rapid rotators similar to Jupiter and Saturn, although most of them may have already established a state of synchronous rotation. In each case the tidal forcing occurs in the frequency range of inertial waves, which will therefore constitute the natural and dominant response of the planet. Moreover, in this frequency range, the Coriolis coupling between the radial and angular motions is strong and the traditional approximation is inappropriate. Therefore two-dimensional computations are required.

1.5. Plan of the paper

In this paper, we revisit the issue of the excitation and dissipation of dynamical tides within gaseous giant planets. The response of the planet to low-frequency tidal forcing separates naturally into an equilibrium tide and a dynamical tide. In the convective regions of the planet the dynamical tide takes the form of inertial waves and we consider a turbulent viscosity associated with convective eddies to act on the tidal disturbance. If the planet has an outer radiative layer, outwardly propagating Hough waves are also excited and we consider them to be damped in the atmosphere. We therefore allow, in principle, for three avenues of tidal dissipation: viscous dissipation of the equilibrium tide, viscous dissipation of inertial waves, and emission of Hough waves. Our analysis permits the planet to rotate differentially, although we focus on the case of uniform rotation in our numerical calculations.

In Section 2, we briefly recapitulate the different components of the tidal potential that are responsible for evolution towards synchronization of the planet's spin and circularization of its orbit. In Section 3, we carry out an analysis of low-frequency oscillation modes in a rotating planet. We formulate the perturbation equations governing both the convective and radiative regions of the planet's interior and analyze the matching conditions between these regions. In Section 4, we consider the tidally forced disturbances, including the equilibrium tide, the dynamical response in both regions, and the matching across the interface. We construct, in Section 5, two numerical schemes to obtain global solutions of the forced

perturbation equations. In Section 6 we present and discuss numerical results appropriate for the internal structure of gaseous giant planets. In Section 7, we compare our results with those obtained in previous investigations. We summarize our findings and discuss their implications in Section 8.

2. COMPONENTS OF THE TIDAL POTENTIAL

We consider two bodies in a mutual Keplerian orbit, and adopt a non-rotating coordinate system with origin at the center of body 1. In our study body 1 will be a giant planet and body 2 its host star. Let $\boldsymbol{r}$ be the position vector of an arbitrary point P in body 1, and let $\boldsymbol{R}(t)$ be the position vector of the center of mass of body 2. When evaluating the tidal force acting within body 1 it is usually adequate to treat body 2 as a point mass, i.e., to neglect its rotational and tidal deformation. The potential of body 2 experienced at the point P, including the indirect potential resulting from the acceleration of the origin of the coordinate system, is then

$$-\frac{GM_2}{|\boldsymbol{R}-\boldsymbol{r}|}+\frac{GM_2}{R^3}(\boldsymbol{R}\cdot\boldsymbol{r})=-\frac{GM_2}{R}+\frac{GM_2}{2R^5}\left[R^2r^2-3(\boldsymbol{R}\cdot\boldsymbol{r})^2\right]+O(r^3). \tag{1}$$

The tidal potential is usually considered to be the non-trivial term of lowest order in r,

$$\Psi=\frac{GM_2}{2R^5}\left[R^2r^2-3(\boldsymbol{R}\cdot\boldsymbol{r})^2\right]. \tag{2}$$

Without loss of generality, let body 2 orbit in the xy-plane, so that its Cartesian coordinates are

$$\boldsymbol{R}=R(\cos\varphi,\sin\varphi,0), \tag{3}$$

while the Cartesian coordinates of the point P are

$$\boldsymbol{r}=r(\sin\theta\cos\phi,\sin\theta\sin\phi,\cos\theta), \tag{4}$$

where (r,θ,ϕ) are spherical polar coordinates. Then

$$\Psi=\frac{GM_2}{2R^3}r^2\left[1-3\sin^2\theta\cos^2(\phi-\varphi)\right]. \tag{5}$$

For a slightly eccentric orbit of semi-major axis a, eccentricity e, and mean motion n, and with a convenient choice for the longitude and time of pericenter passage, we have

$$R=a(1-e\cos nt)+O(e^2),\qquad \varphi=nt+2e\sin nt+O(e^2). \tag{6}$$

The tidal potential may then be expanded in powers of e as

$$\Psi = \Psi^{(0)} + \Psi^{(1)} + O(e^2), \tag{7}$$

where

$$\Psi^{(0)} = \frac{GM_2}{4a^3} r^2 \left\{2 - 3\sin^2\theta\,[1 + \cos(2\phi - 2nt)]\right\}, \tag{8}$$

$$\Psi^{(1)} = \frac{3GM_2}{8a^3} e r^2 \left\{4\cos nt + \sin^2\theta\,[\cos(2\phi - nt) - 7\cos(2\phi - 3nt) - 6\cos nt]\right\}. \tag{9}$$

Let

$$\tilde{P}_\ell^m(\cos\theta) = \left[\frac{(2\ell+1)(\ell-m)!}{2(\ell+m)!}\right]^{1/2} P_\ell^m(\cos\theta), \tag{10}$$

where $0 \le m \le \ell$, denote an associated Legendre polynomial normalized such that

$$\int_0^\pi \left[\tilde{P}_\ell^m(\cos\theta)\right]^2 \sin\theta\, d\theta = 1. \tag{11}$$

The tidal potential correct to $O(e)$ can then be expanded in a series of rigidly rotating solid harmonics of second degree,

$$\Psi^{(0)} + \Psi^{(1)} = \frac{GM_2}{a^3} \mathrm{Re} \sum_{j=1}^{5} A_j r^2 \tilde{P}_2^{m_j}(\cos\theta) e^{i(m_j\phi - \omega_j t)}, \tag{12}$$

where

$$\begin{aligned}
&m_1 = 0, \qquad \omega_1 = 0, \qquad A_1 = \left(\frac{1}{10}\right)^{1/2},\\
&m_2 = 2, \qquad \omega_2 = 2n, \qquad A_2 = -\left(\frac{3}{5}\right)^{1/2},\\
&m_3 = 0, \qquad \omega_3 = n, \qquad A_3 = 3e\left(\frac{1}{10}\right)^{1/2},\\
&m_4 = 2, \qquad \omega_4 = n, \qquad A_4 = e\left(\frac{3}{20}\right)^{1/2},\\
&m_5 = 2, \qquad \omega_5 = 3n, \qquad A_5 = -7e\left(\frac{3}{20}\right)^{1/2}.
\end{aligned} \tag{13}$$

Zahn (1977) gives an equivalent expansion carried to $O(e^2)$.

When body 1 is a differentially rotating planet with angular velocity $\Omega(r,\theta)$, the effective frequency of component j as experienced by the rotating fluid is the Doppler-shifted frequency $\hat{\omega}_j = \omega_j - m_j\Omega$. Component 1 can be neglected because it is independent of time

and causes only a hydrostatic distortion of the planet but no tidal dissipation. The effective forcing frequencies of the remaining four components are

$$\hat{\omega}_2 = 2(n - \Omega), \qquad \hat{\omega}_3 = n, \qquad \hat{\omega}_4 = n - 2\Omega, \qquad \hat{\omega}_5 = 3n - 2\Omega. \tag{14}$$

This prescription assumes that the rotation axis of the planet is perpendicular to its orbit. Otherwise an additional component of the tidal potential appears at first order in the obliquity, having $m_6 = 1$ and $\omega_6 = n$, and therefore $\hat{\omega}_6 = n - \Omega = \hat{\omega}_2/2$.

In the special case of a uniformly rotating planet, the forcing frequency of component j lies in the spectrum of inertial waves if $-2 \le \hat{\omega}_j/\Omega \le 2$. In this frequency range, the Coriolis coupling between the radial and angular motions is strong (Savonije et al. 1995). For any planet being spun down by tidal dissipation towards a synchronized state (i.e., $\Omega > n > 0$), all four effective forcing frequencies lie within the spectrum of inertial waves, as illustrated in Fig. 1. Once synchronism is achieved (i.e., $\Omega = n$), component 2 ceases to cause tidal dissipation but, if the orbit remains elliptical, the three eccentric components of the tidal potential continue to provide forcing at $\hat{\omega} = \pm\Omega$, clearly within the spectrum of inertial waves.

These considerations are directly relevant to the short-period extrasolar planets. All the known satellites of Jupiter and Saturn, except the very distant, retrograde ones, also provide low-frequency tidal forcing within the spectrum of inertial waves. We therefore suggest that the Coriolis force has a dominant influence on tidal interactions in many cases of interest. Except in work by Savonije and co-workers on tides in uniformly rotating stars (Savonije et al. 1995; Savonije & Papaloizou 1997; Papaloizou & Savonije 1997; Witte & Savonije 1999a, 1999b, 2001, 2002; Savonije & Witte 2002), the Coriolis force has been unjustifiably neglected owing to the mathematical, physical, and computational difficulties that it introduces.

3. LOW-FREQUENCY OSCILLATION MODES OF A ROTATING PLANET

3.1. Basic equations

We consider a planet that is predominantly gaseous, but may contain a solid core. We initially consider the fluid regions to be ideal, satisfying Euler's equation of motion,

$$\frac{D\boldsymbol{u}}{Dt} = -\frac{1}{\rho}\nabla p - \nabla\Phi, \tag{15}$$

the equation of mass conservation,

$$\frac{D\rho}{Dt} = -\rho\nabla\cdot\boldsymbol{u}, \tag{16}$$

and the adiabatic condition,

$$\frac{1}{\gamma}\frac{D\ln p}{Dt} - \frac{D\ln \rho}{Dt} = 0, \tag{17}$$

where $\boldsymbol{u}$ is the velocity, ρ the density, p the pressure, γ the adiabatic exponent, and

$$\frac{D}{Dt} = \frac{\partial}{\partial t} + \boldsymbol{u}\cdot\nabla \tag{18}$$

the Lagrangian time-derivative. The gravitational potential satisfies Poisson's equation,

$$\nabla^2\Phi = 4\pi G\rho. \tag{19}$$

When expressed in spherical polar coordinates (r,θ,ϕ), these equations take the form

$$\frac{Du_r}{Dt} - \frac{u_\theta^2}{r} - \frac{u_\phi^2}{r} = -\frac{1}{\rho}\frac{\partial p}{\partial r} - \frac{\partial\Phi}{\partial r}, \tag{20}$$

$$\frac{Du_\theta}{Dt} + \frac{u_r u_\theta}{r} - \frac{u_\phi^2\cos\theta}{r\sin\theta} = -\frac{1}{\rho r}\frac{\partial p}{\partial\theta} - \frac{1}{r}\frac{\partial\Phi}{\partial\theta}, \tag{21}$$

$$\frac{Du_\phi}{Dt} + \frac{u_r u_\phi}{r} + \frac{u_\theta u_\phi\cos\theta}{r\sin\theta} = -\frac{1}{\rho r\sin\theta}\frac{\partial p}{\partial\phi} - \frac{1}{r\sin\theta}\frac{\partial\Phi}{\partial\phi}, \tag{22}$$

$$\frac{D\rho}{Dt} = -\rho\left[\frac{1}{r^2}\frac{\partial}{\partial r}(r^2u_r) + \frac{1}{r\sin\theta}\frac{\partial}{\partial\theta}(u_\theta\sin\theta) + \frac{1}{r\sin\theta}\frac{\partial u_\phi}{\partial\phi}\right], \tag{23}$$

$$\frac{1}{\gamma}\frac{D\ln p}{Dt} - \frac{D\ln\rho}{Dt} = 0, \tag{24}$$

$$\frac{1}{r^2}\frac{\partial}{\partial r}\left(r^2\frac{\partial\Phi}{\partial r}\right) + \frac{1}{r^2\sin\theta}\frac{\partial}{\partial\theta}\left(\sin\theta\frac{\partial\Phi}{\partial\theta}\right) + \frac{1}{r^2\sin^2\theta}\frac{\partial^2\Phi}{\partial\phi^2} = 4\pi G\rho, \tag{25}$$

with

$$\frac{D}{Dt} = \frac{\partial}{\partial t} + u_r\frac{\partial}{\partial r} + \frac{u_\theta}{r}\frac{\partial}{\partial\theta} + \frac{u_\phi}{r\sin\theta}\frac{\partial}{\partial\phi}. \tag{26}$$

3.2. Basic state

The unperturbed state is a steady, axisymmetric planet which may rotate differentially in its fluid regions. We introduce the small parameter ϵ, being a characteristic value of the ratio of the spin frequency to the dynamical frequency $(GM_1/R_1^3)^{1/2}$ of the planet, which

has mass M_1 and radius R_1. Centrifugal distortions of the planet are of fractional order ϵ^2 and so we may pose the expansions

$$\begin{aligned} \rho &= \rho_0(r) + \epsilon^2 \rho_2(r,\theta) + O(\epsilon^4), \\ p &= p_0(r) + \epsilon^2 p_2(r,\theta) + O(\epsilon^4), \\ \Phi &= \Phi_0(r) + \epsilon^2 \Phi_2(r,\theta) + O(\epsilon^4). \end{aligned} \tag{27}$$

We neglect any meridional circulation and set $u_r = u_\theta = 0$. The angular velocity is

$$\frac{u_\phi}{r\sin\theta} = \Omega = \epsilon \Omega_{(1)}(r,\theta). \tag{28}$$

From equations (20) and (25) at order ϵ^0, we obtain the standard equations of structure for a spherical planet. We define the (inward) radial gravitational acceleration $g(r)$ and the Brunt–Väisälä frequency $N(r)$ in the usual way by

$$g = \frac{d\Phi_0}{dr}, \qquad N^2 = \frac{1}{\rho_0}\frac{dp_0}{dr}\left(\frac{d\ln\rho_0}{dr} - \frac{1}{\gamma}\frac{d\ln p_0}{dr}\right). \tag{29}$$

Equation (22) is satisfied identically. In practice the profile of differential rotation is determined by the meridional circulation and by viscous, turbulent, or magnetic stresses that do not feature in the equations as written above. We will not require a solution of the basic state at order ϵ^2 or higher.

Our analysis is based on asymptotic expansions in the small parameter ϵ^2. Jupiter is a relatively rapid rotator, having $\epsilon^2 \approx \Omega^2 R_1^3/GM_1 \approx 0.08$. This number increases to about 0.14 in the case of Saturn, but is greatly reduced, to about 0.0016, if Jupiter is spun down to a period of three days. This last case may be taken as representative of short-period extrasolar planets once they achieve synchronous rotation.

3.3. Linearized equations

We consider the linearized response to a tidal potential component of the form

$$\mathrm{Re}\left[\Psi(r,\theta)\, e^{i(m\phi-\omega t)}\right], \tag{30}$$

where $m \in \mathbf{Z}$ is the azimuthal wavenumber and $\omega \in \mathbf{R}$ the forcing frequency. As in Section 2, we adopt the convention that $m \geq 0$. The induced Eulerian velocity perturbation is

$$\mathrm{Re}\left[\boldsymbol{u}'(r,\theta)\, e^{i(m\phi-\omega t)}\right], \tag{31}$$

and similarly for other perturbed quantities. The linearized equations then take the form

$$-i\hat{\omega}u'_r - 2\Omega\sin\theta\, u'_\phi = -\frac{\partial W}{\partial r} + \frac{1}{\rho^2}\left(\rho'\frac{\partial p}{\partial r} - p'\frac{\partial \rho}{\partial r}\right), \tag{32}$$

$$-i\hat{\omega}u'_\theta - 2\Omega\cos\theta\, u'_\phi = -\frac{1}{r}\frac{\partial W}{\partial \theta} + \frac{1}{\rho^2 r}\left(\rho'\frac{\partial p}{\partial \theta} - p'\frac{\partial \rho}{\partial \theta}\right), \tag{33}$$

$$-i\hat{\omega}u'_\phi + \frac{1}{r\sin\theta}\left(u'_r\frac{\partial}{\partial r} + \frac{u'_\theta}{r}\frac{\partial}{\partial \theta}\right)(\Omega r^2\sin^2\theta) = -\frac{imW}{r\sin\theta}, \tag{34}$$

$$-i\hat{\omega}\rho' + u'_r\frac{\partial \rho}{\partial r} + \frac{u'_\theta}{r}\frac{\partial \rho}{\partial \theta} = -\rho\left[\frac{1}{r^2}\frac{\partial}{\partial r}(r^2u'_r) + \frac{1}{r\sin\theta}\frac{\partial}{\partial \theta}(u'_\theta\sin\theta) + \frac{imu'_\phi}{r\sin\theta}\right], \tag{35}$$

$$-i\hat{\omega}\left(\frac{p'}{\gamma p} - \frac{\rho'}{\rho}\right) + u'_r\left(\frac{1}{\gamma}\frac{\partial \ln p}{\partial r} - \frac{\partial \ln \rho}{\partial r}\right) + \frac{u'_\theta}{r}\left(\frac{1}{\gamma}\frac{\partial \ln p}{\partial \theta} - \frac{\partial \ln \rho}{\partial \theta}\right) = 0, \tag{36}$$

$$\frac{1}{r^2}\frac{\partial}{\partial r}\left(r^2\frac{\partial \Phi'}{\partial r}\right) + \frac{1}{r^2\sin\theta}\frac{\partial}{\partial \theta}\left(\sin\theta\frac{\partial \Phi'}{\partial \theta}\right) - \frac{m^2\Phi'}{r^2\sin^2\theta} = 4\pi G\rho', \tag{37}$$

where

$$\hat{\omega} = \omega - m\Omega \tag{38}$$

is the Doppler-shifted forcing frequency, and

$$W = \frac{p'}{\rho} + \Phi' + \Psi \tag{39}$$

is a modified pressure perturbation. In adiabatically stratified regions, where $\nabla \ln p = \gamma\nabla\ln\rho$, the Eulerian perturbations of pressure and density are related by $p'/p = \gamma\rho'/\rho$, and the terms in parentheses in equations (32) and (33) cancel.

3.4. Free modes of oscillation

We first consider the free modes of oscillation of the planet, neglecting the tidal forcing. We treat the convective regions of the planet as being adiabatically stratified ($\nabla \ln p = \gamma\nabla\ln\rho$), and the radiative regions as being stably stratified such that the Brunt–Väisälä frequency is comparable to the dynamical frequency. Where a radiative region adjoins a convective region, however, there is a transition region in which the Brunt–Väisälä frequency goes to zero. We obtain asymptotic solutions for low-frequency oscillations in each region separately and then match them together. For clarity, we use accented symbols, e.g., $\check{a}$, $\hat{a}$, and $\bar{a}$, to distinguish solution components in convective, radiative, and transition regions, respectively.

As explained in Section 2, we are interested in oscillation frequencies of order ϵ, comparable to the angular velocity of the planet but small compared to the dynamical frequency. Accordingly, we set $\omega = \epsilon\omega_{(1)}$. To achieve such a low frequency in the presence of potentially large restoring forces, the perturbations are highly constrained. They should be almost incompressible (or, more correctly, anelastic) in order to avoid a large acoustic restoring force. In radiative regions the perturbations should also involve predominantly horizontal motions in order to avoid a large buoyant restoring force. In fact, the relevant low-frequency modes are *inertial waves* in convective regions and what we call *generalized Hough waves* in radiative regions. In the solid core, if present, the rigidity is such that no low-frequency modes are permissible.

3.5. Convective regions

In convective regions we seek solutions of the unforced linearized equations of the form

$$\begin{aligned} u'_r &\sim \epsilon\check{u}'_r(r,\theta), \\ u'_\theta &\sim \epsilon\check{u}'_\theta(r,\theta), \\ u'_\phi &\sim \epsilon\check{u}'_\phi(r,\theta), \\ \rho' &\sim \epsilon^2\check{\rho}'(r,\theta), \\ p' &\sim \epsilon^2\check{p}'(r,\theta), \\ \Phi' &\sim \epsilon^2\check{\Phi}'(r,\theta). \end{aligned} \tag{40}$$

The overall amplitude of the perturbations is arbitrary, but the scaling adopted here is relevant to the tidally forced problem considered in Section 4 below. The relative scalings of the perturbations are chosen to satisfy the linearized equations of Section 3.3, which reduce at leading order to

$$-i\hat{\omega}_{(1)}\check{u}'_r - 2\Omega_{(1)}\sin\theta\,\check{u}'_\phi = -\frac{\partial\check{W}}{\partial r}, \tag{41}$$

$$-i\hat{\omega}_{(1)}\check{u}'_\theta - 2\Omega_{(1)}\cos\theta\,\check{u}'_\phi = -\frac{1}{r}\frac{\partial\check{W}}{\partial\theta}, \tag{42}$$

$$-i\hat{\omega}_{(1)}\check{u}'_\phi + \frac{1}{r\sin\theta}\left(\check{u}'_r\frac{\partial}{\partial r} + \frac{\check{u}'_\theta}{r}\frac{\partial}{\partial\theta}\right)(\Omega_{(1)}r^2\sin^2\theta) = -\frac{im\check{W}}{r\sin\theta}, \tag{43}$$

$$\frac{1}{r^2\rho_0}\frac{\partial}{\partial r}(r^2\rho_0\check{u}'_r) + \frac{1}{r\sin\theta}\frac{\partial}{\partial\theta}(\check{u}'_\theta\sin\theta) + \frac{im\check{u}'_\phi}{r\sin\theta} = 0, \tag{44}$$

$$\frac{\check{p}'}{p_0} = \frac{\gamma\check{\rho}'}{\rho_0}, \tag{45}$$

$$\frac{1}{r^2}\frac{\partial}{\partial r}\left(r^2\frac{\partial\check{\Phi}'}{\partial r}\right)+\frac{1}{r^2\sin\theta}\frac{\partial}{\partial\theta}\left(\sin\theta\frac{\partial\check{\Phi}'}{\partial\theta}\right)-\frac{m^2\check{\Phi}'}{r^2\sin^2\theta}=4\pi G\check{\rho}', \tag{46}$$

with

$$\hat{\omega}_{(1)}=\omega_{(1)}-m\Omega_{(1)}, \tag{47}$$

and

$$\check{W}=\frac{\check{p}'}{\rho_0}+\check{\Phi}'. \tag{48}$$

Equations (41)–(44) are decoupled from those that follow, and, when combined with appropriate boundary conditions, define the inertial wave problem. We note that equation (44) is equivalent to the constraint $\nabla\cdot(\rho_0\boldsymbol{u}')=0$ of the anelastic approximation (Ogura & Phillips 1962), which eliminates acoustic waves from the problem. Self-gravitation also plays no role for inertial waves, because $\check{\Phi}'$ simply combines with $\check{p}'$ in the combination $\check{W}$.

3.6. Radiative regions

In radiative regions of the planet, the oscillation frequency is small compared to the Brunt–Väisälä frequency, implying that the motions should be predominantly horizontal in addition to being anelastic. These constraints are satisfied when the radial wavelength is short compared to the radius of the planet, and the perturbations then have a WKB form in the radial direction. Accordingly, we seek solutions of the unforced linearized equations of the form

$$\begin{aligned}
u_r' &\sim \epsilon^2\hat{u}_r'(r,\theta)E(r),\\
u_\theta' &\sim \epsilon\hat{u}_\theta'(r,\theta)E(r),\\
u_\phi' &\sim \epsilon\hat{u}_\phi'(r,\theta)E(r),\\
\rho' &\sim \epsilon\hat{\rho}'(r,\theta)E(r),\\
p' &\sim \epsilon^2\hat{p}'(r,\theta)E(r),\\
\Phi' &\sim \epsilon^2\check{\Phi}'(r,\theta)+\epsilon^3\hat{\Phi}'(r,\theta)E(r),
\end{aligned} \tag{49}$$

with

$$E(r)=\epsilon^s\exp\left[\frac{i}{\epsilon}\int k(r)\,dr\right]. \tag{50}$$

The exponent $s<0$ remains arbitrary until the solutions in adjacent convective and radiative regions can be connected. We show in Section 3.7 below that this procedure yields $s=-1/6$. Note that the term $\epsilon^2\check{\Phi}'(r,\theta)$, which does not have a WKB form, is the smooth continuation of the gravitational potential perturbation associated with the inertial waves in convective regions.

The linearized equations of Section 3.3 then reduce at leading order to

$$0 = -ik\hat{W} - \frac{g\hat{\rho}'}{\rho_0}, \tag{51}$$

$$-i\hat{\omega}_{(1)}\hat{u}'_\theta - 2\Omega_{(1)}\cos\theta\,\hat{u}'_\phi = -\frac{1}{r}\frac{\partial\hat{W}}{\partial\theta}, \tag{52}$$

$$-i\hat{\omega}_{(1)}\hat{u}'_\phi + \frac{\hat{u}'_\theta}{\sin\theta}\frac{\partial}{\partial\theta}(\Omega_{(1)}\sin^2\theta) = -\frac{im\hat{W}}{r\sin\theta}, \tag{53}$$

$$ik\hat{u}'_r + \frac{1}{r\sin\theta}\frac{\partial}{\partial\theta}(\hat{u}'_\theta\sin\theta) + \frac{im\hat{u}'_\phi}{r\sin\theta} = 0, \tag{54}$$

$$i\hat{\omega}_{(1)}\frac{\hat{\rho}'}{\rho_0} + \frac{N^2}{g}\hat{u}'_r = 0, \tag{55}$$

$$-k^2\hat{\Phi}' = 4\pi G\hat{\rho}', \tag{56}$$

with

$$\hat{\omega}_{(1)} = \omega_{(1)} - m\Omega_{(1)}, \tag{57}$$

and

$$\hat{W} = \frac{\hat{p}'}{\rho_0}. \tag{58}$$

Since $\hat{\Phi}'$ appears only in Poisson's equation, self-gravitation is irrelevant for waves of such short radial wavelength. The remaining equations may be combined into the form

$$\mathcal{L}\hat{W} = \frac{k^2r^2}{N^2}\hat{W}, \tag{59}$$

where $\mathcal{L}$ is a linear operator defined by

$$\mathcal{L}w = -\frac{1}{\sin\theta}\left(\frac{\partial}{\partial\theta} + \frac{2m\Omega_{(1)}\cos\theta}{\hat{\omega}_{(1)}\sin\theta}\right)\left[\frac{\sin\theta}{D}\left(\frac{\partial}{\partial\theta} - \frac{2m\Omega_{(1)}\cos\theta}{\hat{\omega}_{(1)}\sin\theta}\right)w\right] + \frac{m^2w}{\hat{\omega}^2_{(1)}\sin^2\theta}, \tag{60}$$

with

$$D = \hat{\omega}^2_{(1)} - 4\Omega^2_{(1)}\cos^2\theta - 2\Omega_{(1)}\frac{\partial\Omega_{(1)}}{\partial\theta}\cos\theta\sin\theta. \tag{61}$$

Let $\{\lambda_i\}$ and $\{w_i(\theta)\}$ be the eigenvalues and eigenfunctions of $\mathcal{L}$, satisfying

$$\mathcal{L}w_i = \lambda_i w_i. \tag{62}$$

If the angular velocity $\Omega_{(1)}$ is independent of r, the eigensolutions will be also. For a general pattern of differential rotation, however, the eigensolutions depend parametrically on r. In

either case, each eigensolution with $\lambda > 0$ corresponds to a freely propagating wave solution (which can be considered a rotationally modified g mode) satisfying the dispersion relation

$$\lambda_i = \frac{k^2 r^2}{N^2}. \tag{63}$$

For a given wave frequency ω and azimuthal wavenumber m, this relation determines the radial wavenumber k at each r. Evanescent eigensolutions with $\lambda < 0$ are also possible in a rotating planet.

As given above, the solution represents a traveling wave with phase velocity $\epsilon^2\omega_{(1)}/k$. A standing wave is formed from a superposition of two such solutions with opposite choices of the sign of k. Depending on how the wave is excited, and on whether it is allowed to reflect from the boundaries of the radiative region, the relevant solution may be a traveling wave, a standing wave or, in the case of partial reflection, an intermediate solution. In the case of a traveling wave the sign of k should be chosen with due regard to the direction of the radial group velocity.

In the absence of dissipation, the waves carry conserved fluxes of energy and angular momentum, owing to the invariance of the basic state with respect to t and ϕ. These conservation relations can be derived from the theory of 'wave action' using a Lagrangian formulation of ideal fluid dynamics (e.g., Hayes 1970). For a traveling wave, the average flux of energy wave action through a spherical surface can be shown to be

$$F = \pi \int_0^\pi \mathrm{Re}\left[\left(\frac{\omega}{\hat{\omega}}\right) p'^* u_r'\right] r^2 \sin\theta \, d\theta \tag{64}$$

$$\sim -\epsilon^{4+2s} \left(\frac{\pi \rho_0 r^2 \omega_{(1)}}{N^2}\right) \mathrm{Re}\,[k] \int_0^\pi |\hat{W}|^2 \sin\theta \, d\theta, \tag{65}$$

and the flux of angular momentum wave action differs only by a factor $m/\omega_{(1)}$. Outwardly propagating waves, having positive radial group velocity, are those with $\mathrm{sgn}(\hat{\omega}_{(1)}/k) < 0$. This property occurs because the frequency of g modes decreases with increasing radial wavenumber. In the absence of dissipation the flux F should be independent of radius.

We note some properties of the operator $\mathcal{L}$. Singular points of the equation $\mathcal{L}w = \lambda w$ occur at the poles and wherever $\hat{\omega}_{(1)} = 0$ ('corotation resonance') or $D = 0$ ('Lindblad resonance'), although the latter is only an apparent singularity. Close to the north pole, two independent solutions are $w \sim \theta^m$ and $w \sim \theta^{-m}$ (or $w \sim 1$ and $w \sim \ln\theta$ in the case $m = 0$). The condition that w be bounded selects the regular solution. This, and a similar condition at the south pole, provide the two boundary conditions for the eigenvalue problem.

In a differentially rotating planet, a corotation resonance can occur, in principle, on any surface of constant angular velocity. As noted by Goldreich & Nicholson (1989), this feature

is expected to present an absorbing barrier to propagating waves. In this paper we disregard the possibility of corotation resonances, but their influence merits further investigation, which we defer to future work.

The operator $\mathcal{L}$ is self-adjoint in the sense that

$$\int_0^\pi u^*(\mathcal{L}v)\sin\theta\,d\theta = \left[\int_0^\pi v^*(\mathcal{L}u)\sin\theta\,d\theta\right]^* \tag{66}$$

for any two functions $u(\theta)$ and $v(\theta)$ satisfying the regularity conditions at the poles. The eigenvalues λ are therefore real and the eigenfunctions corresponding to distinct eigenvalues are orthogonal in the sense that

$$\int_0^\pi w_i^* w_j \sin\theta\,d\theta = 0, \qquad i \neq j. \tag{67}$$

Furthermore, if $w(\theta)$ is a function satisfying the regularity conditions,

$$\int_0^\pi w^*(\mathcal{L}w)\sin\theta\,d\theta = \int_0^\pi \left[\frac{1}{D}\left|\left(\frac{\partial}{\partial\theta} - \frac{2m\Omega_{(1)}\cos\theta}{\hat{\omega}_{(1)}\sin\theta}\right)w\right|^2 + \frac{m^2|w|^2}{\hat{\omega}_{(1)}^2\sin^2\theta}\right]\sin\theta\,d\theta. \tag{68}$$

This equation shows that the eigenvalues of $\mathcal{L}$ are all positive when $D > 0$ throughout $0 < \theta < \pi$. If D changes sign in $0 < \theta < \pi$, there will be sequences of positive and negative eigenvalues.

Later, we will need to know under what conditions the operator $\mathcal{L}$ can be inverted. Provided that the eigenfunctions form a complete set within the relevant function space, the inversion is possible unless $\mathcal{L}$ has a null eigenvalue $\lambda = 0$, in which case the inversion can be performed only within the subspace of functions orthogonal to the null eigenfunction. In the case $m = 0$, the only possible null eigenfunction is $w_0 =$ constant, which exists for all values of $\omega_{(1)}$. In the case $m \neq 0$, this solution does not occur, but there may nevertheless be null eigensolutions for isolated values of $\omega_{(1)}$.

In the case of a non-rotating planet, $\mathcal{L}$ reduces to a multiple of the horizontal Laplacian operator and the eigensolutions are

$$\lambda_i = \frac{n(n+1)}{\omega_{(1)}^2}, \qquad w_i(\theta) = \tilde{P}_n^m(\cos\theta), \qquad n = m + i, \qquad i \geq 0. \tag{69}$$

In the case of a uniformly rotating planet, or one in which the angular velocity is independent of θ, $\mathcal{L}$ reduces to Laplace's tidal operator and the eigenfunctions are the Hough functions (e.g., Chapman & Lindzen 1970). We note that, in the case $m = 0$, Laplace's tidal operator has null eigenfunctions when $\hat{\omega}_{(1)} = -2m\Omega_{(1)}/n(n+1)$ for integers $n \geq m$. These solutions

are known variously as planetary waves, Rossby waves, r modes, or toroidal modes, and correspond to global modes (hence $k \to 0$) of a uniformly rotating radiative region (e.g., Papaloizou & Pringle 1978).

For a general pattern of differential rotation in which Ω depends on θ, we call the eigensolutions 'generalized Hough modes'. The general solution in radiative regions involves a linear combination of generalized Hough waves.

3.7. Matching between convective and radiative regions

In planets and stars, convective and radiative regions can be disposed in a variety of configurations, and planets may also contain solid cores. We consider in detail the case in which a single radiative envelope exists exterior to a single convective region, possibly containing a solid core. This is relevant to short-period extrasolar planets and also to high-mass stars, although in the former case the radiative envelope is shallow. The same principles can be used to construct solutions for alternative arrangements of convective and radiative regions.

Near the boundary $r = r_{\rm b}$ between convective and radiative regions, we assume that N^2 is zero on the convective side and rises linearly from zero on the radiative side, so that

$$\mathcal{D} = \left. \frac{dN^2}{dr} \right|_{r=r_{\rm b}+} > 0. \tag{70}$$

As $r \to r_{\rm b}$ from above, the wavelengths of all the generalized Hough modes tend to infinity because $k \propto N$, and the approximations adopted in Section 3.6 break down. The situation is related to the problem of Lindblad resonances in differentially rotating discs (e.g., Goldreich & Tremaine 1978; Lin & Papaloizou 1979a; Lubow & Ogilvie 1998). By analogy with that problem, the characteristic radial extent of the transition region can be identified as being of order $\epsilon^{2/3}$. We therefore write

$$r = r_{\rm b} + \epsilon^{2/3} x, \tag{71}$$

where x is an inner variable, of order unity within the transition region. We then have

$$N^2 = \epsilon^{2/3} \mathcal{D} x + O(\epsilon^{4/3}). \tag{72}$$

We pose the following expansions for the perturbations within the transition region:

$$\begin{aligned} u_r' &\sim \epsilon^{5/3} \bar{u}_r'(x,\theta), \\ u_\theta' &\sim \epsilon \bar{u}_\theta'(x,\theta), \end{aligned}$$

$$\begin{aligned} u'_\phi &\sim \epsilon \bar{u}'_\phi(x,\theta), \\ \rho' &\sim \epsilon^{4/3}\bar{\rho}'(x,\theta), \\ p' &\sim \epsilon^2 \bar{p}'(x,\theta), \\ \Phi' &\sim \epsilon^2 \check{\Phi}'(r_\mathrm{b},\theta) + \epsilon^{8/3}\bar{\Phi}'(x,\theta). \end{aligned} \tag{73}$$

Note again that the term $\epsilon^2\check{\Phi}'(r_\mathrm{b},\theta)$ is the smooth gravitational potential perturbation associated with the inertial waves in convective regions, evaluated at the boundary.

The linearized equations of Section 3.3 then reduce to

$$0 = -\frac{\partial \bar{W}}{\partial x} - \frac{g\bar{\rho}'}{\rho_0}, \tag{74}$$

$$-i\hat{\omega}_{(1)}\bar{u}'_\theta - 2\Omega_{(1)}\cos\theta\,\bar{u}'_\phi = -\frac{1}{r}\frac{\partial \bar{W}}{\partial \theta}, \tag{75}$$

$$-i\hat{\omega}_{(1)}\bar{u}'_\phi + \frac{\bar{u}'_\theta}{\sin\theta}\frac{\partial}{\partial\theta}(\Omega_{(1)}\sin^2\theta) = -\frac{im\bar{W}}{r\sin\theta}, \tag{76}$$

$$\frac{\partial \bar{u}'_r}{\partial x} + \frac{1}{r\sin\theta}\frac{\partial}{\partial\theta}(\bar{u}'_\theta\sin\theta) + \frac{im\bar{u}'_\phi}{r\sin\theta} = 0, \tag{77}$$

$$i\hat{\omega}_{(1)}\frac{\bar{\rho}'}{\rho_0} + \frac{\mathcal{D}x}{g}\bar{u}'_r = 0, \tag{78}$$

$$\frac{\partial^2\bar{\Phi}'}{\partial x^2} = 4\pi G\bar{\rho}', \tag{79}$$

with

$$\bar{W} = \frac{\bar{p}'}{\rho_0} + \check{\Phi}'. \tag{80}$$

In these equations all coefficients are to be considered independent of x, except where it appears explicitly, and are to be evaluated at $r = r_\mathrm{b}$. Elimination of perturbations in favor of $\bar{W}$ now yields

$$\mathcal{L}\bar{W} + \frac{r^2}{\mathcal{D}}\frac{\partial}{\partial x}\left(\frac{1}{x}\frac{\partial \bar{W}}{\partial x}\right) = 0, \tag{81}$$

where, again, all coefficients are to be evaluated at $r = r_\mathrm{b}$. This is the equivalent of equation (59) in the transition region.

Equation (81) can be solved by separation of variables. Let κ_i be the real solution of

$$\kappa_i^3 = -\frac{\mathcal{D}\lambda_i}{r^2}. \tag{82}$$

Then the general solution of equation (81), regular at the poles, is

$$\bar{W} = \sum_i \bar{W}^{(i)} = \sum_i a_i\left[\mathrm{Ai}'(\kappa_i x) + s_i i\,\mathrm{Bi}'(\kappa_i x)\right] w_i(\theta), \tag{83}$$

where $\{a_i\}$ and $\{s_i\}$ are arbitrary coefficients, and Ai' and Bi' denote the derivatives of the Airy functions of the first and second kinds. This solution must be matched to that in the radiative region at $x \gg 1$, and to the solution in the convective region at $x = 0$.

For generalized Hough modes with $\lambda > 0$, κ is negative and the wave propagates in the radiative region $x > 0$. If the boundary condition at the outer surface of the radiative region is such that the waves are not reflected, the relevant solution is a traveling wave with outwardly directed group velocity. This is achieved by setting either $s_i = \pm 1$, because the asymptotic form of the Airy functions is such that, for $\kappa < 0$,

$$\mathrm{Ai}'(\kappa x) \pm i\,\mathrm{Bi}'(\kappa x) \sim -\pi^{-1/2}(-\kappa x)^{1/4} \exp\left\{\mp i\left[\frac{2}{3}(-\kappa x)^{3/2} + \frac{\pi}{4}\right]\right\} \tag{84}$$

as $x \to \infty$. This matches on to the WKB form of the solution in the radiative region, because the wavenumber can be identified as

$$\mp\epsilon^{-2/3}\frac{d}{dx}\left[\frac{2}{3}(-\kappa x)^{3/2} + \frac{\pi}{4}\right] \sim \mp\epsilon^{-1}\frac{\lambda^{1/2}N}{r}, \tag{85}$$

in agreement with the WKB wavenumber $\epsilon^{-1}k$ given by equation (63). In fact the relevant solution has $s_i = \mathrm{sgn}(\hat{\omega}_{(1)})$.

For modes with $\lambda < 0$, κ is positive and the wave is evanescent in the radiative region. The relevant solution is then $s_i = 0$, because $\mathrm{Ai}'(\kappa x)$ decays exponentially as $\kappa x \to \infty$, while $\mathrm{Bi}'(\kappa x)$ grows exponentially.

To match the solution in the transition region to that in the convective region at $x = 0$, we first compare the ordering schemes (40) and (73), and find that u_r' and ρ' are formally mismatched in order. Now equation (78) implies that $\bar{\rho}' \to 0$ as $x \to 0$, which resolves the mismatch in ρ'. The matching of u_r' implies that the effective boundary condition for inertial waves in the convective region is that

$$\check{u}_r'(r_\mathrm{b}, \theta) = 0. \tag{86}$$

Matching of the other variables is achieved by requiring that W be continuous at $r = r_\mathrm{b}$, i.e.,

$$\check{W}(r_\mathrm{b}, \theta) = \bar{W}(0, \theta). \tag{87}$$

Note that, if W is continuous across the spherical boundary, u_θ' and u_ϕ' are also continuous because they are related to one another only by horizontal derivatives, and in exactly the same way on each side of the boundary. The matching condition

$$\check{W}(r_\mathrm{b}, \theta) = \sum_i a_i \left[\mathrm{Ai}'(0) + s_i i\,\mathrm{Bi}'(0)\right] w_i(\theta) \tag{88}$$

determines the amplitude coefficients according to the orthogonal projection

$$a_i = \frac{\int_0^\pi w_i^* \check{W}(r_{\rm b},\theta)\,\sin\theta\,d\theta}{[{\rm Ai}'(0) + s_i i\,{\rm Bi}'(0)]\int_0^\pi |w_i|^2\,\sin\theta\,d\theta}. \tag{89}$$

The physical interpretation of the matching conditions is that the transition region appears as a rigid boundary for inertial waves in the convective region because the steeply rising entropy gradient suppresses radial motions. The generalized Hough waves in the transition and radiative regions are excited by the modified pressure perturbation W acting at the boundary $r = r_{\rm b}$.

The outward energy flux in generalized Hough waves is found by evaluating equation (65) in the transition region at large x, with the result

$$\begin{aligned} F &= \epsilon^{11/3}\rho_0\omega_{(1)}\,{\rm sgn}(\hat{\omega}_{(1)})\left(\frac{r^2}{\mathcal{D}}\right)^{1/3}\sum_i \lambda_i^{2/3}|a_i|^2\int_0^\pi |w_i|^2\,\sin\theta\,d\theta \\ &= \epsilon^{11/3}\frac{3^{2/3}}{4}\left[\Gamma\left(\frac{1}{3}\right)\right]^2\rho_0\omega_{(1)}\,{\rm sgn}(\hat{\omega}_{(1)})\left(\frac{r^2}{\mathcal{D}}\right)^{1/3}\sum_i \lambda_i^{2/3}\frac{\left|\int_0^\pi w_i^*\check{W}(r_{\rm b},\theta)\,\sin\theta\,d\theta\right|^2}{\int_0^\pi |w_i|^2\,\sin\theta\,d\theta} \end{aligned} \tag{90}$$

where the sum includes only those modes for which $\lambda > 0$, and all quantities are to be evaluated at $r = r_{\rm b}$. Comparison with equation (65) indicates that $s = -1/6$, as anticipated above. A more detailed matching between the transition region and the radiative region is not necessary for our purposes, but the constancy of the energy flux could be used to determine how the amplitudes of the Hough modes vary with radius throughout the radiative region.

It is likely that the waves will become nonlinear and be damped in the outer layers of the planet. In this case the emission of generalized Hough waves at the boundary between convective and radiative regions provides a dissipation mechanism for the inertial waves. The rate of energy loss in Hough modes is formally of order $\epsilon^{11/3}$, while the energy content of the inertial modes is of order ϵ^2. This route of dissipation must be compared with viscous or turbulent damping of the inertial waves in the convective region itself.

3.8. Viscosity and inertial waves

The procedure suggested by the foregoing analysis is to solve the inertial wave problem defined by equations (41)–(44) in the convective region, using the rigid boundary condition (86) at the outer surface. If the planet has a solid core, a rigid boundary condition is also appropriate there. In the absence of a core, regularity conditions apply at $r = 0$. The

amplitudes of the generalized Hough modes in the radiative region can then be computed from equation (89).

In a uniformly rotating planet, equations (41)–(44) admit a dense or continuous spectrum of inertial wave solutions (e.g., Papaloizou & Pringle 1982) occupying the frequency interval $-2|\Omega_{(1)}| \leq \hat{\omega}_{(1)} \leq 2|\Omega_{(1)}|$. In a differentially rotating planet, a similar phenomenon occurs, although the extent of the spectrum is slightly different (e.g., Lin, Papaloizou, & Kley 1993). This property is associated with the fact that the system of equations is spatially hyperbolic, rather than elliptic, for wave frequencies within the dense or continuous spectrum. For such frequencies, the mathematical problem requires the imposition of Cauchy boundary conditions on an open surface, while physical considerations lead to rigid (non-Cauchy) boundary conditions on a closed surface. The inertial wave problem is therefore mathematically ill-posed in the absence of viscosity.

When studying the tidally forced problem, we are interested in calculating the rate of dissipation of energy, or, equivalently, the tidal torque exerted on the planet. For effective forcing frequencies within the range of the dense or continuous spectrum of inertial waves, the possibility exists of resonantly exciting an infinite number of modes. We therefore introduce a small kinematic viscosity ν in convective regions, partly to regularize the problem and partly in an effort to model the effects of turbulent convection on the wave motion. In the presence of viscosity, the inertial wave problem is mathematically well posed and the spectrum is discrete. As the viscosity tends to zero the spectrum becomes increasingly dense (e.g., Dintrans & Ouyed 2001) and the probability of resonant excitation of wave modes increases. It is therefore possible to envisage a situation in which the dissipation rate would not vanish linearly with ν as $\nu \rightarrow 0$. Indeed, it might even be independent of ν as $\nu \rightarrow 0$, as occurs in hydrodynamic turbulence.

In the presence of viscosity it is necessary to introduce additional boundary conditions for the inertial wave problem. If the viscosity is restricted to the convective region $r < r_{\rm b}$, then continuity of the velocity and of the stress requires that the $r\theta$- and $r\phi$-components of the viscous stress tensor vanish at $r = r_{\rm b}$. The boundary conditions at $r = r_{\rm b}$ are therefore

$$\breve{u}'_r = \frac{\partial}{\partial r}\left(\frac{\breve{u}'_\theta}{r}\right) = \frac{\partial}{\partial r}\left(\frac{\breve{u}'_\phi}{r}\right) = 0. \tag{91}$$

If the planet has a solid core of radius $r_{\rm c}$, the no-slip boundary conditions

$$\breve{u}'_r = \breve{u}'_\theta = \breve{u}'_\phi = 0 \tag{92}$$

are appropriate at $r = r_{\rm c}$.

4. TIDALLY FORCED OSCILLATIONS

4.1. The equilibrium tide

The response of a body to tidal forcing is traditionally calculated using the theory of the *equilibrium tide*, in which an initially spherical body adjusts hydrostatically to the varying tidal potential (e.g., Darwin 1880). This approach is usually justified on the basis that the tidal forcing frequency is much less than the dynamical frequency of the body. By introducing an arbitrary phase lag into the response, usually parametrized by the quality factor Q, the theory allows for a tidal torque to be exerted and energy to be dissipated. The efficiency of known tidal interactions in the solar system places constraints on the Q-values of the bodies involved (Goldreich & Soter 1966).

Such a theory may offer a reasonable description of the tidal response of solid bodies, in which the dissipation factor $1/Q$ reflects the imperfect elasticity of the medium. However, it is quite inappropriate for fluid bodies, in which the dissipation is of a different nature and, moreover, a wavelike response, the *dynamical tide*, occurs at low forcing frequencies (Cowling 1941; Zahn 1966). Although, in principle, tidal dissipation in a fluid body can still be parametrized by Q, the required Q-value will depend on the tidal forcing frequency and on the properties of the body in such a complicated way that the parametrization is of questionable value.

In modern studies, the response of a fluid body to tidal forcing is conveniently separated into the equilibrium tide, which represents a large-scale, quasi-hydrostatic distortion of the body (without introducing a phase lag), and the dynamical tide, which usually constitutes a relatively small, mostly wavelike correction that is critically important because of its contribution to the dissipation rate. The equilibrium tide associated with a tidal potential Ψ is a Lagrangian displacement field $\boldsymbol{\xi}$ having the properties (e.g., Goldreich & Nicholson 1989)

$$\xi_r = -\frac{(\Phi'_{(e)} + \Psi)}{g}, \qquad \nabla \cdot \boldsymbol{\xi} = 0. \tag{93}$$

The Eulerian perturbations associated with the equilibrium tide are

$$\boldsymbol{u}'_{(e)} = \epsilon \left[-i\hat{\omega}_{(1)} \boldsymbol{\xi} - r \sin\theta (\boldsymbol{\xi} \cdot \nabla \Omega_{(1)}) \boldsymbol{e}_\phi \right], \tag{94}$$

$$\rho'_{(e)} = -\xi_r \frac{d\rho_0}{dr}, \qquad p'_{(e)} = -\xi_r \frac{dp_0}{dr}, \tag{95}$$

where $\Phi'_{(e)}$ and $\rho'_{(e)}$ are related by

$$\nabla^2 \Phi'_{(e)} = 4\pi G \rho'_{(e)}. \tag{96}$$

Note that $\nabla \cdot \boldsymbol{\xi} = 0$ implies $\nabla \cdot \boldsymbol{u}'_{(e)} = 0$, each implying that the equilibrium tide is incompressible.[3]

We consider a single component of the tidal potential in the form of a spherical harmonic of degree $\ell \geq m$,

$$\Psi = \tilde{\Psi}(r)\tilde{P}_\ell^m(\cos\theta). \tag{97}$$

As noted in Section 2, the more important components of the tidal potential have $\ell = 2$ and $m = 0$, 1, or 2. The solution for the equilibrium tide is of the form

$$\begin{aligned}
\xi_r &= \tilde{\xi}_r(r)\tilde{P}_\ell^m(\cos\theta), \\
\xi_\theta &= \tilde{\xi}_{\rm h}(r)\frac{d}{d\theta}\tilde{P}_\ell^m(\cos\theta), \\
\xi_\phi &= \tilde{\xi}_{\rm h}(r)\frac{im}{\sin\theta}\tilde{P}_\ell^m(\cos\theta), \\
\rho'_{\rm e} &= \tilde{\rho}'_{\rm e}(r)\tilde{P}_\ell^m(\cos\theta), \\
p'_{\rm e} &= \tilde{p}'_{\rm e}(r)\tilde{P}_\ell^m(\cos\theta), \\
\Phi'_{\rm e} &= \tilde{\Phi}'_{\rm e}(r)\tilde{P}_\ell^m(\cos\theta),
\end{aligned} \tag{98}$$

where the radial functions satisfy the ordinary differential equations

$$\tilde{\xi}_r = -\frac{(\tilde{\Phi}'_{\rm e} + \tilde{\Psi})}{g}, \tag{99}$$

$$\frac{1}{r^2}\frac{d}{dr}(r^2\tilde{\xi}_r) - \frac{\ell(\ell+1)}{r}\tilde{\xi}_{\rm h} = 0, \tag{100}$$

$$\tilde{\rho}'_{\rm e} = -\tilde{\xi}_r\frac{d\rho_0}{dr}, \tag{101}$$

$$\tilde{p}'_{\rm e} = -\tilde{\xi}_r\frac{dp_0}{dr}, \tag{102}$$

$$\frac{1}{r^2}\frac{d}{dr}\left(r^2\frac{d\tilde{\Phi}'_{\rm e}}{dr}\right) - \frac{\ell(\ell+1)}{r^2}\tilde{\Phi}'_{\rm e} = 4\pi G\tilde{\rho}'_{\rm e}. \tag{103}$$

The boundary conditions are that the solution should be regular at the center and at the surface of the planet. At the surface, $\tilde{\Phi}'_{\rm e}$ should also match on to a decaying solid harmonic $\propto r^{-(\ell+1)}$, with continuity in the function and its first radial derivative.

Note that the equilibrium tide is not affected by rotation, and involves only a single spherical harmonic. This is not true of the dynamical tide.

---

[3]In expressions such as $\nabla \cdot \boldsymbol{\xi}$ and $\nabla^2\Phi'_{(e)}$ the azimuthal part of the operator is intended to be included, even though a Fourier analysis in ϕ has been carried out.

In both convective and radiative regions, the perturbations $\rho'_{(e)}$, $p'_{(e)}$, and $\Phi'_{(e)}$ associated with the equilibrium tide constitute the dominant part of the response to tidal forcing, and it is convenient to subtract them out. In radiative regions it is also convenient to subtract out the radial velocity perturbation $u'_{r(e)}$, which dominates over the wavelike part.

4.2. Convective regions

In convective regions the forced solution is of the form

$$\begin{aligned} u'_r &\sim \epsilon \check{u}'_r(r,\theta), \\ u'_\theta &\sim \epsilon \check{u}'_\theta(r,\theta), \\ u'_\phi &\sim \epsilon \check{u}'_\phi(r,\theta), \\ \rho' - \rho'_{(e)} &\sim \epsilon^2 \check{\rho}'(r,\theta), \\ p' - p'_{(e)} &\sim \epsilon^2 \check{p}'(r,\theta), \\ \Phi' - \Phi'_{(e)} &\sim \epsilon^2 \check{\Phi}'(r,\theta), \\ W &\sim \epsilon^2 \check{W}(r,\theta). \end{aligned} \tag{104}$$

The linearized equations of Section 3.3 reduce to

$$-i\hat{\omega}_{(1)}\check{u}'_r - 2\Omega_{(1)}\sin\theta\,\check{u}'_\phi = -\frac{\partial \check{W}}{\partial r}, \tag{105}$$

$$-i\hat{\omega}_{(1)}\check{u}'_\theta - 2\Omega_{(1)}\cos\theta\,\check{u}'_\phi = -\frac{1}{r}\frac{\partial \check{W}}{\partial \theta}, \tag{106}$$

$$-i\hat{\omega}_{(1)}\check{u}'_\phi + \frac{1}{r\sin\theta}\left(\check{u}'_r\frac{\partial}{\partial r} + \frac{\check{u}'_\theta}{r}\frac{\partial}{\partial\theta}\right)(\Omega_{(1)}r^2\sin^2\theta) = -\frac{im\check{W}}{r\sin\theta}, \tag{107}$$

$$\frac{1}{r^2\rho_0}\frac{\partial}{\partial r}(r^2\rho_0\check{u}'_r) + \frac{1}{r\sin\theta}\frac{\partial}{\partial\theta}(\check{u}'_\theta\sin\theta) + \frac{im\check{u}'_\phi}{r\sin\theta} = -i\hat{\omega}_{(1)}\xi_r\frac{d\ln\rho_0}{dr}. \tag{108}$$

Equations (105)–(108) are identical to (41)–(44), except for what is effectively a forcing term on the right-hand side of equation (108). The unusual positioning of the forcing term in the equation of mass conservation reflects the fact that the dynamical tide is not forced directly by the tidal potential. Indeed, the tidal forcing is balanced in the equation of motion by the pressure and potential perturbations associated with the equilibrium tide. However, the time-dependence of the associated density perturbation provides an unbalanced term in the equation of mass conservation, which appears as the driving term for $\boldsymbol{u}'$ in the equations as written above. In fact, the equilibrium tide $\boldsymbol{u}'_{(e)}$ satisfies equation (108) exactly, but fails to satisfy the equation of motion because of its contribution to the inertial terms on the

left-hand side. Therefore the dynamical tide is forced very indirectly, through these inertial terms.

Note that the dynamical tide $\boldsymbol{u}' - \boldsymbol{u}'_{(e)}$ in convective regions is anelastic, like the free oscillations studied in Section 3.5, while the equilibrium tide is incompressible. The total tide is therefore neither anelastic nor incompressible, but satisfies $\nabla \cdot (\rho_0 \boldsymbol{u}') = \boldsymbol{u}'_{(e)} \cdot \nabla \rho_0$, which is equivalent to equation (108). In a similar way, although self-gravitation is unimportant for the dynamical tide, which therefore satisfies the Cowling approximation, it cannot be neglected for the equilibrium tide.

4.3. Radiative regions

In radiative regions the forced solution is of the form

$$\begin{aligned}
u'_r - u'_{r(e)} &\sim \epsilon^2 \hat{u}'_r(r,\theta) E(r), \\
u'_\theta &\sim \epsilon \hat{u}'_\theta(r,\theta) E(r), \\
u'_\phi &\sim \epsilon \hat{u}'_\phi(r,\theta) E(r), \\
\rho' - \rho'_{(e)} &\sim \epsilon \hat{\rho}'(r,\theta) E(r), \\
p' - p'_{(e)} &\sim \epsilon^2 \hat{p}'(r,\theta) E(r), \\
\Phi' - \Phi'_{(e)} &\sim \epsilon^2 \check{\Phi}'(r,\theta) + \epsilon^3 \hat{\Phi}'(r,\theta) E(r), \\
W &\sim \epsilon^2 \hat{W}(r,\theta) E(r),
\end{aligned} \tag{109}$$

with $E(r)$ as in Section 3.6. The linearized equations then reduce exactly to equations (51)–(58). This implies that the dynamical tide is not directly forced in radiative regions.

4.4. Matching between convective and radiative regions

In a transition region of the kind considered in Section 3.7 the forced solution is of the form

$$\begin{aligned}
u'_r - u'_{r(e)} &\sim \epsilon^{5/3} \bar{u}'_r(x,\theta), \\
u'_\theta &\sim \epsilon \bar{u}'_\theta(x,\theta), \\
u'_\phi &\sim \epsilon \bar{u}'_\phi(x,\theta), \\
\rho' - \rho'_{(e)} &\sim \epsilon^{4/3} \bar{\rho}'(x,\theta), \\
p' - p'_{(e)} &\sim \epsilon^2 \bar{p}'(x,\theta), \\
\Phi' - \Phi'_{(e)} &\sim \epsilon^2 \check{\Phi}'(r_\mathrm{b},\theta) + \epsilon^{8/3} \bar{\Phi}'(x,\theta),
\end{aligned}$$

$$W \sim \epsilon^2 \bar{W}(x,\theta). \tag{110}$$

The linearized equations reduce to

$$0 = -\frac{\partial \bar{W}}{\partial x} - \frac{g\bar{\rho}'}{\rho_0}, \tag{111}$$

$$-i\hat{\omega}_{(1)}\bar{u}'_\theta - 2\Omega_{(1)}\cos\theta\,\bar{u}'_\phi = -\frac{1}{r}\frac{\partial \bar{W}}{\partial \theta}, \tag{112}$$

$$-i\hat{\omega}_{(1)}\bar{u}'_\phi - i\hat{\omega}_{(1)}\xi_r\frac{\sin\theta}{r}\frac{\partial}{\partial r}(r^2\Omega_{(1)}) + \frac{\bar{u}'_\theta}{\sin\theta}\frac{\partial}{\partial\theta}(\Omega_{(1)}\sin^2\theta) = -\frac{im\bar{W}}{r\sin\theta}, \tag{113}$$

$$-\frac{1}{r^2}\frac{\partial}{\partial r}(i\hat{\omega}_{(1)}r^2\xi_r) + \frac{\partial \bar{u}'_r}{\partial x} + \frac{1}{r\sin\theta}\frac{\partial}{\partial\theta}(\bar{u}'_\theta\sin\theta) + \frac{im\bar{u}'_\phi}{r\sin\theta} = 0, \tag{114}$$

$$i\hat{\omega}_{(1)}\frac{\bar{\rho}'}{\rho_0} + \frac{\mathcal{D}x}{g}\bar{u}'_r = 0, \tag{115}$$

$$\frac{\partial^2\bar{\Phi}'}{\partial x^2} = 4\pi G\bar{\rho}', \tag{116}$$

with

$$\bar{W} = \frac{\bar{p}'}{\rho_0} - \frac{p'_{(e)}\rho_2}{\rho_0^2} + \check{\Phi}'. \tag{117}$$

As in Section 3.7, all coefficients in equations (111)–(115) are to be considered independent of x, except where it appears explicitly, and are to be evaluated at $r = r_{\rm b}$. The equations now contain forcing terms (those involving ξ_r) that are also independent of x. To deal with these, it is convenient to split the solution into a 'particular solution', which is independent of x and satisfies equations (111)–(115) as written, and a 'complementary function', which depends on x and satisfies equations (111)–(115) with the forcing terms omitted. Thus

$$\bar{W}(x,\theta) = \bar{W}^{(p)}(\theta) + \bar{W}^{(c)}(x,\theta), \tag{118}$$

and similarly for $\bar{u}'_\theta$ and $\bar{u}'_\phi$, while $\bar{u}'_r$ and $\bar{\rho}'$ do not appear in the particular solution. The ordinary differential equations defining the particular solution can be combined, if desired, in the form

$$\mathcal{L}\bar{W}^{(p)} = \mathcal{F}, \tag{119}$$

where

$$\mathcal{F} = \frac{1}{\hat{\omega}_{(1)}}\frac{\partial}{\partial r}(\hat{\omega}_{(1)}r^2\xi_r) + \frac{1}{\hat{\omega}_{(1)}\sin\theta}\frac{\partial}{\partial\theta}\left[\frac{2\hat{\omega}_{(1)}\Omega_{(1)}\sin^2\theta\cos\theta}{D}\xi_r\frac{\partial}{\partial r}(r^2\Omega_{(1)})\right] + \frac{m\hat{\omega}_{(1)}}{D}\xi_r\frac{\partial}{\partial r}(r^2\Omega_{(1)}) \tag{120}$$

is a forcing combination independent of x.

For the complementary function, elimination of perturbations in favor of $\bar{W}^{(c)}$ again yields

$$\mathcal{L}\bar{W}^{(c)} + \frac{r^2}{\mathcal{D}}\frac{\partial}{\partial x}\left(\frac{1}{x}\frac{\partial \bar{W}^{(c)}}{\partial x}\right) = 0, \tag{121}$$

with the solution

$$\bar{W}^{(c)} = \sum_i a_i \left[\mathrm{Ai}'(\kappa_i x) + s_i i\,\mathrm{Bi}'(\kappa_i x)\right] w_i(\theta), \tag{122}$$

where $s_i = \mathrm{sgn}(\hat{\omega}_{(1)})$ for propagating modes with $\lambda_i > 0$, and $s_i = 0$ for evanescent modes with $\lambda_i < 0$. The wavelike part of the solution dominates the particular solution at large x.

Matching W to the solution in the convective region at $x = 0$ determines the amplitude coefficients according to

$$a_i = \frac{\int_0^\pi w_i^* \left[\check{W}(r_\mathrm{b},\theta) - \bar{W}^{(p)}\right] \sin\theta\, d\theta}{\left[\mathrm{Ai}'(0) + s_i i\,\mathrm{Bi}'(0)\right] \int_0^\pi |w_i|^2 \sin\theta\, d\theta}. \tag{123}$$

The outward energy flux in generalized Hough waves is then

$$F = \epsilon^{11/3}\frac{3^{2/3}}{4}\left[\Gamma\left(\frac{1}{3}\right)\right]^2 \rho_0 \omega_{(1)}\,\mathrm{sgn}(\hat{\omega}_{(1)})\left(\frac{r^2}{\mathcal{D}}\right)^{1/3} \sum_i \lambda_i^{2/3} \frac{\left|\int_0^\pi w_i^* \left[\check{W}(r_\mathrm{b},\theta) - \bar{W}^{(p)}\right] \sin\theta\, d\theta\right|^2}{\int_0^\pi |w_i|^2 \sin\theta\, d\theta}, \tag{124}$$

where, again, the sum includes only those modes for which $\lambda > 0$, and all quantities are to be evaluated at $r = r_\mathrm{b}$.

The physical interpretation of this analysis is that the particular solution $W^{(p)}$ represents the bulk response of the transition region to residual tidal forcing (i.e., the failure of the equilibrium tide to provide an exact solution to the problem), while the wavelike complementary function is its response to the pressure of the inertial waves acting at the boundary $r = r_\mathrm{b}$, as occurs in the case of free oscillations (Section 3.7).

As discussed in Section 3.6, the inversion of the operator $\mathcal{L}$ to solve equation (119) for $\bar{W}^{(p)}$ requires careful interpretation in cases in which $\mathcal{L}$ has a null eigenvalue. In the case $m = 0$, it is easy to show that $\mathcal{F}$ is orthogonal to the null eigenfunction $w_0 =$ constant. The solution $\bar{W}^{(p)}$ therefore exists but is non-unique, as any multiple of w_0 can be added to it. This ambiguity affects only the amplitude of this non-propagating mode, however, and not the energy flux in propagating Hough modes. In the case $m \neq 0$, if $\mathcal{L}$ has a null eigenvalue for an isolated value of $\omega_{(1)}$, and if $\mathcal{F}$ has a non-zero projection on to the null eigenfunction, the corresponding mode will be resonantly excited and the present analysis breaks down (formally, $W^{(p)} \to \infty$). This phenomenon, called 'toroidal mode resonance' by Papaloizou & Savonije (1997), is discussed further in Section 5.

The matching of u'_r implies that the boundary condition for tidally forced inertial waves in the convective region is

$$\check{u}'_r - \epsilon^{-1} u'_{r(e)} = 0 \qquad \text{at} \quad r = r_{\rm b}, \tag{125}$$

The transition region therefore appears as a rigid boundary for the dynamical tide in the convective region, while the equilibrium tide continues smoothly across the boundary. In the presence of an effective viscosity confined to the convective region, the equivalents of the boundary conditions (91) and (92) are then

$$\check{u}'_r - \epsilon^{-1} u'_{r(e)} = \frac{\partial}{\partial r}\left(\frac{\check{u}'_\theta}{r}\right) = \frac{\partial}{\partial r}\left(\frac{\check{u}'_\phi}{r}\right) = 0 \qquad \text{at} \quad r = r_{\rm b}, \tag{126}$$

$$\check{u}'_r - \epsilon^{-1} u'_{r(e)} = \check{u}'_\theta - \epsilon^{-1} u'_{\theta(e)} = \check{u}'_\phi - \epsilon^{-1} u'_{\phi(e)} = 0 \qquad \text{at} \quad r = r_{\rm c}. \tag{127}$$

The assumption underlying the boundary condition at $r = r_{\rm c}$ is that the core is distorted exactly according to the equilibrium tide, and so the dynamical tide satisfies a no-slip condition. This approximation neglects the influence of the rigidity of the core in modifying its tidal distortion, which is however only a small error for typical cores of several Earth masses.

5. NUMERICAL ANALYSIS FOR UNIFORM OR 'SHELLULAR' ROTATION

5.1. Planet model and equilibrium tide

In the remainder of this paper we construct detailed numerical solutions for a simple model of a planet. Where possible, we omit the ordering parameter ϵ and the ordering subscripts that were needed in deriving the equations in previous sections.

Our numerical method is suited to the case of 'shellular' rotation in which the angular velocity $\Omega(r)$ is independent of latitude (Zahn 1992). Of course, this prescription includes the simple case of uniform rotation, which will be the main focus of our initial investigation. We consider the planet to be fully convective except for a small solid core, $r < r_{\rm c}$, and a shallow radiative envelope, $r_{\rm b} < r < R_1$. We model the planet as a polytrope of index 1, so that the density is

$$\rho = \left(\frac{\pi M_1}{4R_1^3}\right)\frac{\sin kr}{kr}, \tag{128}$$

where k is related to the radius R_1 of the planet by $kR_1 = \pi$. The gravitational acceleration is

$$g = \frac{GM_1}{\pi r^2}(\sin kr - kr\cos kr). \tag{129}$$

While it is common practice to model fully convective giant planets as polytropes of index 1, we neglect any modifications of this structure within the convective region associated with the presence of a core and a radiative envelope.

The tidal potential is of the form

$$\tilde{\Psi} = \frac{GM_2}{a^3} A r^2, \tag{130}$$

where A is a dimensionless constant, as in Section 2. The equations for the equilibrium tide (Section 4.1) imply that

$$\nabla^2(\Phi'_{\rm e} + \Psi) = \frac{4\pi G}{g}\frac{d\rho}{dr}(\Phi'_{\rm e} + \Psi). \tag{131}$$

For a polytrope of index 1 this simplifies to the Helmholtz equation

$$(\nabla^2 + k^2)(\Phi'_{\rm e} + \Psi) = 0, \tag{132}$$

with the solution (regular at $r = 0$)

$$\tilde{\Phi}'_{\rm e} + \tilde{\Psi} = \frac{GM_2}{a^3} B R_1^{5/2} r^{-1/2} J_{5/2}(kr), \tag{133}$$

where B is a dimensionless constant to be determined. At $r = R_1$, $\tilde{\Phi}'_{\rm e}$ must match smoothly on to a decaying solid harmonic $\propto r^{-(\ell+1)}$, and therefore

$$\frac{d\ln|\tilde{\Phi}'_{\rm e}|}{d\ln r} = -3 \qquad \text{at} \quad r = R_1. \tag{134}$$

This condition determines the ratio $B/A = 5/\sqrt{2}$.

The detailed solution for the equilibrium tide is

$$\tilde{\Phi}'_{\rm e} = \frac{GM_2}{a^3} A \left\{ \frac{5R_1^2}{k^3 r^3} \left[(3 - k^2 r^2)\sin kr - 3kr\cos kr \right] - r^2 \right\}, \tag{135}$$

$$\tilde{\xi}_r = -\left(\frac{M_2}{M_1}\right)\left(\frac{R_1}{a}\right)^3 \frac{5A}{k^2 r}\left[\frac{(3 - k^2 r^2)\sin kr - 3kr\cos kr}{\sin kr - kr\cos kr}\right], \tag{136}$$

$$\tilde{\xi}_{\rm h} = \frac{1}{6r}\frac{d}{dr}(r^2\tilde{\xi}_r). \tag{137}$$

We note that, if a less idealized density profile is adopted, the equilibrium tide must be determined by solving the ordinary differential equation (131) numerically.

5.2. Projection of the equations on to spherical harmonics

The basic equations of Section 4.2 governing tidally forced inertial waves in the convective region are

$$-i\hat{\omega}u_r - 2\Omega\sin\theta\, u_\phi = -\frac{\partial W}{\partial r} + \frac{F_r}{\rho}, \tag{138}$$

$$-i\hat{\omega}u_\theta - 2\Omega\cos\theta\, u_\phi = -\frac{1}{r}\frac{\partial W}{\partial \theta} + \frac{F_\theta}{\rho}, \tag{139}$$

$$-i\hat{\omega}u_\phi + \left(2\Omega + \frac{d\Omega}{d\ln r}\right)\sin\theta\, u_r + 2\Omega\cos\theta\, u_\theta = -\frac{imW}{r\sin\theta} + \frac{F_\phi}{\rho}, \tag{140}$$

$$\frac{1}{r^2\rho}\frac{\partial}{\partial r}(r^2\rho u_r) + \frac{1}{r\sin\theta}\frac{\partial}{\partial\theta}(u_\theta\sin\theta) + \frac{imu_\phi}{r\sin\theta} = -i\hat{\omega}\xi_r\frac{d\ln\rho}{dr}, \tag{141}$$

where we specialize to the case of shellular rotation and omit all unnecessary subscripts and superscripts. Included here, as explained in Section 3.8, is a viscous force with components

$$\begin{aligned}
F_r &= \frac{1}{r^2\sin\theta}\left[\frac{\partial}{\partial r}(r^2\sin\theta\, T_{rr}) + \frac{\partial}{\partial\theta}(r\sin\theta\, T_{r\theta}) + imrT_{r\phi}\right] - \frac{T_{\theta\theta}}{r} - \frac{T_{\phi\phi}}{r},\\
F_\theta &= \frac{1}{r^3\sin\theta}\left[\frac{\partial}{\partial r}(r^3\sin\theta\, T_{r\theta}) + \frac{\partial}{\partial\theta}(r^2\sin\theta\, T_{\theta\theta}) + imr^2T_{\theta\phi}\right] - \frac{T_{\phi\phi}\cot\theta}{r},\\
F_\phi &= \frac{1}{r^3\sin^2\theta}\left[\frac{\partial}{\partial r}(r^3\sin^2\theta\, T_{r\phi}) + \frac{\partial}{\partial\theta}(r^2\sin^2\theta\, T_{\theta\phi}) + imr^2\sin\theta\, T_{\phi\phi}\right],
\end{aligned} \tag{142}$$

where

$$\mathbf{T} = 2\mu\mathbf{S} + \mu_{\rm b}(\nabla\cdot\boldsymbol{u})\mathbf{1} \tag{143}$$

is the Navier–Stokes viscous stress tensor, with

$$\mathbf{S} = \frac{1}{2}\left[\nabla\boldsymbol{u} + (\nabla\boldsymbol{u})^{\rm T}\right] - \frac{1}{3}(\nabla\cdot\boldsymbol{u})\mathbf{1} \tag{144}$$

being the traceless shear tensor, $\mu(r)$ the (dynamic) shear viscosity and $\mu_{\rm b}(r)$ the bulk viscosity. The components of $\mathbf{T}$ are

$$\begin{aligned}
T_{rr} &= 2\mu\left(\frac{\partial u_r}{\partial r}\right) + (\mu_{\rm b} - \tfrac{2}{3}\mu)\nabla\cdot\boldsymbol{u},\\
T_{r\theta} &= \mu\left[r\frac{\partial}{\partial r}\left(\frac{u_\theta}{r}\right) + \frac{1}{r}\frac{\partial u_r}{\partial\theta}\right],\\
T_{r\phi} &= \mu\left[r\frac{\partial}{\partial r}\left(\frac{u_\phi}{r}\right) + \frac{imu_r}{r\sin\theta}\right],\\
T_{\theta\theta} &= 2\mu\left(\frac{1}{r}\frac{\partial u_\theta}{\partial\theta} + \frac{u_r}{r}\right) + (\mu_{\rm b} - \tfrac{2}{3}\mu)\nabla\cdot\boldsymbol{u},
\end{aligned}$$

$$
\begin{aligned}
T_{\theta\phi} &= \mu\left[\frac{\sin\theta}{r}\frac{\partial}{\partial\theta}\left(\frac{u_\phi}{\sin\theta}\right)+\frac{imu_\theta}{r\sin\theta}\right],\\
T_{\phi\phi} &= 2\mu\left(\frac{imu_\phi}{r\sin\theta}+\frac{u_r}{r}+\frac{u_\theta\cot\theta}{r}\right)+(\mu_{\rm b}-\tfrac{2}{3}\mu)\nabla\cdot\boldsymbol{u},
\end{aligned}
\tag{145}
$$

with

$$
\nabla\cdot\boldsymbol{u}=\frac{1}{r^2}\frac{\partial}{\partial r}(r^2u_r)+\frac{1}{r\sin\theta}\frac{\partial}{\partial\theta}(u_\theta\sin\theta)+\frac{imu_\phi}{r\sin\theta}. \tag{146}
$$

Following the basic idea of Zahn (1966), we decompose the velocity into 'spheroidal' and 'toroidal' parts and then project all variables on to spherical harmonics such that

$$
\begin{aligned}
u_r &= \sum a_n(r)\tilde{P}_n^m(\cos\theta),\\
u_\theta &= r\sum\left[b_n(r)\frac{d}{d\theta}+c_n(r)\frac{im}{\sin\theta}\right]\tilde{P}_n^m(\cos\theta),\\
u_\phi &= r\sum\left[b_n(r)\frac{im}{\sin\theta}-c_n(r)\frac{d}{d\theta}\right]\tilde{P}_n^m(\cos\theta),\\
W &= \sum id_n(r)\tilde{P}_n^m(\cos\theta).
\end{aligned}
\tag{147}
$$

where the summations are over integers $n\geq m$. Even if the tidal forcing and equilibrium tide involve only one spherical harmonic, the Coriolis force couples spherical harmonics of different degrees. Note that c_n is the amplitude of the 'toroidal' part of the velocity, which is not present in the equilibrium tide but is induced by rotation and is incompressible.

To project equations (138)–(141) on to spherical harmonics, we require the recurrence relations

$$
\cos\theta\,\tilde{P}_n^m(\cos\theta)=q_{n+1}\tilde{P}_{n+1}^m(\cos\theta)+q_n\tilde{P}_{n-1}^m(\cos\theta), \tag{148}
$$

$$
\sin\theta\frac{d}{d\theta}\tilde{P}_n^m(\cos\theta)=nq_{n+1}\tilde{P}_{n+1}^m(\cos\theta)-(n+1)q_n\tilde{P}_{n-1}^m(\cos\theta), \tag{149}
$$

for *normalized* associated Legendre polynomials, where we define the coefficients

$$
q_n=\left(\frac{n^2-m^2}{4n^2-1}\right)^{1/2}, \tag{150}
$$

and it is to be understood that $\tilde{P}_n^m(\cos\theta)=0$ for $n<m$. To deal with the angular components of the equation of motion, equations (139) and (140), we take combinations that correspond to 'divergence' and 'curl':

$$
\begin{aligned}
&\frac{1}{r\sin\theta}\frac{\partial}{\partial\theta}\left[\sin\theta(-i\hat{\omega}u_\theta-2\Omega\cos\theta\,u_\phi)\right]\\
&\quad+\frac{im}{r\sin\theta}\left[-i\hat{\omega}u_\phi+\left(2\Omega+\frac{d\Omega}{d\ln r}\right)\sin\theta\,u_r+2\Omega\cos\theta\,u_\theta\right]\\
&\quad=-\frac{1}{r^2}\left[\frac{1}{\sin\theta}\frac{\partial}{\partial\theta}\left(\sin\theta\frac{\partial W}{\partial\theta}\right)-\frac{m^2W}{\sin^2\theta}\right]+\frac{1}{r\sin\theta}\frac{\partial}{\partial\theta}\left(\frac{F_\theta}{\rho}\right)+\frac{im}{r\sin\theta}\left(\frac{F_\phi}{\rho}\right),
\end{aligned}
\tag{151}
$$

$$\frac{1}{r\sin\theta}\frac{\partial}{\partial\theta}\left\{\sin\theta\left[-i\hat{\omega}u_\phi+\left(2\Omega+\frac{d\Omega}{d\ln r}\right)\sin\theta\,u_r+2\Omega\cos\theta\,u_\theta\right]\right\}$$
$$-\frac{im}{r\sin\theta}(-i\hat{\omega}u_\theta-2\Omega\cos\theta\,u_\phi)=\frac{1}{r\sin\theta}\frac{\partial}{\partial\theta}\left(\frac{F_\phi}{\rho}\right)-\frac{im}{r\sin\theta}\left(\frac{F_\theta}{\rho}\right). \qquad (152)$$

Equation (138) then gives

$$-i\hat{\omega}a_n-2im\Omega rb_n+2\Omega r\left[(n-1)q_nc_{n-1}-(n+2)q_{n+1}c_{n+1}\right]$$
$$=-i\frac{dd_n}{dr}+\frac{1}{\rho}\frac{d}{dr}\left[2\mu\frac{da_n}{dr}+(\mu_{\rm b}-\tfrac{2}{3}\mu)\Delta_n\right]+\frac{4\mu}{\rho}\frac{d}{dr}\left(\frac{a_n}{r}\right)$$
$$-n(n+1)\frac{\mu}{\rho}\left[\frac{a_n}{r^2}+r^2\frac{d}{dr}\left(\frac{b_n}{r^2}\right)\right], \qquad (153)$$

where

$$\Delta_n=\frac{1}{r^2}\frac{d}{dr}(r^2a_n)-n(n+1)b_n. \qquad (154)$$

Equations (151) and (152) give

$$-n(n+1)i\hat{\omega}b_n-\frac{im}{r}\left(2\Omega+\frac{d\Omega}{d\ln r}\right)a_n-2im\Omega b_n$$
$$+2\Omega\left[(n-1)(n+1)q_nc_{n-1}+n(n+2)q_{n+1}c_{n+1}\right]=-n(n+1)\frac{id_n}{r^2}$$
$$+\frac{n(n+1)}{\rho}\left\{\frac{1}{r^6}\frac{d}{dr}(\mu r^4a_n)+(\mu_{\rm b}-\tfrac{2}{3}\mu)\frac{\Delta_n}{r^2}+\frac{1}{r^4}\frac{d}{dr}\left(\mu r^4\frac{db_n}{dr}\right)-2[n(n+1)-1]\frac{\mu b_n}{r^2}\right\} \qquad (155)$$

and

$$-n(n+1)i\hat{\omega}c_n+\frac{1}{r}\left(2\Omega+\frac{d\Omega}{d\ln r}\right)\left[(n+1)q_na_{n-1}-nq_{n+1}a_{n+1}\right]$$
$$-2\Omega\left[(n-1)(n+1)q_nb_{n-1}+n(n+2)q_{n+1}b_{n+1}\right]-2im\Omega c_n$$
$$=\frac{n(n+1)}{\rho}\left\{\frac{1}{r^4}\frac{d}{dr}\left(\mu r^4\frac{dc_n}{dr}\right)-[n(n+1)-2]\frac{\mu c_n}{r^2}\right\}, \qquad (156)$$

respectively. Finally, equation (141) gives

$$\frac{1}{r^2\rho}\frac{d}{dr}(r^2\rho a_n)-n(n+1)b_n=-i\hat{\omega}\tilde{\xi}_r\frac{d\ln\rho}{dr}\delta_{n\ell}, \qquad (157)$$

where δ is the Kronecker delta function.

The couplings are such that, if $\ell=m=2$, the quantities a_n, b_n, and d_n are non-zero only for even values $n\geq 2$, while c_n is non-zero only for odd values $n\geq 3$. If $\ell=2$ and

$m = 1$, the quantity c_1 is also non-zero. Finally, if $\ell = 2$ and $m = 0$, the quantity d_0 is also non-zero, but a_0 and b_0 can be taken to vanish, and equations (155) and (157) are not required in the case $n = 0$.

The boundary conditions (126) and (127) translate into

$$a_n + i\hat{\omega}\tilde{\xi}_r\delta_{n\ell} = \frac{a_n}{r^2} + \frac{db_n}{dr} = \frac{dc_n}{dr} = 0 \qquad \text{at} \quad r = r_{\rm b}, \tag{158}$$

$$a_n + i\hat{\omega}\tilde{\xi}_r\delta_{n\ell} = rb_n + i\hat{\omega}\tilde{\xi}_{\rm h}\delta_{n\ell} = rc_n = 0 \qquad \text{at} \quad r = r_{\rm c}. \tag{159}$$

The viscous dissipation rate per unit volume is

$$2\mu\mathbf{S}^2 + \mu_{\rm b}(\nabla\cdot\boldsymbol{u})^2, \tag{160}$$

and the time-averaged tidal dissipation rate in the convective region can be evaluated as

$$D_{\rm visc} = \pi\int_{r_{\rm c}}^{r_{\rm b}}\sum_n D_n\, r^2\, dr, \tag{161}$$

where

$$D_n = \mu\left[3\left|\frac{da_n}{dr} - \frac{\Delta_n}{3}\right|^2 + n(n+1)\left(\left|\frac{a_n}{r} + r\frac{db_n}{dr}\right|^2 + \left|r\frac{dc_n}{dr}\right|^2\right)\right.$$
$$\left. +(n-1)n(n+1)(n+2)\left(|b_n|^2 + |c_n|^2\right)\right] + \mu_{\rm b}|\Delta_n|^2. \tag{162}$$

5.3. Method of solution

We truncate the system of equations at even order L, so that $a_n = b_n = c_n = d_n = 0$ for $n > L$, and thereby obtain a large but finite number of linear, inhomogeneous ordinary differential equations constituting a two-point boundary-value problem. The order of the system is in fact $3L$.

5.3.1. Principal method

Our principal method of solution makes use of a Chebyshev pseudospectral approach (e.g., Boyd 2001) as used by, e.g., Rieutord et al. (2001) in their study of free inertial waves in an incompressible fluid contained in a spherical annulus. This method is well suited to the problem as it provides spectral accuracy, superior to any finite-difference method with a

similar number of radial nodes, and naturally supplies additional resolution in the boundary layer just outside the solid core.

We introduce the Chebyshev coordinate x such that $-1 < x < 1$ and

$$r = \left(\frac{1-x}{2}\right) r_{\rm c} + \left(\frac{1+x}{2}\right) r_{\rm b}, \tag{163}$$

and reorganize the differential equations by defining a new set of dependent variables

$$X_i = c_{2i-1}, \qquad Y_i = a_{2i}, \qquad Z_i = \frac{db_{2i}}{dr}, \qquad 1 \le i \le \frac{L}{2}, \tag{164}$$

using equation (157) to substitute for b_n wherever it appears. For each value of i we then obtain an equation involving the quantities

$$\frac{d^2X_i}{dx^2}, \quad \frac{dX_i}{dx}, \quad X_i, \quad \frac{dY_i}{dx}, \quad Y_i, \quad \frac{dY_{i-1}}{dx}, \quad Y_{i-1} \tag{165}$$

from equation (156). Differentiating equation (157) with respect to r, we obtain an equation involving the quantities

$$\frac{d^2Y_i}{dx^2}, \quad \frac{dY_i}{dx}, \quad Y_i, \quad Z_i. \tag{166}$$

Finally, eliminating d_n between equations (153) and (155), we obtain an equation involving the quantities

$$\frac{dX_i}{dx}, \quad X_i, \quad \frac{d^2Y_i}{dx^2}, \quad \frac{dY_i}{dx}, \quad Y_i, \quad \frac{d^2Z_i}{dx^2}, \quad \frac{dZ_i}{dx}, \quad Z_i, \quad \frac{dX_{i+1}}{dx}, \quad X_{i+1}. \tag{167}$$

The functions X_i, Y_i, and Z_i, for the appropriate values of i, are represented by their values at the Gauss–Lobatto collocation nodes

$$x_j = \cos\left(\frac{j\pi}{N}\right), \qquad 0 \le j \le N, \tag{168}$$

where N is the Chebyshev truncation order. Each differential equation is then represented at each of the internal collocation nodes, using the first and second Chebyshev collocation derivative matrices. At the boundary nodes, the boundary conditions are represented instead, again using the Chebyshev collocation derivative where needed.

The result of this procedure is a block-tridiagonal system of linear, inhomogeneous algebraic equations. Each block is of dimension $3(N+1)$ and relates to the functions c_{n-1}, a_n, and b_n for a single value of n. There are L blocks along the diagonal, and blocks immediately above and below the diagonal, which originate from the Coriolis terms in the equation of motion. The blocks are dense owing to the structure of the Chebyshev collocation derivative matrix. We solve the system by a standard procedure for block-tridiagonal matrices, which involves $O(LN^3)$ operations and has a memory requirement $O(LN^2)$, although this can be reduced to $O(N^2)$ if ample temporary storage is available on disk.

5.3.2. Alternative method

Our alternative method is based on a direct integration of the differential equations using a fifth-order Runge–Kutta method with adaptive stepsize control. This method does not work when the viscosity is very small, because the equations are then very stiff, but we use it to verify the results obtained by the principal method in an accessible parameter regime.

We recast the system as a set of $3L$ first-order differential equations for the functions

$$a_{2i}, \quad b_{2i}, \quad c_{2i-1}, \quad d_{2i}, \quad \nu r^4 \frac{db_{2i}}{dr}, \quad \nu r^4 \frac{dc_{2i-1}}{dr}, \qquad 1 \le i \le \frac{L}{2}, \tag{169}$$

where $\nu = \mu/\rho$ is the kinematic viscosity. To eliminate da_n/dr and d^2a_n/dr^2 from the equations, we use equation (157) to express these quantities in terms of b_n and db_n/dr. To start the integration at $r = r_\mathrm{b}$ we must guess $3L/2$ initial values in addition to those specified by the boundary conditions, and there are $3L/2$ corresponding boundary conditions to satisfy at $r = r_\mathrm{c}$. As the problem is linear, a conventional shooting method is not required. Instead, we integrate the equations once from r_c to r_b using null initial values, to obtain a 'particular solution'. We then integrate the equations $3L/2$ times, omitting the forcing terms, setting a different one of the initial values to unity each time (the others being null). This approach generates a set of 'complementary functions' that spans the space of admissible initial values. The desired solution is then the particular solution plus a linear combination of the complementary functions; the coefficients of the complementary functions are found by imposing the boundary conditions at r_b, requiring the inversion of a square matrix of dimension $3L/2$.

5.4. Computation of the Hough functions

In order to determine the amplitudes with which the Hough waves are excited in the radiative region, according to equation (124), the numerical solution at the boundary $r = r_\mathrm{b}$ must be projected on to the Hough functions. In the case of shellular rotation, the operator $\mathcal{L}$ given by equation (60) reduces to Laplace's tidal operator, the eigenfunctions of which have often been expanded in associated Legendre polynomials (e.g., Longuet-Higgins 1968 and references therein). We make use of the identity

$$\tilde{P}_n^m(\cos\theta) = \hat{\omega}_{(1)}^2 \mathcal{L}\left[A_n \tilde{P}_n^m(\cos\theta) + B_{n+1}\tilde{P}_{n+2}^m(\cos\theta) + B_{n-1}\tilde{P}_{n-2}^m(\cos\theta)\right], \tag{170}$$

valid for $n \geq 2$, where

$$A_n = \frac{1}{n^2(n+1)^2}\left\{n(n+1) + fm - f^2\left[\frac{(n-1)^2(n+1)^2 q_n^2}{(n-1)n + fm} + \frac{n^2(n+2)^2 q_{n+1}^2}{(n+1)(n+2) + fm}\right]\right\}, \tag{171}$$

$$B_n = -\frac{f^2 q_n q_{n+1}}{n(n+1) + fm}, \tag{172}$$

and $f = 2\Omega_{(1)}/\hat{\omega}_{(1)}$. Equation (170) is readily verified by direct substitution. It becomes indeterminate in the case $m \neq 0$ when $f = -n(n+1)/m$ for integers $n \geq m$, owing to the existence of a null eigenfunction of $\mathcal{L}$ corresponding to a toroidal mode, as discussed in Section 3.6.

To solve the eigenvalue problem $\mathcal{L}w = \lambda w$ we consider the equivalent problem $(\hat{\omega}_{(1)}^2\mathcal{L})^{-1}w = \Lambda w$, where $\Lambda = (\hat{\omega}_{(1)}^2\lambda)^{-1}$. In cases when $\mathcal{L}$ has a null eigenvalue, we consider the restriction of this equation to the subspace of functions orthogonal to the null eigenfunction. Expanding w in normalized associated Legendre polynomials,

$$w = \sum e_n \tilde{P}_n^m(\cos\theta), \tag{173}$$

where the sum is over even integers $n \geq 2$, we obtain from equation (170)

$$A_n e_n + B_{n-1}e_{n-2} + B_{n+1}e_{n+2} = \Lambda e_n. \tag{174}$$

We truncate at the same order $n = N$ as for the solution in the convective region, and thereby obtain an eigenvalue problem involving a tridiagonal, real symmetric matrix,

$$\begin{bmatrix} A_2 & B_3 & 0 & 0 & \cdots & 0 & 0 \\ B_3 & A_4 & B_5 & 0 & \cdots & 0 & 0 \\ 0 & B_5 & A_6 & B_7 & \cdots & 0 & 0 \\ 0 & 0 & B_7 & A_8 & \cdots & 0 & 0 \\ \cdots & \cdots & \cdots & \cdots & \cdots & \cdots & \cdots \\ 0 & 0 & 0 & 0 & \cdots & A_{N-2} & B_{N-1} \\ 0 & 0 & 0 & 0 & \cdots & B_{N-1} & A_N \end{bmatrix} \begin{bmatrix} e_2 \\ e_4 \\ e_6 \\ e_8 \\ \cdots \\ e_{N-2} \\ e_N \end{bmatrix} = \Lambda \begin{bmatrix} e_2 \\ e_4 \\ e_6 \\ e_8 \\ \cdots \\ e_{N-2} \\ e_N \end{bmatrix}. \tag{175}$$

It is clear from this representation that, in the case of a non-rotating planet ($f = 0$), the matrix is diagonal and the eigenvalues are the diagonal elements $[n(n+1)]^{-1}$, in agreement with equation (69). More generally, the eigensolutions of equation (175) are readily obtained by standard numerical methods. The inner product in equation (124) is easily computed in the Legendre polynomial representation, because

$$\int_0^\pi \left[\sum_n a_n \tilde{P}_n^m(\cos\theta)\right]^* \left[\sum_{n'} b_{n'} \tilde{P}_{n'}^m(\cos\theta)\right] \sin\theta\, d\theta = \sum_n a_n^* b_n. \tag{176}$$

To determine the particular solution in the transition region, rather than working with equation (119), we project equations (112)–(114) for the particular solution on to spherical harmonics in the manner of equation (147), leading to (in an obvious notation)

$$-n(n+1)i\hat{\omega}b_n^{(p)} - \frac{im}{r}\left(2\Omega + \frac{d\Omega}{d\ln r}\right)\tilde{a}_n - 2im\Omega b_n^{(p)} + 2\Omega\left[(n-1)(n+1)q_n c_{n-1}^{(p)} + n(n+2)q_{n+1}c_{n+1}^{(p)}\right] = -n(n+1)\frac{id_n^{(p)}}{r^2}, \tag{177}$$

$$-n(n+1)i\hat{\omega}c_n^{(p)} + \frac{1}{r}\left(2\Omega + \frac{d\Omega}{d\ln r}\right)\left[(n+1)q_n\tilde{a}_{n-1} - nq_{n+1}\tilde{a}_{n+1}\right] - 2\Omega\left[(n-1)(n+1)q_n b_{n-1}^{(p)} + n(n+2)q_{n+1}b_{n+1}^{(p)}\right] - 2im\Omega c_n^{(p)} = 0, \tag{178}$$

$$\frac{1}{r^2}\frac{d}{dr}(r^2\tilde{a}_n) - n(n+1)b_n^{(p)} = 0, \tag{179}$$

where $\tilde{a}_n = -i\hat{\omega}\tilde{\xi}_r\delta_{n\ell}$. It is then straightforward to solve algebraically for the coefficients $d_n^{(p)}$ defining the desired function $\bar{W}^{(p)}(\theta)$. When $\ell = 2$, the only non-zero coefficients are $\tilde{a}_2$, $b_2^{(p)}$, $c_1^{(p)}$ (when $m < 2$), $c_3^{(p)}$, $d_2^{(p)}$, and $d_4^{(p)}$. In the course of obtaining this solution, a singularity arises if the coefficient of $c_n^{(p)}$ in equation (178) vanishes. This gives rise to a 'toroidal mode resonance' as discussed in Section 4.4. The only such resonances for $\ell = 2$ tidal forcing in a planet with shellular rotation occur at $\hat{\omega} = -\Omega/3$ (when $m = 2$), or at $\hat{\omega} = -\Omega$ and $\hat{\omega} = -\Omega/6$ (when $m = 1$).

6. NUMERICAL RESULTS

6.1. Model parameters

We present results for a uniformly rotating planet with a solid core of fractional radius $r_{\rm c}/R_1 = 0.2$ and a convective–radiative boundary of fractional radius $r_{\rm b}/R_1 = 0.9$. These values are suggested by the models of short-period extrasolar planets constructed by Bodenheimer, Lin, & Mardling (2001).

The kinematic shear viscosity ν is assumed to be uniform and is parametrized by the dimensionless Ekman number

$$Ek = \frac{\nu}{2\Omega R_1^2}, \tag{180}$$

while the bulk viscosity, which we found to be unimportant, is set to zero. Current models (Guillot et al. 2003) suggest that the microscopic viscosity in the interior of Jupiter is of

the order of $10^{-2}\,\mathrm{cm}^2\,\mathrm{s}^{-1}$, corresponding to $Ek \sim 10^{-18}$. The eddy viscosity associated with turbulent convection is much larger, corresponding to $Ek \sim 10^{-7}$. However, the characteristic timescale of the eddies is a year or longer, making the convection inefficient at damping tidal disturbances with typical periods of a few days. Therefore the estimate $Ek \sim 10^{-7}$ should probably be reduced by several orders of magnitude, perhaps using the prescription of Goldreich & Keeley (1977). In this initial study, we make no attempt to model the detailed variations of the effective viscosity, but investigate the systematic behavior of the solutions as the uniform kinematic viscosity is reduced into the regime $Ek \ll 1$.

Almost all the results reported here are obtained by the principal method, using a standard numerical resolution of $L = N = 100$, for which each calculation takes approximately 30 seconds on a modern workstation. As discussed below, this resolution allows numerically converged results to be obtained at Ekman numbers at least as small as 10^{-7}. We have also carried out a small number of calculations for isolated forcing frequencies at a very high resolution of $L = N = 500$, each taking several hours on a workstation, but allowing access to yet smaller Ekman numbers.

We have computed the tidal dissipation rate by viscous dissipation in the convective region and via the emission of Hough waves at the convective–radiative boundary for forcing frequencies in the range $-3\Omega < \hat{\omega} < 3\Omega$, comfortably spanning the spectrum of inertial waves. Only the most important case of $m = 2$ forcing was considered. To investigate the effect of a small but non-zero viscosity, the calculations were carried out for $Ek = 10^{-4}$, 10^{-5}, 10^{-6}, and 10^{-7}.

In the case of the uniformly rotating planet, the calculations were also repeated omitting certain terms in the governing equations, in order to test the validity of earlier and more tractable approaches to the problem. In the *traditional approximation* (e.g., Chapman & Lindzen 1970) the latitudinal component of the angular velocity is neglected in computing the Coriolis force. This amounts to neglecting the $\Omega \sin\theta$ terms in equations (138) and (140), while the Hough modes are unaffected. The traditional approximation, where valid, is useful because it allows the linearized equations to be solved by separation of variables, although we do not make use of that property here. In the *no-Coriolis approximation* the Coriolis force is completely neglected and the Hough modes reduce to spherical harmonics. This is equivalent to considering a non-rotating planet except that the Doppler shift of the forcing frequency is taken into account.

6.2. Dimensionless dissipation rates

It is convenient to express the tidal dissipation rate in a dimensionless form. The natural unit for viscous dissipation is

$$U_{\rm visc} = \left(\frac{M_2}{M_1}\right)^2 \left(\frac{R_1}{a}\right)^6 |A|^2 M_1 R_1^2 |\Omega|^3. \tag{181}$$

Use of this unit means that the dimensionless viscous dissipation rate $D_{\rm visc}/U_{\rm visc}$ depends only on $\hat{\omega}/\Omega$ and Ek (in principle also on $r_{\rm c}/R_1$ and $r_{\rm b}/R_1$ if these are varied). We note that $D_{\rm visc}$ captures the viscous dissipation of the equilibrium tide in addition to the damping of any inertial waves that are excited as a dynamical tide, and $D_{\rm visc}$ is therefore non-zero even under the no-Coriolis approximation.

To calculate the dissipation rate via Hough waves, we note that the waves carry both energy and angular momentum fluxes, their ratio being the angular pattern speed ω/m. When the waves damp, their angular momentum is deposited locally in the planet. Part of the energy of the waves is then required in order to change the spin of the planet, while the remainder is dissipated locally. A simple calculation shows that the dissipation rate is

$$D_{\rm Hough} = \left(\frac{\hat{\omega}}{\omega}\right) F, \tag{182}$$

where F is the energy flux in equation (124) (factors of ϵ and ordering subscripts being omitted).

The dissipation rate via the emission of Hough waves is naturally expressed in terms of the unit

$$U_{\rm Hough} = f_{\rm Hough} U_{\rm visc}, \tag{183}$$

where

$$f_{\rm Hough} = \frac{\rho(r_{\rm b})}{\rho(0)} \left(\frac{\Omega^2}{r_{\rm b}\mathcal{D}}\right)^{1/3}. \tag{184}$$

is a model-dependent, dimensionless quantity. The first factor in $f_{\rm Hough}$, being the ratio of the density at the convective–radiative boundary to the central density of the polytropic model, is highly uncertain, being possibly in the range $10^{-4} - 10^{-3}$ for short-period extrasolar planets, according to the models of spherically irradiated and tidally heated planets by Bodenheimer et al. (2001). The second factor involves the quantity $\mathcal{D}$, which is also very uncertain but is raised only to a weak power. For planets that are distant from their host stars, such as Jupiter, $f_{\rm Hough}$ is probably so small that tidal dissipation via Hough waves is entirely negligible.

According to the conventional theory of the equilibrium tide, in which the efficiency of tidal dissipation is parametrized by a quality factor Q (e.g., Goldreich & Soter 1966), the tidal dissipation rate in a body of negligible rigidity would be

$$\left(\frac{5k_2}{4Q}\right)\frac{GM_2^2R_1^5}{a^6}|A|^2|\hat{\omega}| = \frac{1}{f_Q Q}\left|\frac{\hat{\omega}}{\Omega}\right| U_{\rm visc}, \tag{185}$$

where k_2 is the second-order Love number, and

$$f_Q = \left(\frac{4}{5k_2}\right)\frac{\Omega^2 R_1^3}{GM_1} \tag{186}$$

is a dimensionless number of order ϵ^2. We can therefore express the numerically determined tidal dissipation rates in terms of effective Q-values given by

$$Q_{\rm visc}^{-1} = f_Q\left(\frac{D_{\rm visc}}{U_{\rm visc}}\right)\left|\frac{\Omega}{\hat{\omega}}\right|, \qquad Q_{\rm Hough}^{-1} = f_Q f_{\rm Hough}\left(\frac{D_{\rm Hough}}{U_{\rm Hough}}\right)\left|\frac{\Omega}{\hat{\omega}}\right|. \tag{187}$$

For Jupiter, using the volumetric radius for R_1 and the value $k_2 \approx 0.38$ from Gavrilov & Zharkov (1977), we obtain $f_Q \approx 0.18$; when Jupiter is spun down to a period of three days, illustrative of a short-period extrasolar planet, we obtain $f_Q \approx 0.0033$.

We note that Goldreich & Soter (1966) assume that $k_2 = 3/2$, as for a homogeneous body, and therefore the effective Q-values appropriate for use with their formulae are approximately four times larger than the values we quote below.

6.3. Standard model and variations

Fig. 2 shows the viscous dissipation rate as a function of forcing frequency, for the standard model. The four panels correspond to Ekman numbers 10^{-4}, 10^{-5}, 10^{-6}, and 10^{-7}. The quantity plotted is the base-10 logarithm of $(D_{\rm visc}/U_{\rm visc})|\Omega/\hat{\omega}|$, which is directly related to the effective Q-value. The dotted line in panel (d) corresponds to a fiducial value of $Q_{\rm visc} = 10^5$ for Jupiter, or approximately 50 times higher for a short-period extrasolar planet. Fig. 3 shows the dissipation rate via Hough waves for the same model. Although the values obtained are much larger, they must be scaled down by the small and uncertain factor $f_{\rm Hough}$ before they can be compared with Fig. 2. Figs 4–7 show the equivalent results obtained when either the no-Coriolis approximation or the traditional approximation is adopted.

It is clear from Fig. 2 that the results become more complicated, and the computations more challenging, as the viscosity is reduced. The numerical convergence of the solutions is examined in two resolution studies in Figs 8 and 9. The first of these (Fig. 8) is carried out at

a forcing frequency $\hat{\omega} = \Omega$ within the spectrum of inertial waves but not associated with an obvious resonant feature. The figure shows that higher resolution is required at lower Ekman numbers, and that the dissipation rate can be either underestimated or overestimated if the resolution is insufficient. The standard resolution $L = N = 100$ clearly gives numerically converged results for all the Ekman numbers considered in Fig. 2. The second resolution study (Fig. 9) is carried out at a forcing frequency $\hat{\omega} = 0.489\,\Omega$, which lies near the peak of the largest resonant feature seen in Fig. 2. In this case the standard resolution is just adequate to capture the peak dissipation rate at $Ek = 10^{-7}$ with a small error.

Fig. 10 shows, as a dotted line, an expanded view of part of panel (d) of Fig. 2, the graph of viscous dissipation rate for $Ek = 10^{-7}$. The solid line, for comparison, comes from a calculation at $Ek = 10^{-8}$, for which the increased numerical resolution $L = N = 200$ was necessary.

Finally, Fig. 11 illustrates the spatial structure of the velocity field induced by tidal forcing in the convective region. This calculation, at $Ek = 10^{-9}$, is performed at the very high resolution of $L = N = 500$, and the forcing frequency $\hat{\omega} = -1.1181\,\Omega$ is chosen to be close to the peak of a large resonance.

6.4. The Coriolis effect and the traditional approximation

We begin by comparing the results for the uniformly rotating planet in the full model (Figs 2 and 3) with those obtained under the no-Coriolis approximation (Figs 4 and 5). It is clear that, when the Coriolis force is included, a number of resonant features are superimposed on the otherwise smooth variation of the viscous dissipation rate with forcing frequency. As expected, the resonances are restricted to the interval $-2 \le \hat{\omega}/\Omega \le 2$ corresponding to the spectrum of inertial waves in the convective region. For $Ek = 10^{-4}$ the inertial waves show up as two resonant peaks in the dissipation rate. However, as Ek is reduced further, a host of resonances come into play. This trend is consistent with the idea that the spectrum of inertial waves is dense or continuous in the absence of viscosity, while it consists of a discrete set of damped modes in the presence of viscosity. When $Ek = 10^{-4}$ the discrete nature of the modes is clearly evident, but when $Ek = 10^{-7}$ the individual resonances can barely be discerned, except for the most prominent examples, and a resonant response is almost guaranteed for any forcing frequency within the spectrum of inertial waves. Under the no-Coriolis approximation the convective regions of the planet have no wavelike response and no dynamical tide is excited. The slow, large-scale motion associated with the equilibrium tide is damped by viscosity, leading to a dissipation rate that vanishes linearly with the viscosity. The same dependence does not occur in the full model for frequencies

within the spectrum of inertial waves. This behaviour reflects the fact that the characteristic spatial scale of the tidally forced inertial waves diminishes as the viscosity is reduced. Rather as occurs in hydrodynamic turbulence, the dissipation rate then has a non-trivial finite limit as the viscosity tends to zero.

The dissipation rate via Hough waves is differently normalized, owing to the model-dependent prefactor $f_{\rm Hough}$. If this factor is of the order of $10^{-4} - 10^{-3}$, as may occur in short-period extrasolar planets, the Hough dissipation rate could dominate over the viscous dissipation rate. A comparison of Figs 2 and 3 indicates that the Hough dissipation rate responds to the inertial-mode resonances when the full Coriolis effect is used. This result reflects the fact that the Hough waves are excited partly by the pressure of the inertial waves at the convective–radiative boundary. These resonant features become stronger and sharper as the Ekman number is reduced, but otherwise the Hough dissipation rate is essentially independent of the viscosity. The feature at $\hat{\omega} = -\Omega/3$ is the toroidal mode resonance mentioned in Section 5.4. In the neighborhood of this forcing frequency, a global toroidal mode is excited in the radiative region, contrary to the assumptions of this paper, and the Hough dissipation rate cannot be trusted. The no-Coriolis approximation fails to reproduce any of these features but, generally, significantly overestimates the Hough dissipation rate. This discrepancy may be attributable to the fact that, depending on their frequency, the Hough modes are confined by the Coriolis force to propagate only in certain ranges of latitude, unlike the g modes in a non-rotating planet.

Now comparing Figs 2 and 3 with Figs 6 and 7, we find that, within the inertial region, the traditional approximation gives a totally inaccurate representation of the tidal dissipation rate. While the traditional approximation does allow for a resonant response in the convective region, the details are quite wrong and the viscous dissipation rate is generally overestimated by about two orders of magnitude. This difference may occur because of a artificial decoupling between the angular and radial structures of the response that occurs when the traditional approximation is employed. This decoupling implies that, when the conditions for resonance are met, a global amplification of the response occurs. We conclude that, within the spectrum of inertial waves, the traditional approximation is, if anything, even worse than the no-Coriolis approximation, and should therefore never be used for inertial waves in gaseous giant planets.

6.5. The low-viscosity limit

Returning to the full model, we see clearly from the expanded view in Fig. 10 that the viscous dissipation rate does not simply vanish linearly with the viscosity. Instead, as

the Ekman number is reduced (in this case by a factor of 10) the resonant peaks become more numerous, sharper, and taller. The frequency-averaged viscous dissipation rate for the interval shown in Fig. 10 is very nearly *independent of the viscosity*, decreasing by approximately four per cent when the Ekman number is reduced by a factor of 10. In fact, the frequency sampling in Fig. 10 is such that the resonant peaks for the case $Ek = 10^{-8}$ are not perfectly captured, and this inaccuracy may be sufficient to account for the four per cent reduction.

This finding suggests what may be a very important result: although the effective Q-value derived from the dissipation of inertial waves at very low Ekman number may be an exceedingly complicated function of the forcing frequency, a robust average Q-value may be obtained that is asymptotically independent of the viscosity as $Ek \to 0$. In Appendix A we present a toy model that may explain this effect. The toy model, based on a simplified Cartesian geometry, has the advantage of possessing an analytical solution from which it can be shown that the frequency-averaged dissipation rate is exactly independent of the viscosity. We suggest that this property may be typical of situations in which forcing is applied to systems that exhibit a dense or continuous spectrum in the absence of dissipation.

It is conceivable that the dissipation rate, averaged locally in frequency, may be essentially independent of the details of the dissipation mechanism, whether it is due to a Navier–Stokes viscosity, damping by turbulent convection, or nonlinear wave damping. We are far from having demonstrated such a result. Nevertheless, our results suggest that a Q-value of the order of 10^5 can be obtained for Jupiter or Saturn through this mechanism. The value for a synchronized short-period extrasolar planet would be some 50 times greater owing to its slower rotation.

Fig. 11 illustrates the spatial structure of the tidal response in the convective region. In line with work by Rieutord et al. (2001) on free inertial waves in an incompressible fluid contained in a spherical annulus, we find that the disturbance is localized near rays, which are the characteristics of the spatially hyperbolic equations governing inertial waves, and are seen to reflect many times from the inner and outer boundaries. In a uniformly rotating planet the rays are straight and a simple relation exists between the wave frequency and the angle made by the rays with the vertical. A mild near-singularity occurs when the rays approach the axis of rotation. The overall wave pattern does not appear as neat as that in the calculations by Rieutord et al. (2001), perhaps because the density is non-uniform, but more probably because of an interference effect between the equilibrium and dynamical tides.

6.6. Effects of differential rotation

We have also made a very preliminary investigation of the possible effects of differential rotation. Unfortunately, without a reliable theory of how differential rotation is generated by convection and other processes in giant planets and stars, the choice of angular velocity profile is unconstrained. We considered the case of a linear profile $\Omega(r)$ of angular velocity in the convective region. There are clear similarities between the graphs of viscous dissipation rate versus forcing frequency (which we omit here) and those shown in Fig. 2 for a uniformly rotating planet. Even with a differential rotation of 20 per cent, however, the resonant response is substantially richer and stronger. The tidal response also looks qualitatively similar to that shown in Fig. 11, although the rays are curved in a differentially rotating planet.

We emphasize that we have not considered the possible effects of corotation resonances. While such resonances in the radiative region may absorb outgoing Hough waves, as noted by Goldreich & Nicholson (1989), there may also be a direct tidal torque and energy dissipation associated with tidal forcing at the corotation resonance, as occurs in differentially rotating disks (e.g., Goldreich & Tremaine 1980). There is also the possibility of an angular velocity that depends on latitude. The numerical method used in this paper is not well suited to such a situation, unless Ω depends in a sufficiently simple way on θ that the couplings between different spherical-harmonic components of the velocity field are strongly restricted. Therefore there remains much to be investigated with regard to tides in differentially rotating planets and stars.

7. COMPARISON WITH PREVIOUS WORK

The previous work most closely related to the present paper is that by Savonije & Papaloizou (1997) and Papaloizou & Savonije (1997). The former paper presents a numerical analysis of the linearized response of a uniformly rotating high-mass star to $\ell = m = 2$ tidal forcing. Unlike the planet considered in our calculations, the star is predominantly radiative and has only a small convective core. In comparison with our study, Savonije & Papaloizou (1997) take a more direct numerical approach to the full linearized equations, including non-adiabatic effects and a small viscosity, but retaining only terms of first order in the angular velocity. Perhaps because the convective core is small, they find that main effects of rotation occur through the resonant excitation of Hough modes in the radiative region, rather than inertial modes in the convective region. Indeed, they find a number of toroidal mode resonances for negative forcing frequencies, whereas precisely one such resonance is allowed in our analysis. Our calculation is more dedicated to the exacting task of resolving

the tidally forced inertial waves in the convective region and examining more carefully the limit of small viscosity. The reduction of the basic equations that we carry out allows us to solve the resulting equations much more efficiently, and the numerical method that we employ is particularly well suited to this problem.

The accompanying paper by Papaloizou & Savonije (1997) provides an asymptotic analysis of low-frequency tidal forcing in the same type of star. There is much in common between their concisely expressed analysis and the present paper. We have attempted to give a fuller exposition of the problem, formally justifying the approximations involved and allowing for the important possibility of differential rotation. We have thereby generalized the derivation of reduced equations for inertial modes and Hough modes. Furthermore, our analysis should be useful for future direct numerical simulations of tides, as it clarifies the role of the anelastic and Cowling approximations. These approximations are satisfied by the dynamical tide but not by the equilibrium tide (in Papaloizou & Savonije 1997 the effect of self-gravitation on the equilibrium tide is neglected).

Related work for non-rotating stars and planets has also been published by Goldreich & Nicholson (1989), Lubow et al. (1997), and Goodman & Dickson (1998), who arrive at asymptotic expressions for the tidal dissipation rate through the emission of g modes at a convective–radiative interface. There is a close formal relation between these expressions and our equation (124). However, the expression can only be evaluated, in the case of a rotating star or planet, if the inertial wave problem in the convective region has been solved numerically. In this connection it would be interesting to re-examine the problem of tidal forcing in rotating solar-type stars with convective envelopes (cf. Terquem et al. 1998; Goodman & Dickson 1998) taking into account either uniform or differential rotation. In the latter case the angular velocity profile of the solar convective envelope, inferred from helioseismic studies, could be used as a guide.

8. SUMMARY AND CONCLUSIONS

In this paper we have revisited the classical problem of the response of a giant planet to low-frequency tidal forcing. Much of our general analysis of this problem applies equally to tidal forcing in stars. The novel feature of our approach is that we take into account the slow and possibly non-uniform rotation of the planet. (Here 'slow' rotation means that we include the full Coriolis force but not the centrifugal distortion of the planet.) Convective regions of the planet then support low-frequency inertial waves with an intricate spatial structure and a rich frequency spectrum, while radiative regions support (generalized) Hough modes, some of which may be regarded as g modes of high radial order, modified by the (differential)

rotation. We have argued that, in many cases of interest, such as that of an extrasolar planet that orbits close to its host star, the effective tidal forcing frequency lies within the spectrum of inertial waves in the convective regions of the planet, and a resonant response can be expected. As a result, the rate of tidal dissipation may be greatly enhanced relative to a model that neglects the rotation of the planet. The dissipation occurs both through the viscous or turbulent dissipation of the inertial waves in the convective region and through the emission of generalized Hough waves that propagate through the radiative envelope towards the surface, where they presumably damp. Enhancement of the tidal dissipation rate implies a more rapid synchronization of the planet's spin with its orbit, a faster circularization of the orbit, and a more intense heating of the planet, which may lead in turn to inflation and even Roche-lobe overflow (Gu et al. 2003).

We have presented a systematic asymptotic analysis of the linearized response of a differentially rotating planet to tidal forcing with a frequency that is small compared to the dynamical frequency of the planet. The response separates naturally into an equilibrium tide, which represents a large-scale, quasi-hydrostatic distortion of the planet in the imposed tidal potential, and a dynamical tide, which constitutes a mostly wavelike correction. We obtain the reduced system of equations governing the dynamical tide in convective and radiative regions separately, and explain the asymptotic matching procedure between the two solutions.

In convective regions, which we model as being adiabatically stratified, the dynamical tide takes the form of an indirectly forced inertial wave confined in a spherical annulus. The reduced equations are intrinsically two-dimensional and require a numerical solution. Moreover, for effective forcing frequencies within the dense or continuous spectrum of free inertial waves, the problem is mathematically ill-posed unless viscosity is included. A question of particular interest is how the dissipation rate varies with the viscosity in the limit that the viscosity tends to zero.

In radiative regions, the dynamical tide involves predominantly horizontal motions and takes the form of a wave (or evanescent disturbance) with a short radial wavelength. A separation of variables is possible, and we find that the angular structure of the wave is governed by a generalization of Laplace's tidal operator. We call the resulting solutions generalized Hough modes and discuss some mathematical properties of the operator concerned.

Our analysis clarifies the role in the tidal problem of certain well known approximations to the equations of fluid dynamics. We find that the so-called traditional approximation, in which the latitudinal component of the angular velocity is neglected, is not applicable to inertial waves in convective regions and should never be used for this purpose. In fact, it gives highly misleading results for the tidal dissipation rate, perhaps worse than neglecting

the Coriolis force altogether. On the positive side, we argue that the dynamical tide satisfies both the anelastic and Cowling approximations, which eliminate acoustic waves and self-gravitation, respectively, from the problem. However, the equilibrium tide satisfies neither of these approximations. These considerations are important not only for analytical or semi-analytical studies but also for direct numerical simulations of tidal forcing. Such simulations will be needed in order to determine properly how the dynamical tide interacts with turbulent convection, as well as the role of nonlinearity in the tidal problem. It is highly convenient and appropriate to simulate convection with a numerical method based on the anelastic and Cowling approximations. Our analysis indicates that the dynamical tide can also be captured within this approach, and shows how the subtle, indirect forcing of the dynamical tide by the equilibrium tide can be achieved through the inertial terms in the equation of motion.

We have presented the results of full numerical calculations of the tidal response for an idealized model of a giant planet that is predominantly convective but also contains a solid core and has a thin radiative envelope. The numerical method is suited to the case of 'shellular' rotation in which the angular velocity is independent of latitude, and we have focused mainly on the case of uniform rotation. High-resolution calculations, using a pseudospectral method, are required to access the physically interesting regime of small Ekman number (small viscosity) and reveal the intricate spatial structure of the inertial waves while properly resolving the dissipative structures. We have calculated the tidal dissipation rate, both by viscous dissipation in the convective region and via the emission of Hough waves, as a function of the tidal forcing frequency, for the important case of a tidal potential proportional to the $\ell = m = 2$ solid harmonic, and for forcing frequencies that span the spectrum of inertial waves. We find that the viscous dissipation rate is strongly enhanced, relative to a calculation in which the Coriolis force is neglected, in a number of inertial-mode resonant peaks that become more numerous, sharper, and taller as the Ekman number is reduced. As a result, the viscous dissipation rate does not vanish linearly with the viscosity. Depending on the physical conditions at the convective–radiative boundary, the Hough dissipation rate may possibly exceed the viscous dissipation rate, and also responds to the inertial-mode resonances. A single 'toroidal mode resonance' is also possible, in which residual forcing excites a large-scale mode (related to a Rossby wave), rather than a short-wavelength response, in the radiative region. When the planet rotates differentially, the inertial-mode resonances are yet stronger and more numerous, and the viscous dissipation rate is further enhanced.

Examination of the spatial structure of the tidal response in the convective region shows, in line with work by Rieutord et al. (2001) on free inertial waves in an incompressible fluid contained in a spherical annulus, that the disturbance is localized near rays, which are the

characteristics of the spatially hyperbolic equations governing inertial waves, and are seen to reflect many times from the inner and outer boundaries. The rays are straight or curved depending on whether the planet rotates uniformly or differentially.

The dissipation rate associated with inertial waves at very low Ekman number is, in principle, a highly erratic function of the forcing frequency (Fig. 2). As we will discuss in future work, when realistic scenarios for tidal evolution are considered, there are various reasons why it may be more appropriate to apply a smoothed version of this 'fractal' curve rather than taking every resonant peak literally. We have presented both numerical evidence (Fig. 10), and an analytical demonstration based on a toy model (Appendix A), that the frequency-averaged tidal dissipation rate associated with inertial waves may be asymptotically independent of the viscosity in the limit of small Ekman number. If correct, this result is most important because the Ekman number based on the microscopic viscosity in the interior of Jupiter is exceptionally small and beyond the range of any numerical calculation. Even the eddy viscosity based on turbulent convection gives rise to a very small Ekman number, which should probably be further reduced owing to the mismatch between the typical tidal forcing frequency and the characteristic timescale of the convective motion.

The resulting tidal dissipation rates are not adequately represented by a constant Q-value as is commonly adopted in parametrized models. One reason for this is that the dissipation rate associated with inertial waves scales naturally with the spin frequency of the planet in a way that is not captured in the constant-Q model. Nevertheless, the effective Q-values obtained are of the order of 10^5 for Jupiter or Saturn, or some 50 times greater for a synchronized short-period extrasolar planet owing to its slower rotation.

These values are probably adequate to explain the historical evolution and current state of the Galilean satellites (e.g., Peale 1999). We consider the alternative model of Ioannou & Lindzen (1993b) improbable as it requires the interior of Jupiter to be subadiabatically stratified, in contradiction of current models (Guillot et al. 2003) which suggest that it has a minuscule superadiabatic gradient owing to the high efficiency with which convection can transport the required heat flux.

In the case of short-period extrasolar planets, a Q-value of the order of 10^7 following synchronization is probably sufficient to explain the circularization of their orbits (cf. Marcy et al. 1997). The additional route of dissipation via the emission of Hough waves in an outer radiative layer may play a role here, although this mechanism is subject to significant uncertainties. The dissipation of inertial waves in the convective region provides a deep source of heating that can inflate the planet, as may have been observed in the case of the transiting planet HD 209458 b (Brown et al. 2001).

In conclusion, we have shown that it is both important and feasible, although numerically challenging, to include the effects of rotation when studying the response of a planet or star to tidal forcing. Our general analysis lays the ground work for future numerical studies including more realistic interior models and, possibly, the effects of differential rotation or nonlinearity. In our preliminary numerical investigation we have demonstrated that a robust enhancement of tidal dissipation results from the inclusion of rotational effects, which can account for the rapid evolution of tidally interacting systems. There remains much of interest to be explored in this problem.

GIO acknowledges the hospitality of UCO/Lick Observatory, where this work was initiated, and also the support of the Royal Society through a University Research Fellowship. This work is supported in part by NASA through NAG5-13177 and NSF through NSF-AST-9987417.

A. DISSIPATION OF INERTIAL WAVES IN A TOY MODEL

In this appendix we present a toy model that explains some aspects of the viscous dissipation of forced inertial waves. Although the model does not capture many of the subtleties of the tidal-forcing problem, it has the advantage of possessing an analytical solution.

We consider an incompressible fluid of uniform density ρ and kinematic viscosity ν. The fluid initially rotates with uniform angular velocity $\mathbf{\Omega}$, with a pressure gradient balancing the centrifugal force and any gravitational force.

A body force $\boldsymbol{f}$ per unit mass excites small disturbances satisfying the linearized equations (written in the rotating frame)

$$\frac{\partial \boldsymbol{u}}{\partial t} + 2\mathbf{\Omega} \times \boldsymbol{u} = -\frac{1}{\rho}\nabla p + \nu \nabla^2 \boldsymbol{u} + \boldsymbol{f}, \tag{A1}$$

$$\nabla \cdot \boldsymbol{u} = 0, \tag{A2}$$

where $\boldsymbol{u}$ and p are the Eulerian perturbations of velocity and pressure.

The fluid is contained in a square box, $0 < x < L$ and $0 < z < L$, referred to Cartesian coordinates (x, y, z) such that $\mathbf{\Omega} = \Omega\, \boldsymbol{e}_z$. For the purposes of illustration, we assume that all quantities are independent of y, and adopt the boundary conditions

$$u_x = u_y = \frac{\partial u_z}{\partial x} = 0 \tag{A3}$$

on $x = 0, L$ and

$$\frac{\partial u_x}{\partial z} = \frac{\partial u_y}{\partial z} = u_z = 0 \tag{A4}$$

on $z = 0, L$. Apart from the first condition on u_y, these can be interpreted as meaning that the boundaries are rigid and stress-free.

We adopt units of mass, length, and time such that $\rho = 1$, $L = \pi$ and $2\Omega = 1$. For a periodic forcing, all quantities may be assumed to have the form

$$\begin{aligned} u_x &= \mathrm{Re}\left[u(x,z)\, e^{-i\omega t}\right], \qquad & u_y &= \mathrm{Re}\left[v(x,z)\, e^{-i\omega t}\right], \\ u_z &= \mathrm{Re}\left[w(x,z)\, e^{-i\omega t}\right], \qquad & p &= \mathrm{Re}\left[\psi(x,z)\, e^{-i\omega t}\right], \\ f_x &= \mathrm{Re}\left[f(x,z)\, e^{-i\omega t}\right], \qquad & f_z &= \mathrm{Re}\left[h(x,z)\, e^{-i\omega t}\right]. \end{aligned} \tag{A5}$$

We assume for simplicity that $f_y = 0$.

The linearized equations then reduce to

$$-i\omega u - v = -\partial_x \psi + \nu(\partial_x^2 + \partial_z^2)u + f, \tag{A6}$$

$$-i\omega v + u = \nu(\partial_x^2 + \partial_z^2)v, \tag{A7}$$

$$-i\omega w = -\partial_z \psi + \nu(\partial_x^2 + \partial_z^2)w + h, \tag{A8}$$

$$\partial_x u + \partial_z w = 0, \tag{A9}$$

subject to

$$u = v = \partial_x w = 0 \qquad \text{at} \quad x = 0, \pi \tag{A10}$$

and

$$\partial_z u = \partial_z v = w = 0 \qquad \text{at} \quad z = 0, \pi. \tag{A11}$$

For free modes of oscillation ($f = h = 0$), solutions exist of the form

$$\begin{aligned} u &= u_{mn} \sin mx \cos nz, \qquad & v &= v_{mn} \sin mx \cos nz, \\ w &= w_{mn} \cos mx \sin nz, \qquad & \psi &= \psi_{mn} \cos mx \cos nz, \end{aligned} \tag{A12}$$

with m and n non-negative integers, not both equal to zero. The dispersion relation of these viscously damped inertial modes is

$$\tilde{\omega}^2 = \frac{n^2}{m^2 + n^2}, \tag{A13}$$

where

$$\tilde{\omega} = \omega + i\nu(m^2 + n^2). \tag{A14}$$

In the absence of viscosity, the eigenfrequencies are real and dense in the interval $-1 \leq \omega \leq 1$. Viscous damping causes the eigenfrequencies to move below the real axis, increasingly so for modes of higher 'order'.

We return to the forced problem where ω is real and prescribed. The force components f and h can be expanded in Fourier series (the sums are over non-negative integers m, n)

$$\begin{aligned} f &= \sum f_{mn} \sin mx \cos nz, \\ h &= \sum h_{mn} \cos mx \sin nz. \end{aligned} \tag{A15}$$

The solution to the forced problem is then

$$\begin{aligned} u &= \sum u_{mn} \sin mx \cos nz, \\ v &= \sum v_{mn} \sin mx \cos nz, \\ w &= \sum w_{mn} \cos mx \sin nz, \\ \psi &= \sum \psi_{mn} \cos mx \cos nz, \end{aligned} \tag{A16}$$

with

$$u_{mn} = \frac{i\tilde{\omega} n(nf_{mn} - mh_{mn})}{(m^2+n^2)\tilde{\omega}^2 - n^2}, \tag{A17}$$

$$v_{mn} = \frac{n(nf_{mn} - mh_{mn})}{(m^2+n^2)\tilde{\omega}^2 - n^2}, \tag{A18}$$

$$w_{mn} = -\frac{i\tilde{\omega} m(nf_{mn} - mh_{mn})}{(m^2+n^2)\tilde{\omega}^2 - n^2}, \tag{A19}$$

$$\psi_{mn} = \frac{n(1-\tilde{\omega}^2)h_{mn} - m\tilde{\omega}^2 f_{mn}}{(m^2+n^2)\tilde{\omega}^2 - n^2}. \tag{A20}$$

Of particular interest is the average rate of viscous dissipation per unit volume,

$$D = \frac{1}{\pi^2} \int_0^\pi \int_0^\pi \langle -\boldsymbol{u} \cdot \nu \nabla^2 \boldsymbol{u} \rangle \, dx \, dz. \tag{A21}$$

This evaluates to

$$D = \frac{\nu}{8} \sum (m^2+n^2) \left(|u_{mn}^2| + |v_{mn}^2| + |w_{mn}^2| \right), \tag{A22}$$

and can then be related to the forcing in the form

$$D = \frac{\nu}{8} \sum \frac{(m^2+n^2)|\tilde{\omega}^2| + n^2}{|(m^2+n^2)\tilde{\omega}^2 - n^2|^2} \, (m^2+n^2)|nf_{mn} - mh_{mn}|^2. \tag{A23}$$

The variation of D with ω and ν is very complicated. As $\nu \to 0$ for fixed ω, D eventually tends linearly to zero, unless ω is one of the eigenvalues of the inviscid problem (which form a dense set of measure zero), in which case D tends to infinity. However, an 'average' dissipation rate associated with the spectrum of inertial waves can be identified by integrating D over all positive (or negative) frequencies, with the simple result

$$\int_0^\infty D\, d\omega = \frac{\pi}{16} \sum \frac{|n f_{mn} - m h_{mn}|^2}{m^2 + n^2}, \tag{A24}$$

which is *exactly independent of the viscosity*.

Fig. 12 illustrates how D varies with ω for several values of ν, for a simple forcing of the form $f_{mn} = 1/mn^2$, $h_{mn} = 0$. (In fact, for generic forcing, $f_{mn} = O(1/mn^2)$ for large m, n.) As seen in the tidal-forcing problem, the dissipation is enhanced in the neighborhood of inertial-mode resonances in the interval $-1 \le \omega \le 1$. As ν is reduced the resonant peaks become more numerous, sharper, and taller, but the integrated dissipation rate remains exactly the same. In fact, the contribution of each mode to the integrated dissipation rate is independent of the viscosity, and the strongest resonances, which are with modes of lowest 'order', retain their identity and importance as ν is reduced.

REFERENCES

Armitage, P. J., Livio, M., Lubow, S. H., & Pringle, J. E. 2002, MNRAS, 334, 248

Artymowicz, P. 1992, PASP, 104, 769

Bodenheimer, P., Hubickyj, O., & Lissauer, J. J. 2000, Icarus, 143, 2

Bodenheimer, P., Lin, D. N. C., & Mardling, R. A. 2001, ApJ, 548, 466

Boss, A. P. 1997, Science, 276, 1836

Boyd, J. P. 2001, Chebyshev and Fourier Spectral Methods, 2nd edn (Mineola: Dover)

Brown, T. M., Charbonneau, D., Gilliland, R. L., Noyes, R. W., & Burrows, A. 2001, ApJ, 552, 699

Burkert, A., Lin, D. N. C., Bodenheimer, P., Jones, C., & Yorke, H. 2003, in preparation

Cameron, A. G. W. 1978, Moon Planets, 18, 5

Cartwright, D. E. 2000, Tides (Cambridge: Cambridge Univ. Press)

Chapman, S., & Lindzen, R. S. 1970, Atmospheric Tides (Dordrecht: Reidel)

Cowling, T. G. 1941, MNRAS, 101, 367

Darwin, G. H., 1880, Phil. Trans. R. Soc. London, 171, 713

Dintrans, B., & Ouyed, R. 2001, A&A, 375, L47

Dobbs-Dixon, I., Lin, D. N. C., & Mardling, R. A. 2003, ApJ, submitted

Eckart, C. 1960, Hydrodynamics of Oceans and Atmospheres (London: Pergamon)

Eggleton, P. P., Kiseleva, L. G., & Hut, P. 1998, ApJ, 499, 853

Fischer, D. A., & Valenti, J. A. 2003, in preparation

Gavrilov, S. V., & Zharkov, V. N. 1977, Icarus, 32, 443

Giuricin, G., Mardirossian, F., & Mezzetti, M. 1984a, A&A, 134, 365

Giuricin, G., Mardirossian, F., & Mezzetti, M. 1984b, A&A, 135, 393

Gold, T., & Soter, S. 1969, Icarus, 11, 356

Goldreich, P. 1965, MNRAS, 130, 159

Goldreich, P., & Keeley, D. A. 1977, ApJ, 211, 934

Goldreich, P., & Nicholson, P. D. 1977, Icarus, 30, 301

Goldreich, P., & Nicholson, P. D. 1989, ApJ, 342, 1079

Goldreich, P., & Sari, R. 2003, ApJ, 585, 1024

Goldreich, P., & Soter, S. 1966, Icarus, 5, 375

Goldreich, P., & Tremaine, S. 1978, ApJ, 222, 850

Goldreich, P., & Tremaine, S. 1980, ApJ, 241, 425

Gonzalez, G., Laws, C., Sudhi, T., & Reddy, B. E. 2001, AJ, 121, 423

Goodman, J., & Dickson, E. S. 1998, ApJ, 507, 938

Goodman, J., & Oh, S. P. 1997, ApJ, 486, 403

Greenspan, H. P. 1968, The Theory of Rotating Fluids (Cambridge: Cambridge Univ. Press)

Gu, P.-G., Lin, D. N. C., & Bodenheimer, P, H. 2003, ApJ, 588, 509

Guillot, T., Hubbard, W. B., Stevenson, D. J., & Saumon, D. 2003, in Bagenal, F., et al., eds, Jupiter, in press

Hayes, W. D. 1970, Proc. R. Soc. London A, 320, 187

Hough, S. S. 1897, Phil. Trans. R. Soc. London A, 189, 201

Hough, S. S. 1898, Phil. Trans. R. Soc. London A, 191, 139

Hubbard, W. B., 1984, Planetary Interiors (New York: van Nostrand Reinhold)

Hut, P. 1981, A&A, 99, 126

Ida, S., & Lin, D. N. C. 2003, ApJ, submitted

Ioannou, P. J., & Lindzen, R. S. 1993a, ApJ, 406, 252

Ioannou, P. J., & Lindzen, R. S. 1993b, ApJ, 406, 266

Ioannou, P. J., & Lindzen, R. S. 1994, ApJ, 424, 1005

Jeffreys, H. 1920, MNRAS, 80, 309

Kuiper, G. P., 1951, in Hynek, J. A., ed., Astrophysics (New York: McGraw-Hill), 357

Laughlin, G., & Adams, F. C. 1997, ApJ, 491, 51

Lin, D. N. C., 1997, in Wickramasinghe, D. T., Bicknell, G. V., & Ferrario, L., eds, Accretion Phenomena and Related Outflows, IAU Colloquium 163 (San Francisco: ASP), 321

Lin, D. N. C., Bodenheimer, P., & Richardson, D. C. 1996, Nature, 380, 606

Lin, D. N. C., & Papaloizou, J. C. B. 1979a, MNRAS, 186, 799

Lin, D. N. C., & Papaloizou, J. C. B. 1979b, MNRAS, 188, 191

Lin, D. N. C., & Papaloizou, J. C. B. 1986, ApJ, 309, 846

Lin, D. N. C., Papaloizou, J. C. B., & Kley, W. 1993, ApJ, 416, 689

Lissauer, J. J. 1993, ARA&A, 31, 129

Longuet-Higgins, M. S. 1968, Phil. Trans R. Soc. London A, 262, 511

Lubow, S. H., & Ogilvie, G. I. 1998, ApJ, 504, 983

Lubow, S. H., Tout, C. A., & Livio, M. 1997, ApJ, 484, 866

Marcy, G. W., Butler, R. P., Williams, E., Bildsten, L., Graham, J. R., Ghez, A. M., & Jernigan, J. G. 1997, ApJ, 481, 926

Mardling, R. A., & Lin, D. N. C. 2002, ApJ, 573, 829

Mathieu, R. D. 1994, ARA&A, 32, 465

Mayor, M., & Queloz, D. 1995, Nature, 378, 355

Munk, W. H., & MacDonald, G. J. F. 1960, The Rotation of the Earth (Cambridge: Cambridge Univ. Press)

Murray, C. D., & Dermott, S. F. 1999, Solar System Dynamics (Cambridge: Cambridge Univ. Press)

Murray, N., Hansen, B., Holman, M., & Tremaine, S. 1998, Science, 279, 69

Ogura, Y., & Phillips, N. A. 1962, J. Atmos. Sci., 19, 173

Papaloizou, J. C. B., Nelson, R. P., & Masset, F. 2001, ApJ, 366, 263

Papaloizou, J. C. B., & Pringle, J. E. 1978, MNRAS, 182, 423

Papaloizou, J. C. B., & Pringle, J. E. 1981, MNRAS, 195, 743

Papaloizou, J. C. B., & Pringle, J. E. 1982, MNRAS, 200, 49

Papaloizou, J. C. B., & Savonije, G. J. 1997, MNRAS, 291, 651

Papaloizou, J. C. B., & Terquem, C. 1999, ApJ, 521, 823

Peale, S. J. 1999, ARA&A, 37, 533

Peale, S. J., Cassen, P., & Reynolds, R. T. 1979, Science, 203, 892

Pollack, J. B., Hubickyj, O., Bodenheimer, P., Lissauer, J. J., Podolak, M., & Greenzweig, Y. 1996, Icarus, 124, 62

Primini, F., Rappaport, S., & Joss, P. C. 1977, ApJ, 217, 543

Rasio, F. A., & Ford, E. B. 1996, Science, 274, 954

Rasio, F. A., Tout, C. A., Lubow, S. H., & Livio, M. 1996, ApJ, 470, 1187

Rieutord, M., Georgeot, B., & Valdettaro, L. 2001, J. Fluid Mech., 435, 103

Rieutord, M., & Valdettaro, L. 1997, J. Fluid Mech., 341, 77

Sandquist, E., Taam, R. E., Lin, D. N. C., & Burkert, A. 1998, ApJ, 506, 65

Santos, N. C., Israelian, G., & Mayor, M. 2001, A&A, 373, 1019

Sasselov, D. D., & Lecar, M. 2000, ApJ, 528, 995

Savonije, G. J., & Papaloizou, J. C. B. 1983, MNRAS, 203, 581

Savonije, G. J., & Papaloizou, J. C. B. 1984, MNRAS, 207, 685

Savonije, G. J., & Papaloizou, J. C. B. 1997, MNRAS, 291, 633

Savonije, G. J., Papaloizou, J. C. B., & Alberts, F. 1995, MNRAS, 277, 471

Savonije, G. J., & Witte, M. G. 2002, A&A, 386, 211

Taylor, G. I. 1920, Phil. Trans. R. Soc. London A, 220, 1

Terquem, C., Papaloizou, J. C. B., Nelson, R. P., & Lin, D. N. C. 1998, ApJ, 502, 788

Thomson, W. (Lord Kelvin) 1882, Proc. R. Soc. Edinburgh, 11, 396

Trilling, D. E., Lunine, J. I., & Benz, W. 2002, A&A, 394, 241

Unno, W., Osaki, Y., Ando, H., & Shibahashi, H. 1979, Nonradial Oscillations of Stars (Tokyo: Univ. Tokyo Press)

Weidenschilling, S. J., & Marzari, F. 1996, Nature, 384, 619

Witte, M. G., & Savonije, G. J. 1999a, A&A, 341, 842

Witte, M. G., & Savonije, G. J. 1999b, A&A, 350, 129

Witte, M. G., & Savonije, G. J. 2001, A&A, 366, 840

Witte, M. G., & Savonije, G. J. 2002, A&A, 386, 222

Yoder, C. F., & Peale, S. J. 1981, Icarus, 47, 1

Zahn, J.-P. 1966, Ann. Astrophys., 29, 313

Zahn, J.-P. 1970, A&A, 4, 452

Zahn, J.-P. 1977, A&A, 57, 383

Zahn, J.-P. 1989, A&A, 220, 112

Zahn, J.-P. 1992, A&A, 265, 115

Zhang, K., Earnshaw, P., Liao, X., & Busse, F. H. 2001, J. Fluid Mech., 437, 103

This preprint was prepared with the AAS LaTeX macros v5.0.

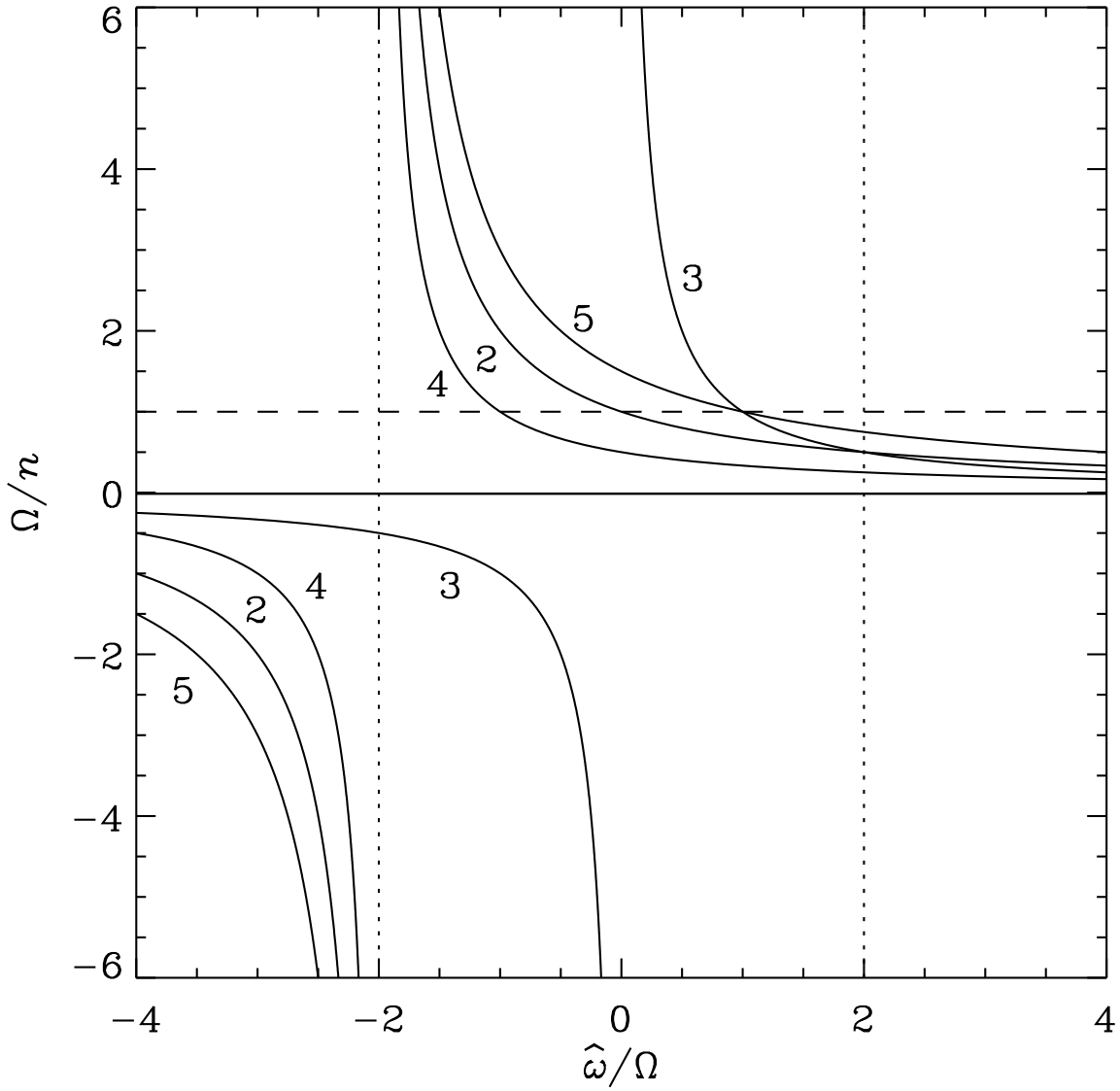

Fig. 1.— Tidal forcing frequencies and the spectrum of inertial waves in a uniformly rotating planet. The ratio of the (spin) angular velocity of the planet to the mean motion of the orbit is plotted against the ratio of the effective forcing frequency to the angular velocity of the planet, for components 2–5 of the tidal potential. The dotted lines indicate the extent of the spectrum of inertial waves. A short-period extrasolar planet being spun down towards the synchronized state descends the tracks from near the top of the diagram to the dashed line.

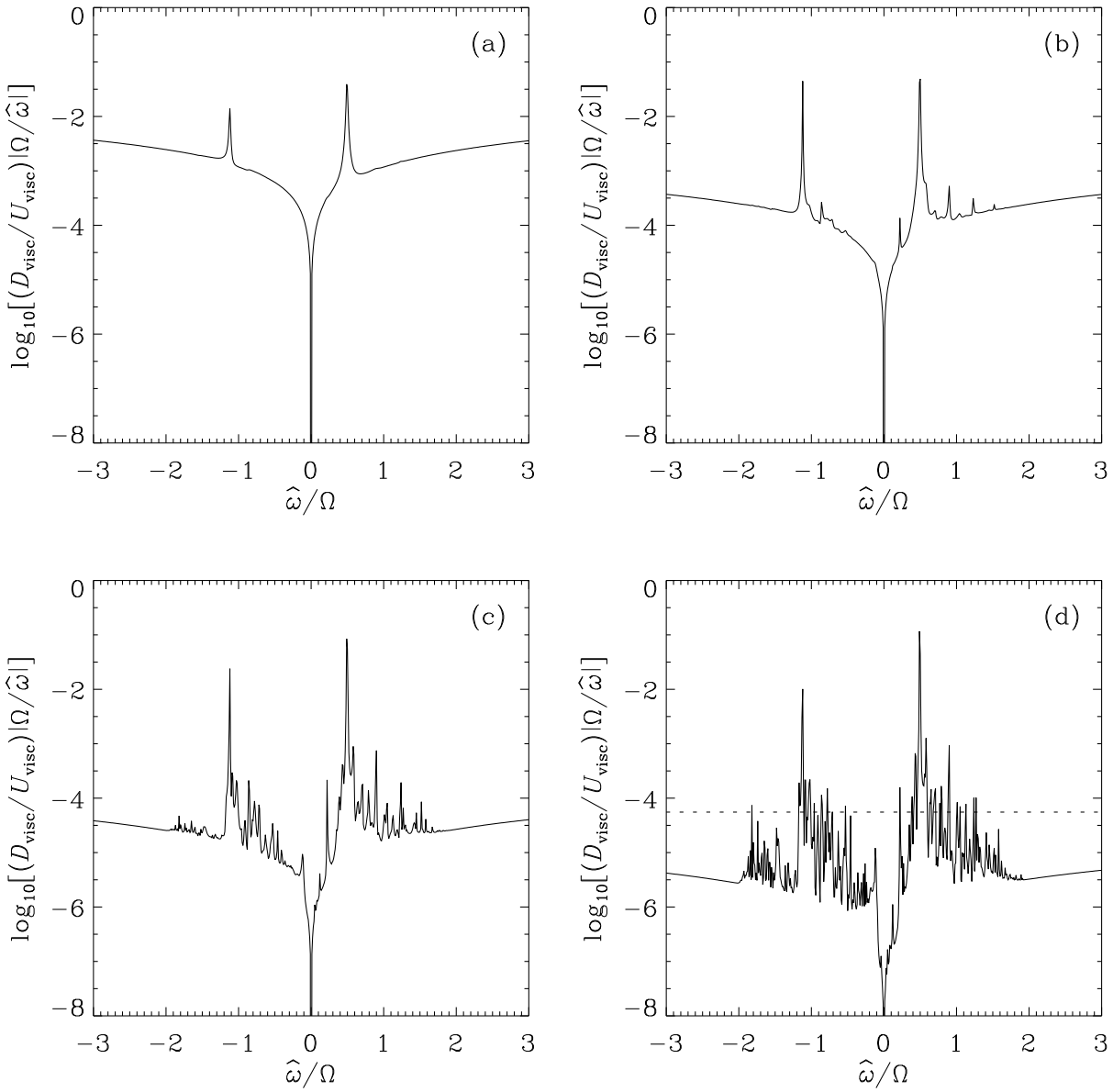

Fig. 2.— Tidal dissipation rate by viscosity in a uniformly rotating planet, according to the full model. The dissipation rate is scaled for comparison with equation (187). Panels (a), (b), (c), and (d) are for Ekman numbers 10^{-4}, 10^{-5}, 10^{-6}, and 10^{-7}, respectively. The spectrum of inertial waves corresponds to the interval $[-2, 2]$. The dotted line in panel (d) indicates the dissipation rate in Jupiter corresponding to an effective quality factor $Q_{\rm visc} = 10^5$.

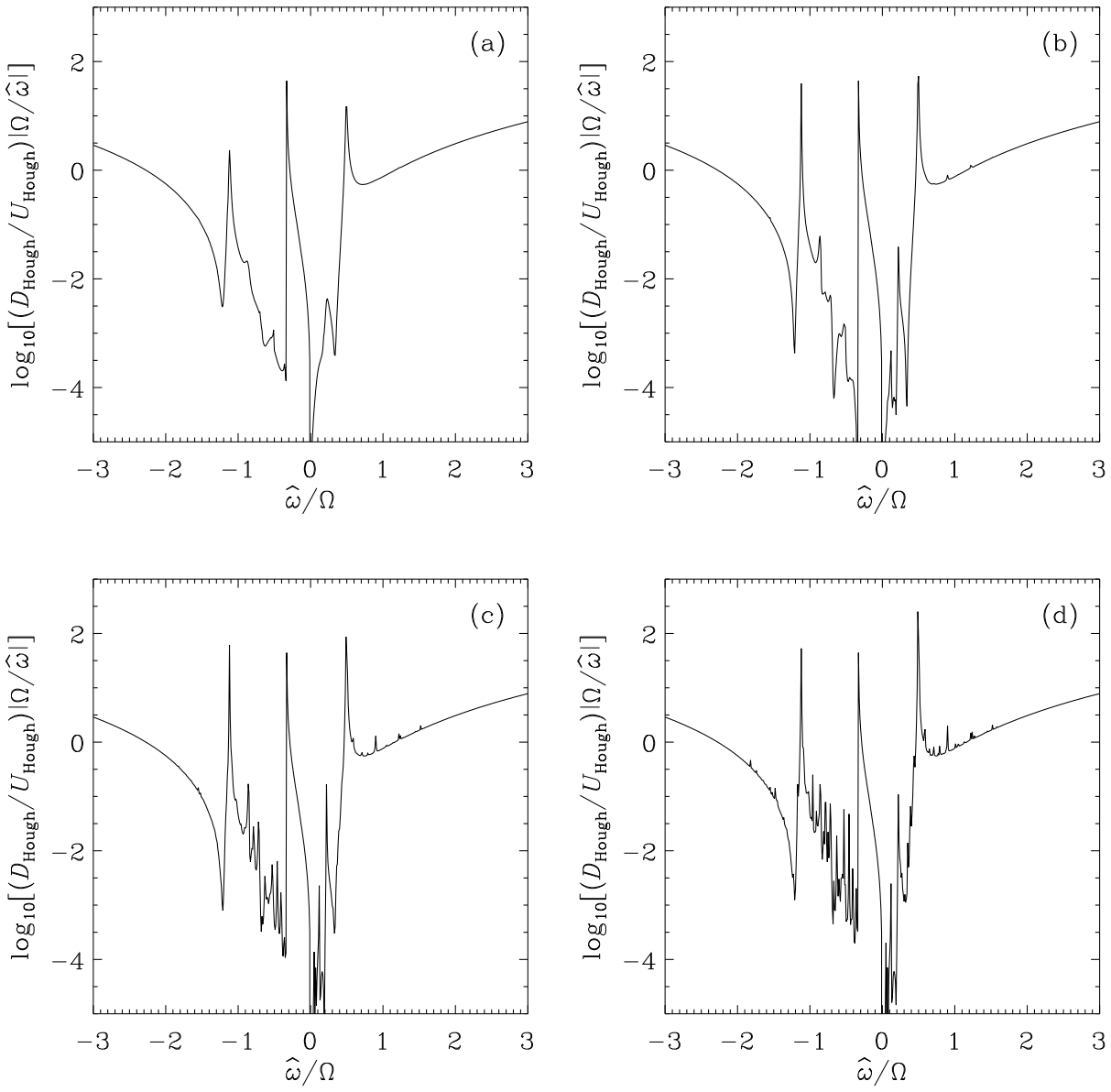

Fig. 3.— Tidal dissipation rate via Hough waves in a uniformly rotating planet, according to the full model. The dissipation rate is scaled for comparison with equation (187). Panels (a), (b), (c), and (d) are for Ekman numbers 10^{-4}, 10^{-5}, 10^{-6}, and 10^{-7}, respectively.

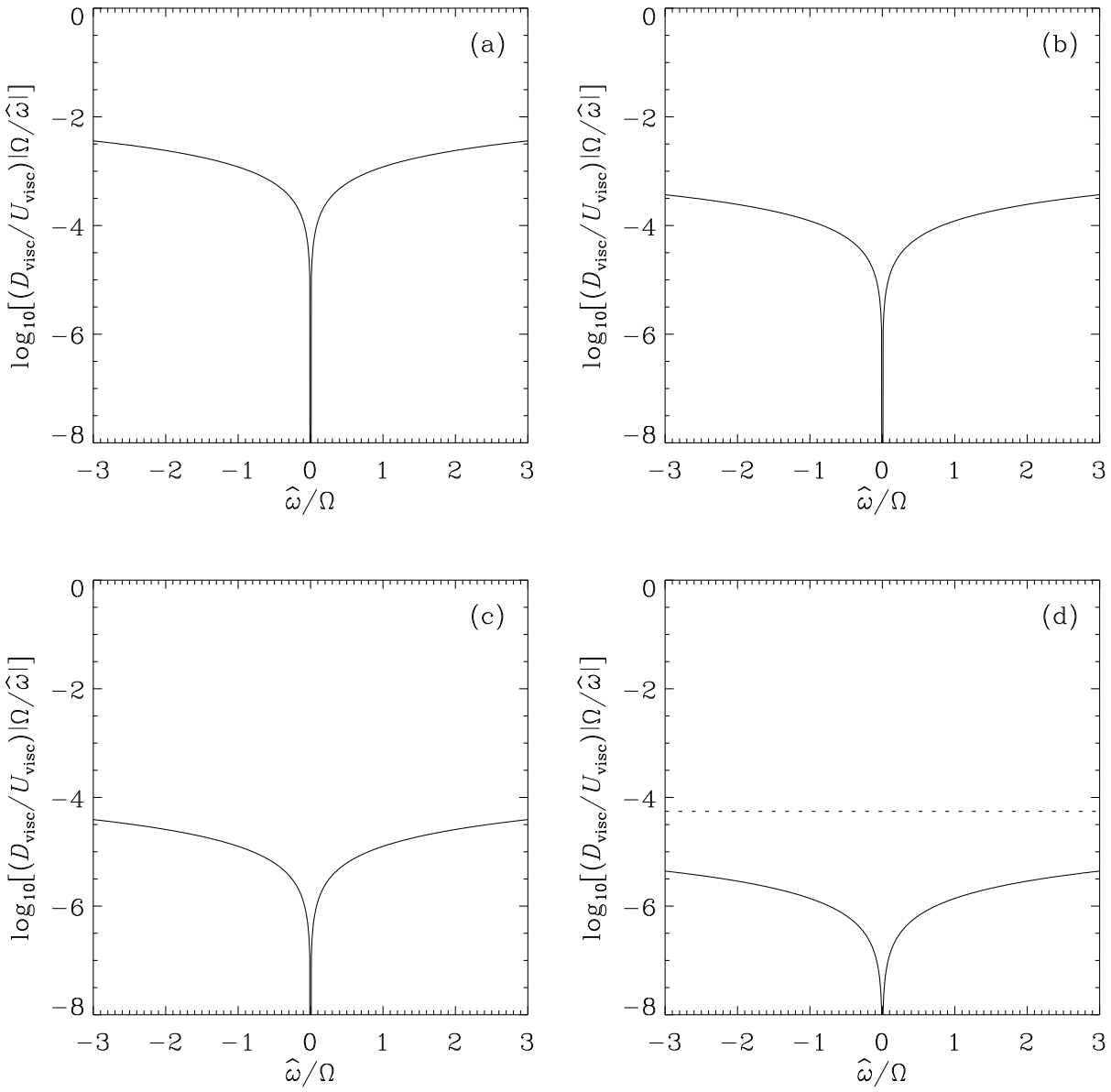

Fig. 4.— Tidal dissipation rate by viscosity in a uniformly rotating planet, according to the no-Coriolis approximation. The parameters are as in Fig. 2.

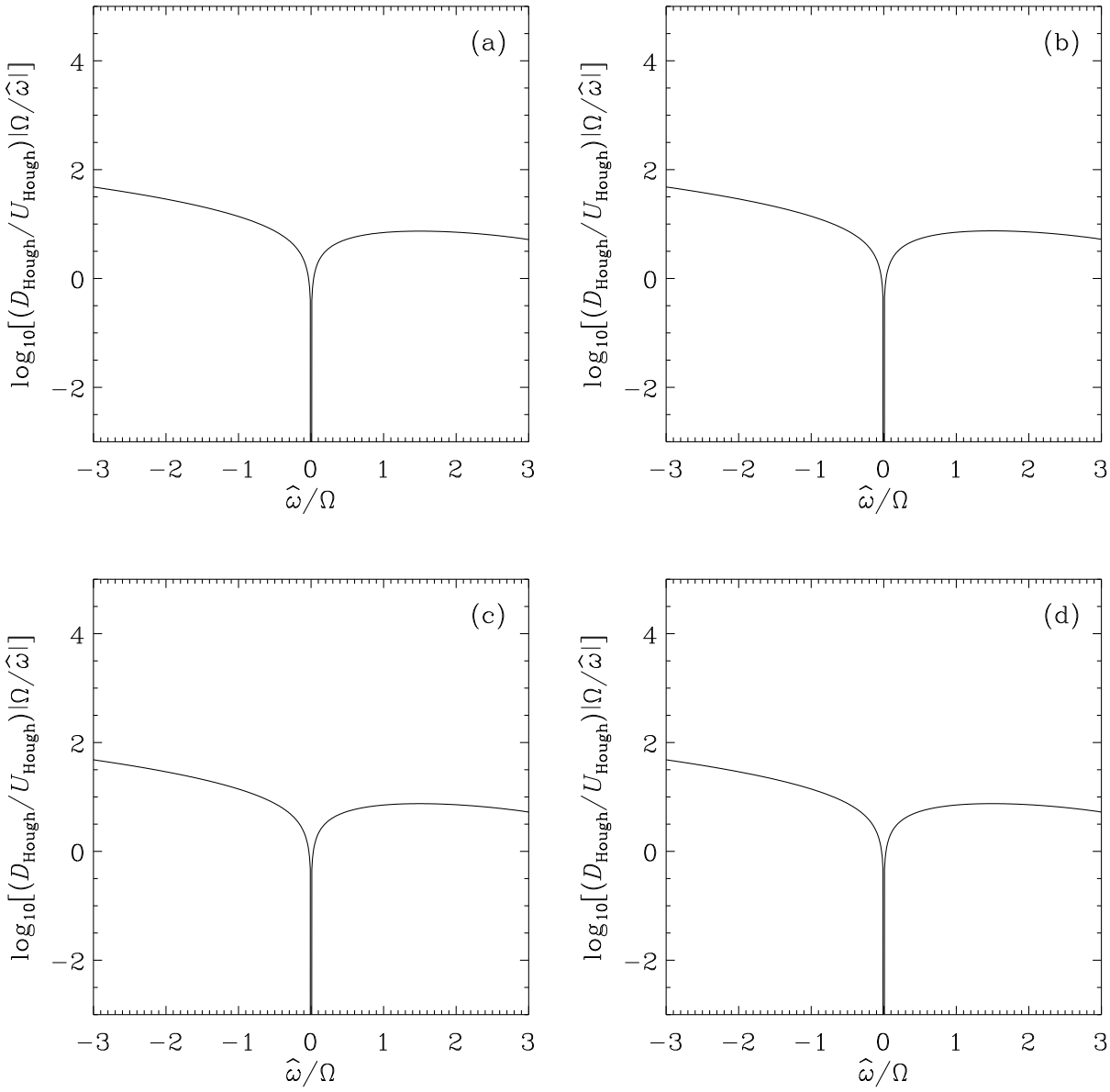

Fig. 5.— Tidal dissipation rate via Hough waves in a uniformly rotating planet, according to the no-Coriolis approximation. The parameters are as in Fig. 3.

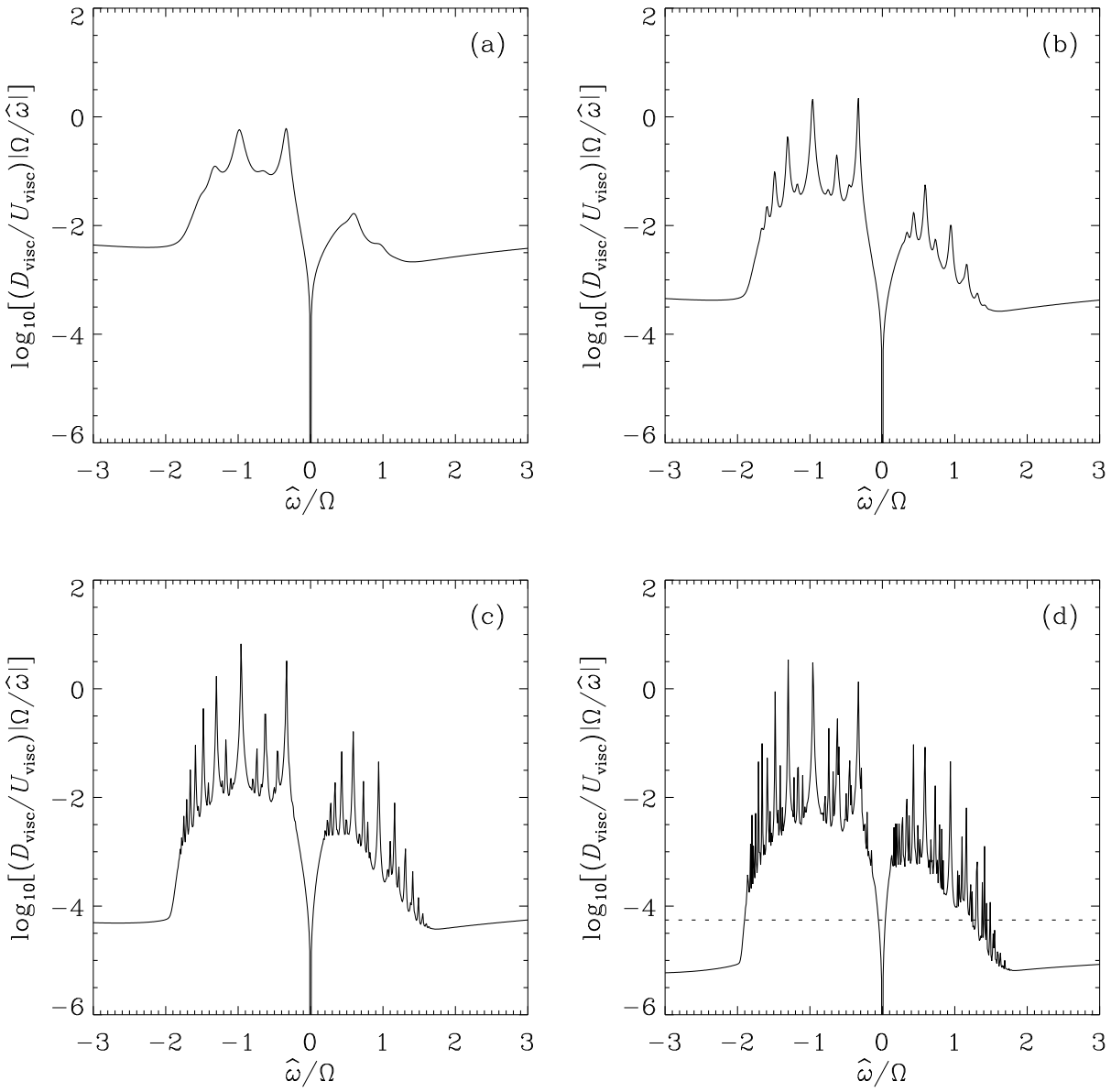

Fig. 6.— Tidal dissipation rate by viscosity in a uniformly rotating planet, according to the traditional approximation. The parameters are as in Fig. 2.

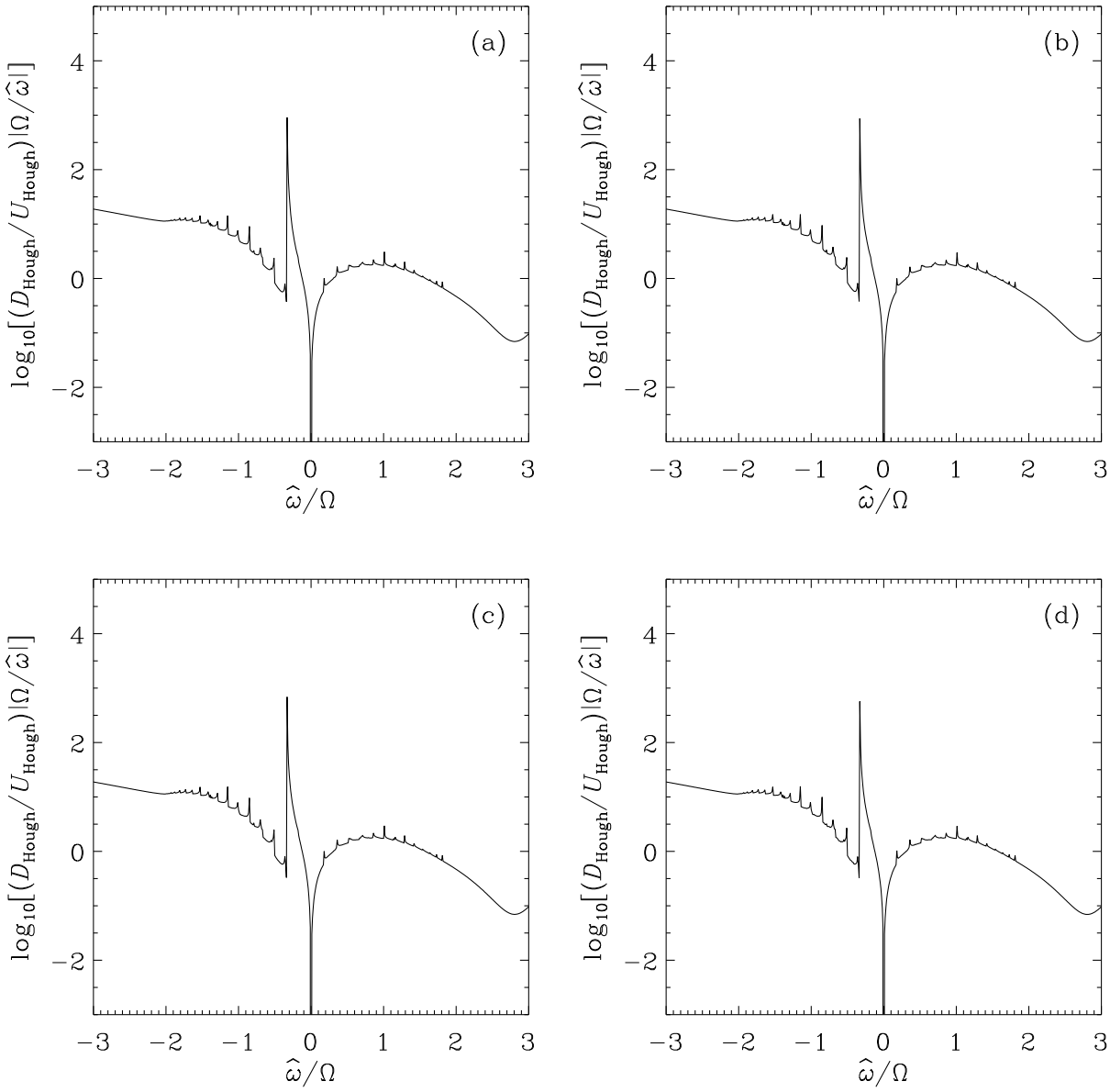

Fig. 7.— Tidal dissipation rate via Hough waves in a uniformly rotating planet, according to the traditional approximation. The parameters are as in Fig. 3.

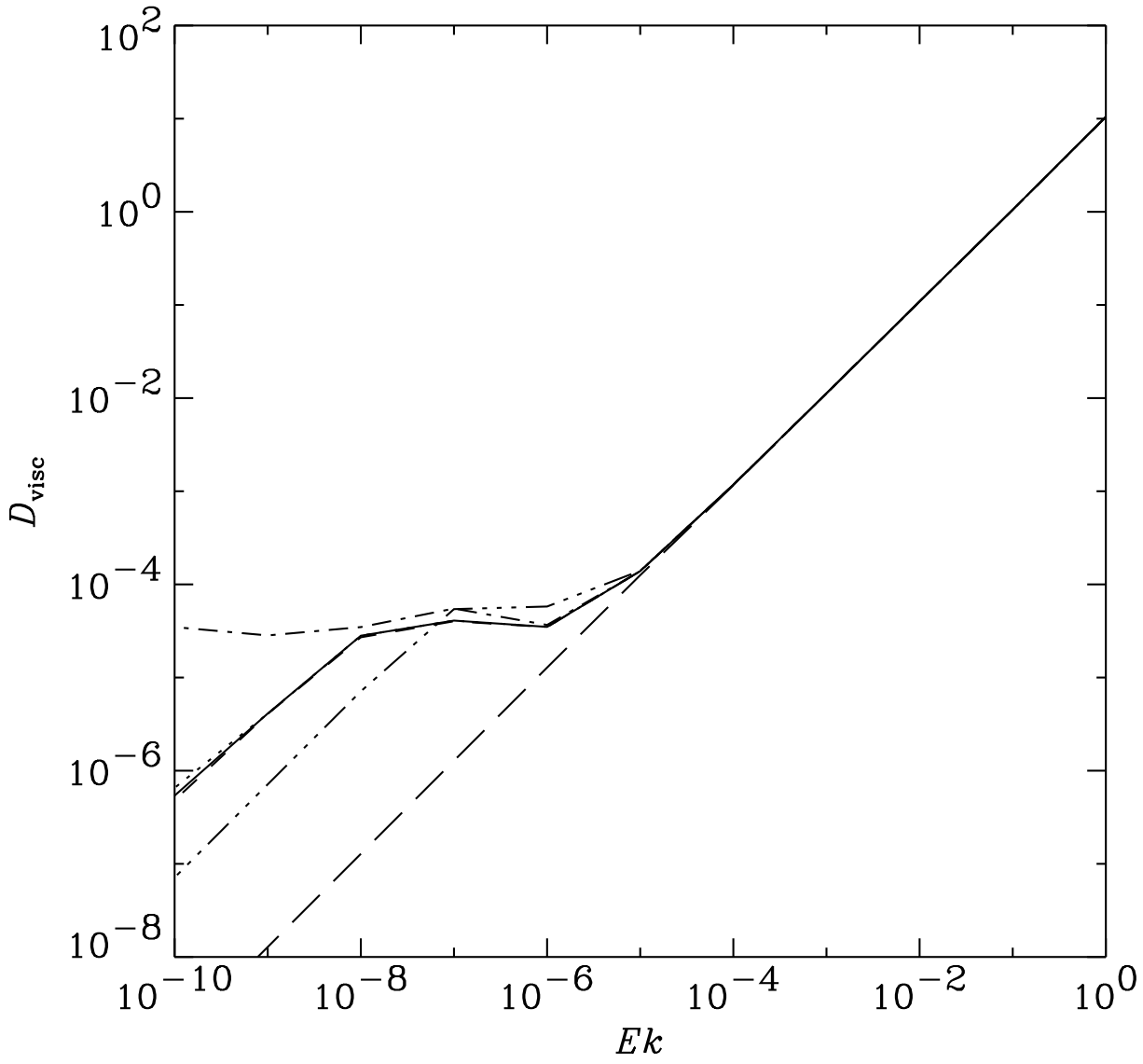

Fig. 8.— Resolution study away from resonance. The viscous dissipation rate for a forcing frequency $\hat{\omega} = \Omega$, not associated with an obvious resonant feature, is plotted versus the Ekman number for numerical resolutions $L = N = 500$ (solid line), 200 (dotted line), 100 (dashed line), 50 (dash-dotted line), 20 (dash-triple-dotted line), and 10 (long-dashed line). The three highest resolutions give results that are almost indistinguishable by eye. The alternative numerical method reproduces the curve for $Ek > 10^{-3}$ to very high accuracy, but cannot be used for smaller Ek.

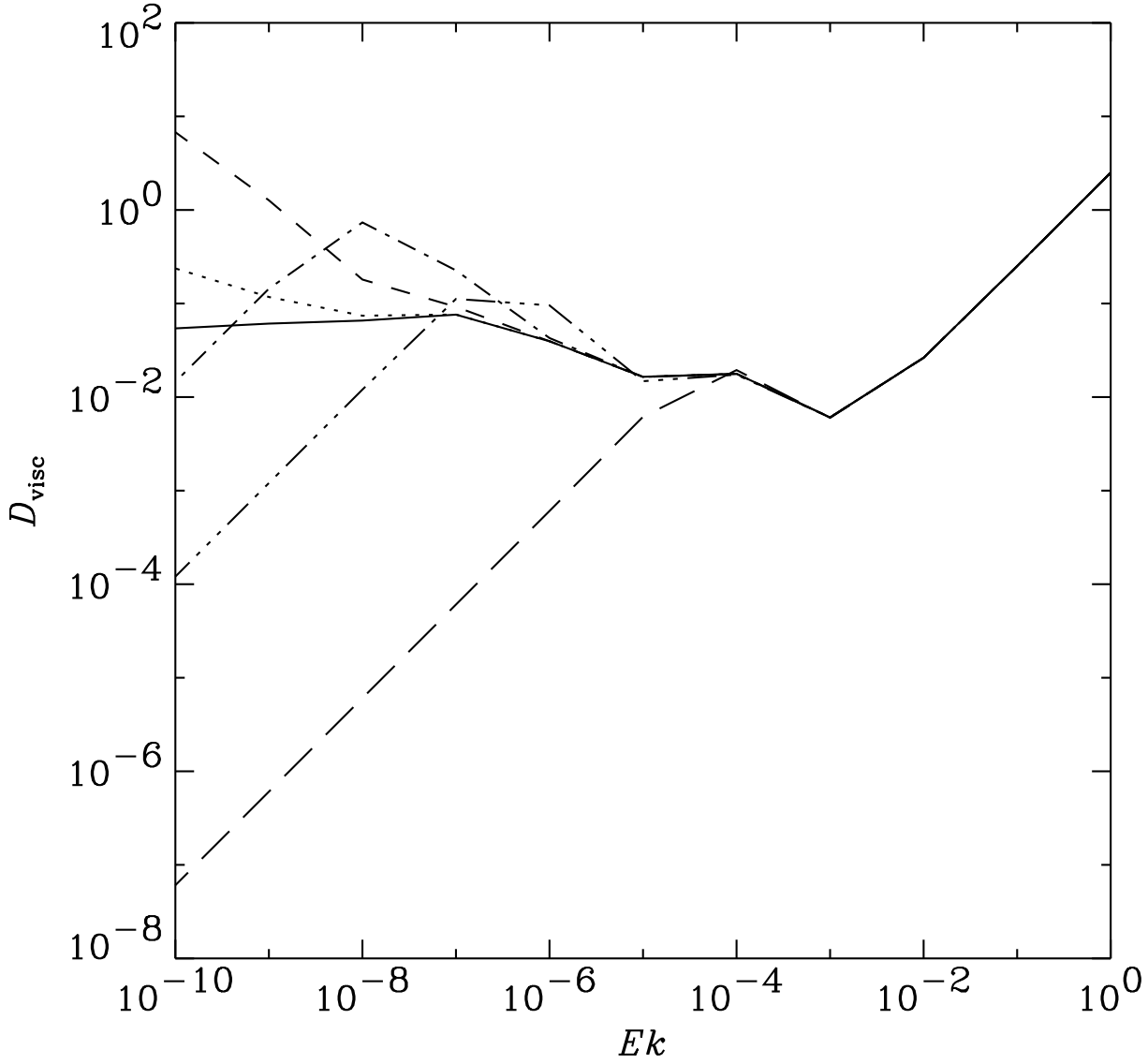

Fig. 9.— Resolution study on resonance. As for Fig. 8, but for a forcing frequency $\hat{\omega} = 0.489\,\Omega$, associated with the largest resonant feature seen in Fig. 2.

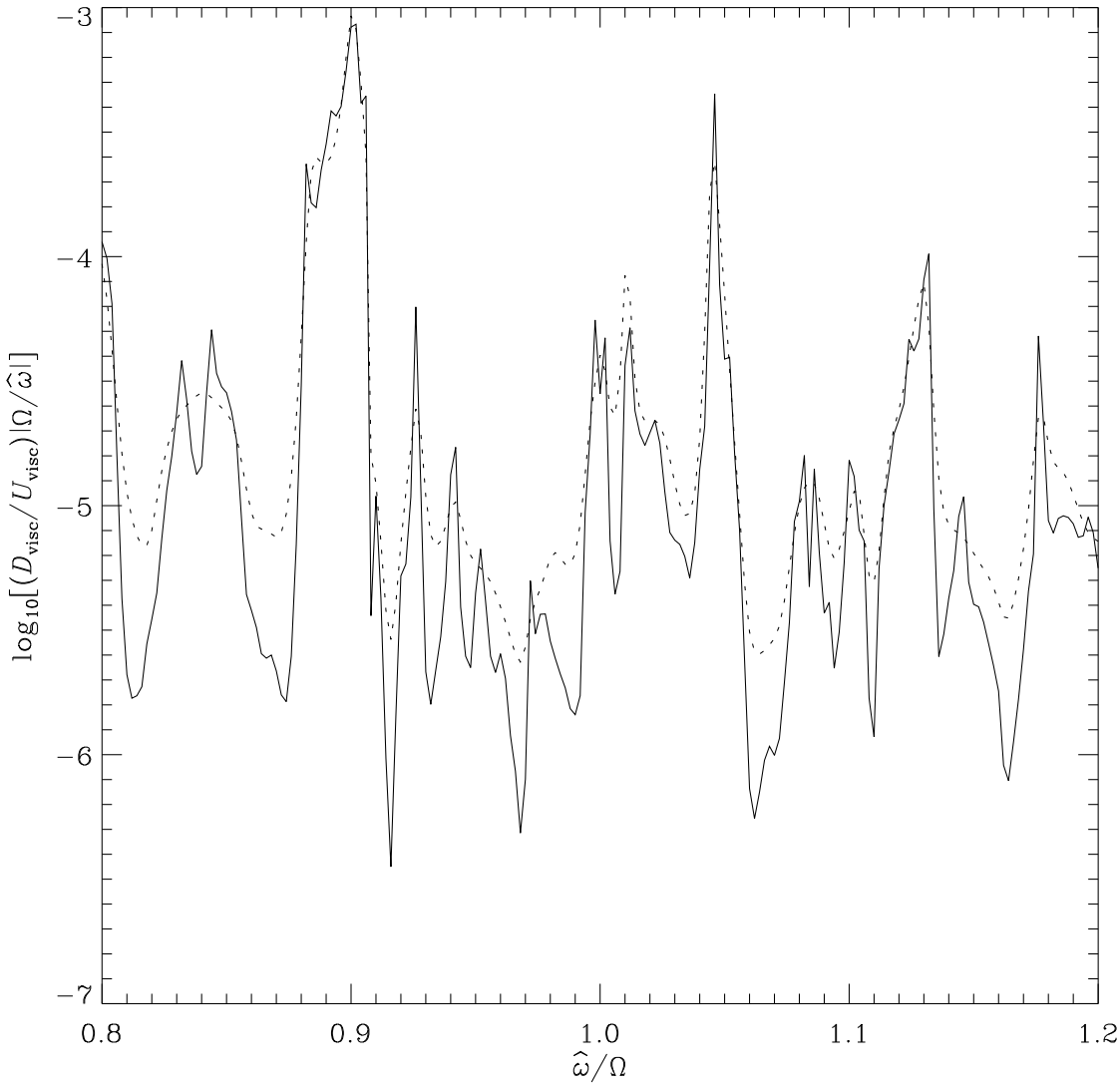

Fig. 10.— Expanded view of the graph of viscous dissipation rate in the full model, for forcing frequencies close to $\hat{\omega} = \Omega$. The dotted line corresponds to $Ek = 10^{-7}$ and is equivalent to panel (d) of Fig. 2. The solid line corresponds to $Ek = 10^{-8}$ and is calculated at a higher resolution of $L = N = 200$. The peaks of the curve are not perfectly captured at the frequency sampling of $\Delta\hat{\omega}/\Omega = 0.002$. Although the viscosities differ by a factor of ten, the frequency-averaged dissipation rates over this interval differ by at most a few per cent.

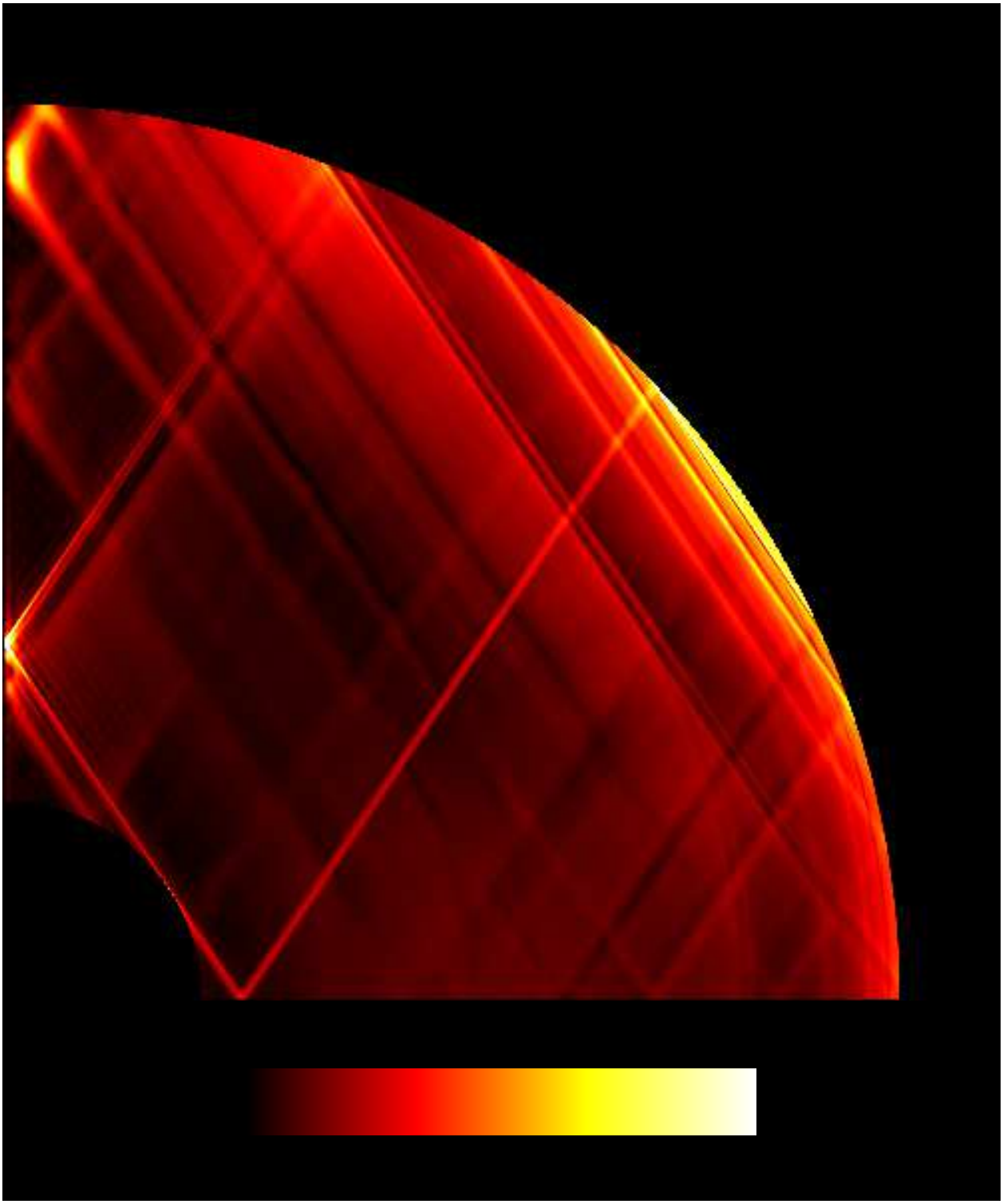

Fig. 11.— High-resolution calculation ($L = N = 500$, $Ek = 10^{-9}$) of the tidal response of a uniformly rotating planet. The root-mean-square velocity of the total tide (equilibrium plus dynamical) is plotted in a meridional slice through the convective region only. The velocity scale is linear, black representing zero. The forcing frequency is chosen to be near the peak of an inertial-mode resonance.

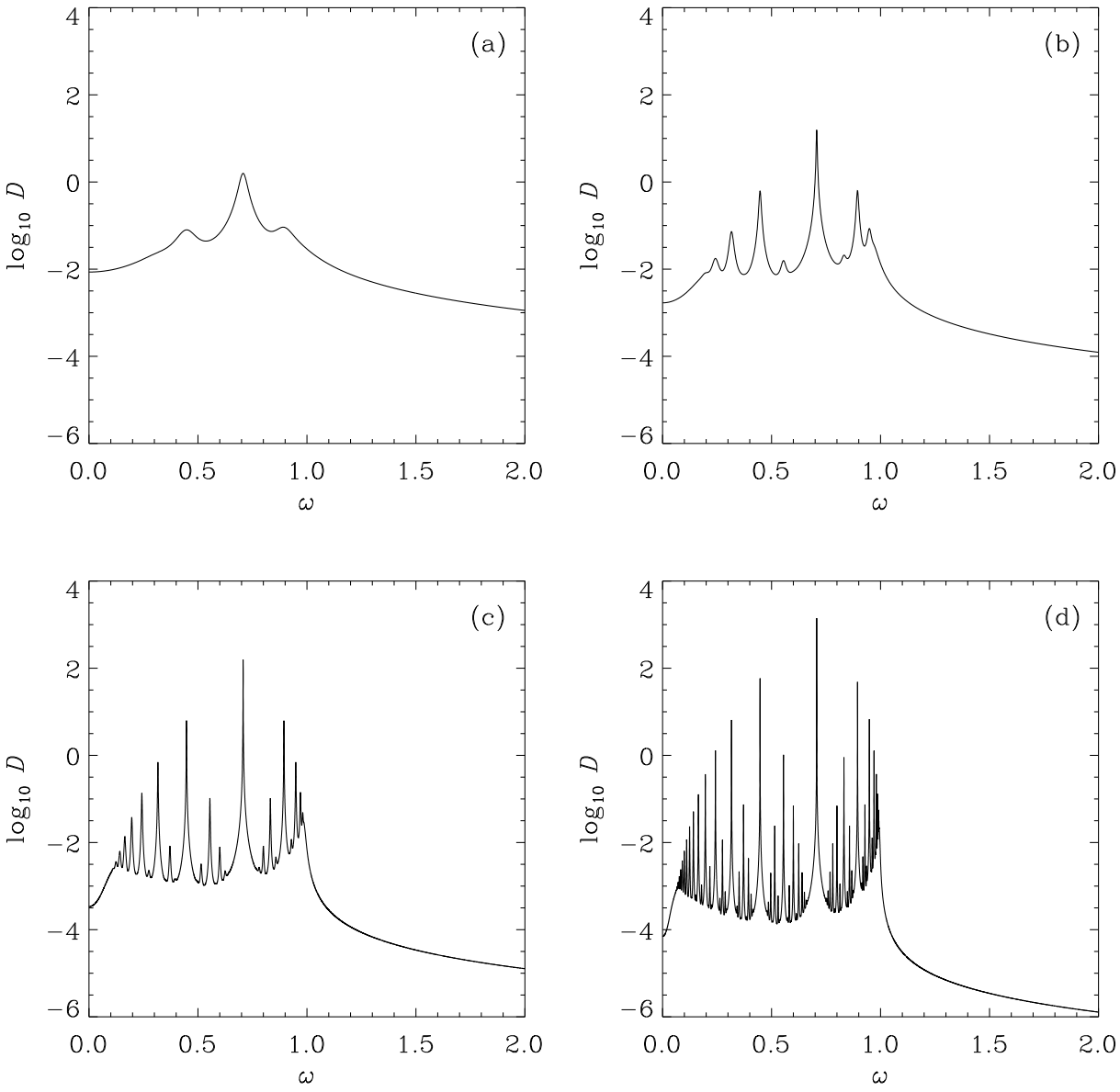

Fig. 12.— Variation of the viscous dissipation rate with forcing frequency, in the toy model for forced inertial waves (Appendix A). Panels (a), (b), (c), and (d) are for dimensionless viscosities $\nu = 10^{-2}$, 10^{-3}, 10^{-4}, and 10^{-5}, respectively. The spectrum of inertial waves corresponds to $-1 \leq \omega \leq 1$, and the graphs are symmetric about $\omega = 0$.